

GENERALIZED INTEGRAL TRANSFORMS AND WAVELET BASED NUMERICAL SCHEMES FOR FRACTIONAL DIFFERENTIAL EQUATIONS

A THESIS SUBMITTED TO
THE BHARATHIDASAN UNIVERSITY, TIRUCHIRAPPALLI
IN PARTIAL FULFILLMENT OF THE REQUIREMENTS
FOR THE DEGREE OF
DOCTOR OF PHILOSOPHY IN MATHEMATICS

SUBMITTED BY

R. ANUSUYA DEVI

(Ref. No. 010779/ Ph.D.K1/ Mathematics/ F-T(2-4)/ January 2019)/Date:11.01.2019

UNDER THE SUPERVISION OF
Dr. R. ARULDOSS, M.Sc., M.Phil., Ph.D.,



DEPARTMENT OF MATHEMATICS
GOVERNMENT ARTS COLLEGE(AUTONOMOUS)
KUMBAKONAM - 612 002
TAMIL NADU, INDIA
JULY 2022

DECLARATION

I hereby declare that this work has been carried out by me under the guidance and supervision of **Dr. R. ARULDOSS, M.Sc., M.Phil., Ph.D.**, and this work has not been submitted elsewhere for any other Degree, Diploma, Associateship, Fellowship or any other similar title.

Place : (R. ANUSUYA DEVI)
Date : Research Scholar,
Department of Mathematics,
Government Arts College (Autonomous),
Kumbakonam, Tamilnadu, India.

CERTIFICATE

I certify that this thesis entitled “**GENERALIZED INTEGRAL TRANSFORMS AND WAVELET BASED NUMERICAL SCHEMES FOR FRACTIONAL DIFFERENTIAL EQUATIONS**”, submitted by **Mrs. R. ANUSUYA DEVI, M.Sc., M.Phil.**, for the degree of Doctor of Philosophy in Mathematics of the Bharathidasasn University is a record of research work done by her under my guidance and that it has not been previously formed the basis for the award of any Degree, Diploma, Associateship, Fellowship or any other similar title.

Place :

(**Dr. R. ARULDOSS**)

Date :

Research Advisor,
Assistant Professor,
Department of Mathematics,
Government Arts College (Autonomous),
Kumbakonam, Tamilnadu, India.

Document Information

Analyzed document	R. ANUSUYA DEVI - Mathematics - Final Thesis.pdf (D142231765)
Submitted	7/20/2022 9:05:00 AM
Submitted by	Dr.S.Vanitha
Submitter email	vanitha@bdu.ac.in
Similarity	6.3%
Analysis address	navitha.bdu@analysis.arkund.com

Sources included in the report









SA	Thapar Institute Of Engineering And Technology / Thesis work of gagan msc math_removed.pdf Document Thesis work of gagan msc math_removed.pdf (D110664288) Submitted by: sanjeev.smca@thapar.edu Receiver: sanjeev.smca.thapar@analysis.arkund.com	 1
SA	Savutribai Phule Pune University / Shrinath Dilip Manjarekar.pdf Document Shrinath Dilip Manjarekar.pdf (D56166309) Submitted by: plag.cpe@unipune.ac.in Receiver: plag.cpe.unipune@analysis.arkund.com	 3
SA	Bharathidasan University, Tiruchirappally / Jernith.pdf Document Jernith.pdf (D41812768) Submitted by: bdulib@gmail.com Receiver: bdulib.bdu@analysis.arkund.com	 5
SA	Tumkur University / Jayaprakasha.P.C-Mathematics-15MT002-Thesis.pdf Document Jayaprakasha.P.C-Mathematics-15MT002-Thesis.pdf (D112611378) Submitted by: basralravi@gmail.com Receiver: basralravi.tumkur@analysis.arkund.com	 8
SA	Scientia Iranica, Sharif University of Tech / M. Khader- Scientia_ScientiaP1287_FullPaper.pdf Document M. Khader- Scientia_ScientiaP1287_FullPaper.pdf (D14222276) Submitted by: scientia@sharif.edu Receiver: scientia.shuniv@analysis.arkund.com	 1
SA	Baba Ghulam Shah Badshah University, Rajouri / Original.pdf Document Original.pdf (D48153609) Submitted by: rameshpandita90@gmail.com Receiver: rameshpandita90.bgsbu@analysis.arkund.com	 8
SA	Thapar Institute Of Engineering And Technology / Final Thesis work.pdf Document Final Thesis work.pdf (D110815744) Submitted by: sanjeev.smca@thapar.edu Receiver: sanjeev.smca.thapar@analysis.arkund.com	 1
SA	Anna University, Chennai / AS-J-3-Published version.pdf Document AS-J-3-Published version.pdf (D41962241) Submitted by: harikrish.10@gmail.com Receiver: harikrish.10.annauniv@analysis.arkund.com	 10

Table of Contents

Table of Contents	iii
Abstract	vii
Acknowledgements	ix
List of publications	xi
1 Introduction	1
1.1 A brief history of Fractional Calculus	1
1.1.1 Fractional derivatives and integrals	10
1.2 Fractional differential equations	13
1.3 Integral transforms	15
1.4 Wavelets	16
1.4.1 Multiresolution Analysis	23
1.4.2 Advantages of wavelet theory	25
1.4.3 Comparison of wavelet transform with Fourier transform	26
2 Numerical solutions of fractional differential equations using Aboodh Transform method and a generalized fractional integral transform with exponential type kernel	28
2.1 Introduction	28

2.2	Aboodh transform method	29
2.2.1	Properties of Aboodh transform	30
2.2.2	Solutions of Fractional Differential Equations using Aboodh transform method	31
2.3	A generalized fractional integral transform with exponential type kernel	37
2.3.1	Sufficient conditions for the existence of the generalized fractional integral transform with exponential type kernel	39
2.3.2	Duality relation between the fractional Laplace transform and the generalized fractional integral transform with exponential type kernel	40
2.3.3	Operational Properties of generalized fractional integral transform with exponential type kernel	41
2.3.4	Convolution theorem using generalized fractional integral transform with exponential type kernel	44
2.3.5	Inversion theorem using generalized fractional integral transform with exponential type kernel	45
2.3.6	Solutions of fractional differential equations using generalized fractional integral transform with exponential type kernel	46
2.3.7	Example 1	46
2.3.8	Example 2	47
3	Numerical solutions of fractional differential equations by Euler wavelet method	49
3.1	Introduction	49
3.2	Euler wavelet based numerical scheme	50
3.3	Function approximation by Euler wavelets	52
3.4	Error analysis for the Euler wavelet bases	54

3.5	Operational matrix of the fractional integration of Euler wavelets . . .	55
3.6	Numerical Examples	57
3.6.1	Example 3	58
3.6.2	Example 4	59
3.6.3	Example 5	60
3.6.4	Example 6	61
3.6.5	Example 7	63
4	Numerical solutions of fractional differential equations with variable coefficients by Bernoulli wavelet method	66
4.1	Introduction	66
4.2	Bernoulli wavelet based numerical scheme	67
4.3	Properties of Bernoulli polynomials and Bernoulli wavelets	69
4.4	Function approximation by Bernoulli wavelets	70
4.5	Operational matrix of fractional order integration of Bernoulli wavelets	71
4.6	Convergence Analysis	73
4.7	Algorithm for the Bernoulli wavelet based numerical scheme	75
4.8	Numerical Examples	76
4.8.1	Example 8	76
4.8.2	Example 9	78
5	Numerical solutions of multi-order fractional differential equations by Chebyshev wavelet method	82
5.1	Introduction	82
5.2	Chebyshev wavelet based numerical scheme	84
5.3	Function approximation by Chebyshev wavelets	85
5.4	The Chebyshev wavelet Operational matrix of fractional integration .	86
5.5	Numerical Examples	88

5.5.1	Example 10	88
5.5.2	Example 11	91
5.5.3	Example 12	92
6	Applications of Bernoulli wavelets	94
6.1	Introduction	94
6.2	Applications	95
6.2.1	Example 13	95
6.2.2	Example 14	97
6.2.3	Example 15	99
6.2.4	Example 16	100
	Conclusion	103
	Bibliography	106

Abstract

In recent years, fractional calculus has been the focus of various scientific studies. The main objective of this thesis is to explore different fractional integral transforms with exponential type kernels and wavelet based numerical schemes for solving fractional differential equations.

In the first Chapter, we discuss the history of fractional calculus, definitions of fractional derivatives and integrals.

In the second Chapter, we apply Aboodh integral transform to solve some fractional differential equations and determine the relationship between Aboodh transform and the Laplace transform. Also we introduce a fractional integral transform which is a generalization of many integral transforms having exponential type kernels and discuss some of its properties. We also discuss the sufficient conditions for the existence of the newly introduced fractional integral transform with exponential type kernel. Finally, we conclude that the generalized fractional integral transform with exponential type kernel is an efficient and useful technique for solving many fractional differential equations.

In the third Chapter, we introduce a numerical scheme based on Euler wavelets and obtain numerical solutions of some fractional differential equations using an efficient Euler wavelet operational matrix. We finally conclude that the Euler wavelet based

numerical scheme is preferable to many other numerical schemes since the obtained numerical results are more consistent with the exact solutions.

In the fourth Chapter, we introduce a novel numerical scheme based on Bernoulli wavelets and utilize the operational matrix of Bernoulli wavelets to transform fractional differential equations with variable coefficients into simultaneous algebraic equations. The main advantage of the Bernoulli wavelet based numerical scheme is its fast convergency and its high degree of accuracy.

In the fifth Chapter, we derive a new fractional integration operational matrix of the Chebyshev wavelets and elucidate the solution process, the simplicity and the efficiency of the Chebyshev wavelet operational matrix by some illustrative examples. Finally we conclude that the numerical solutions attained by the Chebyshev wavelet scheme are in a good agreement with the exact solutions.

In the sixth chapter, we employ the numerical technique based on Bernoulli wavelets for finding the approximate solutions of fractional electrical circuits namely, LC, RL, RC and RLC.

Acknowledgements

It is my pleasure to acknowledge several individuals who played key roles for the completion of my Ph.D thesis.

First and foremost, I would like to convey my heartfelt gratitude to my supervisor, Dr. R. Aruldoss, for his wise counsel and encouraging observations during my studies. From the beginning until the end of this research work, he has provided all necessary facilities and assistance. This thesis would not have been feasible without his unwavering support and encouragement.

I would sincerely like to thank and deeply grateful to Prof. K. Duraiarasan, Principal, Government Arts College (Autonomous), Kumbakonam, for offering me this opportunity to accomplish this thesis.

With great pleasure, I express sincere thanks to Dr. P. Murali Krishna, Asst. Professor of Mathematics, Amrita Vishwa Vidhyapeetham, Coimbatore, for his immense help, constructive comments and discussion.

I will always remember my friends that I have made during my research work and with whom I have cherished some joyous moments and refreshing exchanges.

I would like to express my gratitude to my parents and family for their blessings, moral support and encouragement.

From the bottom of my heart, I thank my husband Ananth Kumar and my son

Sai Sakthi for their great sacrifice, kind co-operation, patience and understanding throughout the course of this work. Their invaluable companionship, warmth, strong faith in my capabilities has always helped me to be assertive in difficult times.

List of publications

[1] R. Arul Doss and R. Anusuya Devi, “An expeditious wavelet-based numerical scheme for solving fractional differential equations”, *Computational and Applied mathematics*, Vol. 40, Issue 2(2021). **A SPRINGER Publication, UGC CARE list-Group II, Scopus and Web of Science**

[2] R. Arul Doss and R. Anusuya Devi, “A novel numerical scheme based on Bernoulli wavelets for fractional differential equations with variable coefficients”, *Advances and Applications in Mathematical Sciences*, Vol. 21, Issue 5(2022).
UGC CARE list-Group I and II, Web of Science

[3] R. Arul Doss and R. Anusuya Devi, “An efficient fractional integration operational matrix of the Chebyshev wavelets and its applications for multi-order fractional differential equations”, *South East Asian Journal of Mathematics and Mathematical Sciences*, Vol. 18, No. 1(2022), pp. 147-158.

UGC CARE list-Group I and II, Scopus

[4] R. Arul Doss and R. Anusuya Devi, “A generalized fractional integral transform with exponential type kernel”, *Malaya Journal of Matematic*, Vol. 8, No. 2(2020), pp. 544-550.

UGC CARE list - Group I, as of February 2020

- [5] R. Arul Doss and R. Anusuya Devi, “Aboodh transform for solving fractional differential equations”, *Global journal of pure and applied mathematics*, Vol. 16, No. 2(2020), pp. 145-153, ISSN:0973-1768.
- [6] R. Arul Doss and R. Anusuya Devi, “A numerical approach based on Bernoulli wavelets for fractional electrical circuits”, *Quest Journal of Research in Applied Mathematics*, Vol. 8, Issue 2(2022), pp. 10-17.

List of Tables

2.1	Integral transforms with exponential type kernel	38
2.2	Conversion of Sadik transform to various integral transforms	38
2.3	Conversion of the generalized fractional integral transform with exponential type kernel into existing fractional integral transforms	39
3.1	Comparisons between numerical solutions attained by Euler wavelet based numerical scheme(EWM) for $M=3$ and various numerical methods	58
3.2	Comparisons of maximum absolute errors for different values of k and β	60
3.3	Comparisons between numerical solutions attained by Euler wavelet based numerical scheme and Legendre wavelet method	61
3.4	Absolute errors for $M = 3$ and different values of j	62
3.5	Comparison of maximum absolute errors for Euler wavelet based numerical scheme with $j = 3, M = 3$ and Adams-type Predictor-Corrector method	62
3.6	Absolute errors for different values of k and for $\alpha = 1.5$	64
3.7	Comparison of maximum absolute errors for $\alpha = 1.5, M = 3$ and different values of j	64

4.1	Maximum absolute errors for various choices of j and N	78
4.2	Adams type Predictor-Corrector method [20].	78
4.3	Absolute errors for various choices of j and for $N = 2$	80
5.1	Absolute errors of example 10 for various values of \hat{n}	90
5.2	Absolute errors of example 11 for various values of \hat{n}	91
5.3	Maximum absolute errors of example 12 for various values of \hat{n}	92
6.1	Numerical results of LC circuit($L = 1, C = 1, R_0 = 0.01$ and for $\beta = 2$)	96
6.2	Numerical results of RL circuit($R = 10, L = 1, Q_0 = 0.01, V = 10$ and for $\beta = 1$)	97
6.3	Numerical results of RC circuit ($R = 10, C = 1, Q_0 = 20$ and for $\beta = 1$)	99
6.4	Numerical results of RLC circuit ($R=10, L=10, C=10, Q_0 = 0.01$ and for $\beta = 1$)	101

List of Figures

4.1	Comparison of Numerical solutions of Example 5.1 for $k = 8$ ($j = 3, N = 2$) and $k = 16$ ($j = 4, N = 2$) with the Exact solutions.	79
4.2	Comparison of Numerical solutions of Example 5.2 for $k = 8$ ($j = 3, N = 2$) and $k = 16$ ($j = 4, N = 2$) with the Exact solutions.	80
5.1	Comparison of the numerical and exact solutions for example 11	91
6.1	Current versus Time graph ($L = 1, C = 1, R_0 = 0.01$ and $\beta = 2$)	96
6.2	Current versus Time graph ($R = 10, L = 1, Q_0 = 0.01, V = 10$ and $\beta = 1$)	98
6.3	Voltage versus Time graph ($R = 10, C = 1, Q_0 = 20$ and $\beta = 1$)	100
6.4	Current versus Time graph ($R = 10, L = 10, C = 10, Q_0 = 0.01$ and $\beta = 1$)	102

Chapter 1

Introduction

1.1 A brief history of Fractional Calculus

Fractional Calculus [46, 56, 47] is a natural extension of classical calculus. It is a 300-year-old mathematical tool that has been gradually developed to the present day. It also does not imply a fraction of any calculus-differential, integral or calculus of variations.

L'Hospital questioned Leibniz in 1695, "What if n be $\frac{1}{2}$?" Leibniz unexpectedly responded, "...You may see from that, sir, that a quantity like $d^{\frac{1}{2}}xy$ or $d^{1:2}xy$ can be expressed by an infinite series. Despite the fact that infinite series and geometry are not particularly related, infinite series only permits the use of exponents that are positive and negative integers and does not yet know how to employ fractional exponents...". Leibniz had a special insight into the unknowable, as do other outstanding mathematicians. He stumbled onto fractional derivatives and realized that his work will soon lead to great things. He had no idea what they would mean. He continued

in the same letter: “As a result, it follows that $x\sqrt{dx} : x$ will equal $d^{\frac{1}{2}}x$. This appears to be an index from which future useful findings might be formed...”. The insight of Leibniz did not end there. Three years later, he discussed how to use fractional derivatives in Wallis’ infinite product for $\frac{1}{2\pi}$ in a letter to John Wallis. He writes: “...Differential calculus might have been utilised to accomplish this result,...”. It should be clear that Leibniz gave fractional derivatives more than a passing thought; he must have devoted a lot of effort to the subject.

The idea of fractional derivatives was experimented by Euler, another great mathematician. 43 years after Leibniz published his controversial ideas on fractional derivatives, in his dissertation published in 1738, Euler stated: “... when n is a positive integer, and if p should be a function of x , the ratio $d^n p$ to dx^n can always be expressed algebraically, so that if $n = 2$ and $p = x^3$, then $d^2 x^3$ to dx^2 is $6x$ to 1. The question now is what kind of ratio can be created if n is a fraction. It is clear why this situation is challenging, because d^n can be determined by further differentiation if n is a positive integer. But if n is a fraction, then there is no obvious method to do it. However, one might be able to speed up the process with the use of interpolation, which I have already explained in my dissertation...”

The formula for the m^{th} derivative of $y = x^n$, where n is a positive integer, was established by Lacroix and published in his 700-page long book on Calculus in 1819.

$$D^m y = \frac{n!}{(n-m)!} x^{n-m}, \quad (1.1.1)$$

where $m(\leq n)$ is an integer.

He further established the formula for the fractional derivative by replacing the factorial symbol with the gamma function.

$$D^\alpha x^\beta = \frac{\Gamma(\beta + 1)}{\Gamma(\beta - \alpha + 1)} x^{\beta - \alpha}, \quad (1.1.2)$$

where α and β are fractional numbers. In particular, he calculated

$$D^{\frac{1}{2}} x = \frac{\Gamma(2)}{\Gamma(\frac{3}{2})} x^{\frac{1}{2}} = 2\sqrt{\frac{x}{\pi}}. \quad (1.1.3)$$

However, Joseph Liouville (1809–1882), in 1832, explicitly expanded the derivative of integral order n

$$D^n e^{bx} = b^n e^{bx} \quad (1.1.4)$$

to the derivative of arbitrary order β

$$D^\beta e^{bx} = b^\beta e^{bx}. \quad (1.1.5)$$

Liouville arrived at the formula by using the series expansion of a function $f(x)$.

$$D^\beta f(x) = \sum_{m=0}^{\infty} C_m b_m^\beta e^{b_m x}, \quad \text{Re } b_m > 0, \quad (1.1.6)$$

where

$$f(x) = \sum_{n=0}^{\infty} c_n \exp(b_n x), \quad \text{Re } b_n > 0. \quad (1.1.7)$$

Liouville's first fractional derivative formula is given in formula (1.1.6). Whether they are complex, irrational, or derivatives of any order β , it can be applied as a formula.

However, it can only be utilized for functions of the form (1.1.7). In order to extend his first definition, Liouville developed a second definition of a fractional derivative based on the gamma function (1.1.6).

$$\Gamma(\beta)x^{-\beta} = \int_0^{\infty} t^{\beta-1}e^{-xt}dt, \quad \beta > 0, \quad (1.1.8)$$

$$D^{\alpha}x^{-\beta} = (-1)^{\alpha}\frac{\Gamma(\alpha + \beta)}{\Gamma(\beta)}x^{-\alpha-\beta}, \quad \beta > 0. \quad (1.1.9)$$

This is called Liouville's second definition of fractional derivative. He solved problems in potential theory by using both of his definitions. Though his second definition only applies to rational functions, Liouville's first definition is limited to a certain class of functions having the form (1.1.7). It was determined that neither of his definitions was appropriate for a large class of functions. As stated in (1.1.9), the derivative of a constant function ($\beta = 0$) is zero because (1.1.2) provides a non zero value for the fractional derivative of a constant function ($\beta = 0$) in the form

$$D^{\alpha}1 = \frac{x^{\alpha}}{\Gamma(1 - \alpha)} \neq 0. \quad (1.1.10)$$

The following integral representations of $f(x)$ and its derivatives were discovered by Fourier in 1822.

$$f(x) = \frac{1}{2\pi} \int_{-\infty}^{\infty} f(\zeta)d\zeta \int_{-\infty}^{\infty} \text{cost}(x - \zeta)dt \quad (1.1.11)$$

and

$$D^n f(x) = \frac{1}{2\pi} \int_{-\infty}^{\infty} f(\zeta)d\zeta \int_{-\infty}^{\infty} t^n \text{cost}\left\{(x - \zeta) + \frac{n\pi}{2}\right\}dt. \quad (1.1.12)$$

Formally, replacing arbitrary real α with integer n produces

$$D^\alpha f(x) = \frac{1}{2\pi} \int_{-\infty}^{\infty} f(\zeta) d\zeta \int_{-\infty}^{\infty} t^\alpha \text{cost}\left\{(x - \zeta) + \frac{\alpha\pi}{2}\right\} dt. \quad (1.1.13)$$

For fractional derivatives, Peacock (1833) supported the Liouville definitions whereas other mathematicians chose the Lacroix formula (1.1.2). The two definitions of a fractional derivative did not agree with one another as a result. Despite significant subsequent advancements of fractional calculus, this controversy has rarely been resolved.

Greer (1858–1859) developed formulas in the form of (1.1.4) for the fractional derivatives of trigonometric functions.

$$\begin{aligned} D^\alpha e^{iax} &= i^\alpha a^\alpha e^{iax} = i^\alpha a^\alpha (\cos ax + i \sin ax) \\ &= a^\alpha \left(\cos \frac{\pi\alpha}{2} + i \sin \frac{\pi\alpha}{2} \right) (\cos ax + i \sin ax) \end{aligned} \quad (1.1.14)$$

The fractional derivatives of trigonometric functions are given by

$$\begin{aligned} D^\alpha (\cos ax) &= a^\alpha \left(\cos \frac{\pi\alpha}{2} \cos ax - \sin \frac{\pi\alpha}{2} \sin ax \right) \\ &= a^\alpha \cos \left(ax + \frac{\pi\alpha}{2} \right), \\ D^\alpha (\sin ax) &= a^\alpha \left(\cos ax \sin \frac{\pi\alpha}{2} + \sin ax \cos \frac{\pi\alpha}{2} \right) \\ &= a^\alpha \sin \left(ax + \frac{\pi\alpha}{2} \right) \end{aligned} \quad (1.1.15)$$

When $\alpha = \frac{1}{2}$ and $a = 1$, Greer's formulas are as follows:

$$\begin{aligned} D^{\frac{1}{2}} \cos x &= \cos \left(x + \frac{\pi}{4} \right), \\ D^{\frac{1}{2}} \sin x &= \sin \left(x + \frac{\pi}{4} \right) \end{aligned} \quad (1.1.16)$$

Similarly, fractional derivatives for hyperbolic functions can be obtained.

For modern mathematicians, Sonin and Letnikov built the basis for the concept of fractional derivatives. Sonin published a paper titled “On Differentiation with Arbitrary Index” in 1869, and Letnikov published four papers on the same topic between 1868 and 1872. Both mathematicians started their work with Cauchy’s integral formula:

$$D^m f(z) = \frac{m!}{2\pi i} \int_c \frac{f(\eta)}{(\eta - z)^{m+1}} d\eta,$$

where “c” denotes a closed contour that rotates once anticlockwise. Sonin and Letnikov were off to a great start since it was permitted to generalize $m!$ both knew about the gamma function and how $m! = \Gamma(m + 1)$ when $m!$ takes on arbitrary values of integers. They were aware that a simple pole would appear in the close circuit’s contour when m was an integer. They understood that instead of a simple pole, they would have a branch cut if m was not an integer. Although Sonin and Letnikov were aware of the problem, they did not suggest a solution. Unfortunately for Sonin and Letnikov, Laurent found the solution twelve years later, in 1884. Despite being an untrained scientist (as stated by Miller and Ross) and not a mathematician, Oliver Heaviside, a genius later in his life, has received the name of “hero”. He published a number of papers on linear functional operators in 1892, and by using unorthodox techniques, he was able to solve a number of engineering problems, including the equation relating to submarine cables and the transmission of electrical currents

in cables. Heaviside operational calculus is a collection of his brilliant approaches, results, and applications. However, his work was viewed with distrust and suspicion during the time he developed it. Because he was unable to provide solid proofs for his work, he became a laughing stock among mathematicians. In 1919, Bromwich set out to rigorously confirm all of Heaviside's work, which he accomplished.

Even though there have been a huge number of new mathematicians throughout this time, it is surprising that only a small number of research papers have been written on the subject of fractional derivatives over the past 82 years. The few "greats" are Thomas J. Osler, Davis Erdelyi, Hardy, Kobler, Littlewood, Love, Riesz, Samko, Sneddon, Weyl, and Al-Bassam. One would think that there would be hundreds, if not thousands, of research articles with all these new mathematicians entering the field. Even Davis claimed this in 1936: "...By 1900, it is reasonable to consider that the formal development of operational procedures had come to a halt. The theory of integral equations was just starting to capture mathematicians' attention and reveal the possibilities of operational methods..." In 82 years, it appears like not a lot of imaginations were being inspired. The year 1974 then arrived, however.

During the final decades of the nineteenth century, Heaviside successfully constructed his operational calculus without using exact mathematical explanations. He first proposed the concept of fractional derivatives in his study of electric transmission lines in 1892.

The research on fractional derivatives really started off in 1974. The first international conference on fractional calculus was conducted in 1974. The University of New Haven functioned as the venue, Askey, Mikolas, and many other mathematicians, including our own Dr. Thomas J. Osler attended along with some of the mathematicians named above. “Great explosion” was really the title above. Many of those previously listed were inspired by the 1974 conference. There have been roughly 400 papers on fractional derivatives published in just a little more than five years, which is more than since mathematics began.

Then came the 1980’s. Ten years later, in 1984, there was a second international conference on fractional calculus. It took place in Glasgow, Scotland, at the University of Strathclyde. It seems that mathematicians had jumped on the proverbial bandwagon from all around the world. Mathematicians from Japan, the Soviet Union, England, India, Canada, Venezuela, Scotland, and a host of smaller nations all have written on the topic. Some of these mathematicians that wrote on the fractional calculus include Saigo(1980), Owa(1990) and Nishimoto (1984, 1987, 1989, 1991) who wrote a four-volume set on applications. The three mathematicians mentioned above are from Japan. Soviet authors Marichev and Kilbas published an encyclopaedia on the topic in 1987. It also included applications. In the 1980s, Indian authors Rauna and Saxena published a number of publications. In their research on fractional derivatives, Srivastava from Canada, Kalla from Venezuela, and McBride from Scotland

all achieved a great deal. In the 1980s and 1990s, even our own Dr. Thomas Osler co-authored or published 10 publications on the topic.

It might be important to note that Abel's (1801–1829) solution of an integral equation arising from the formulation of the tautochronous problem is the first known application of fractional calculus. This problem includes finding the shape of a frictionless plane curve via the origin in a vertical plane in order to establish the shape that a particle of mass m can fall along in a time that is independent of the starting position. The concept that the derivative of a constant is not always equal to zero is the foundation for the solution to the Abel problem.

The number of mathematicians in the world today would lead one to believe that there would be countless volumes of published publications on the topic. Unfortunately, the majority of mathematicians are unaware of the possibilities and uses of fractional calculus. Many would not even know where to start if given a simple problem. Even worse is the fact many have only heard of fractional derivatives in passing and some not at all.

Various investigations on fractional calculus were published in engineering literature in the second half of the 20th century. Recent advancements in fractional calculus is developed by contemporary applications in differential and integral equations, viscoelasticity, physics, fluid mechanics, mathematics, biology, signal processing, and electrochemistry. There is no doubt that fractional calculus has been developed into

a wonderful new mathematical analysis for dealing with a wide range of problems in mathematics, science, and engineering.

1.1.1 Fractional derivatives and integrals

The idea of Fractional derivatives is a powerful tool for analysing the memory and hereditary qualities of many materials and processes in nature. The psychology and life sciences are new applications fields for fractional calculus, and it is used to define the time variation of people's emotions. In addition to the applications listed above, fractional calculus is used in a variety of domains with mathematics. For example, fractional operators can be used to investigate certain special functions analytically.

In the literature, there are several different definitions of fractional derivatives and integrals. They include the Riemann-Liouville, Caputo, Hadamard, Granwald-Letnikov, Erdelyi-Kober, Marchaud and Riesz-Feller fractional derivatives and integrals. Except in a few circumstances, these concepts are not identical in general. B. Riemann and J. Liouville are responsible for the most widely definitions of fractional derivative and integral, which are known as the Riemann-Liouville fractional derivative and integral. However, in some circumstances, the Riemann-Liouville derivative may yield the Caputo fractional derivative, which was developed by Caputo and adopted by Caputo and Mainardi. Among all these, the following are two most widely used definitions:

1. The Riemann-Liouville fractional derivative of $y(x)$ of order β is given by

$$D^\beta y(x) = \begin{cases} \frac{1}{\Gamma(n-\beta)} \left(\frac{d}{dx}\right)^n \int_0^x \frac{y(t)}{(x-t)^{\beta-n+1}} dt, & 0 \leq n-1 < \beta < n, \\ \left(\frac{d}{dx}\right)^n y(x), & \beta = n, \quad n \in \mathbb{N}. \end{cases}$$

The Riemann-Liouville fractional integral of $f(x)$ of order β is given by

$$I^\beta f(x) = \begin{cases} \frac{1}{\Gamma(\beta)} \int_0^x (x-t)^{\beta-1} f(t) dt, & x > 0, \beta > 0, \\ f(x), & \beta = 0. \end{cases}$$

2. The left sided Caputo fractional derivative $D^\beta y(t)$ or $y^{(\beta)}$ for $y \in L_1[a, b]$, is originally defined as follows.

$$D^\beta y(t) = I^{m-\beta} y^{(m)}(t) = \frac{1}{\Gamma(m-\beta)} \int_a^t (t-x)^{m-\beta-1} y^{(m)}(x) dx,$$

where $m = [a]$ is the smallest integer greater than or equal to m and $\beta \in \mathbb{R}^+$.

The Caputo fractional derivative satisfies the following properties for $f \in L_1[0, 1]$, $\beta, \gamma \geq 0$ and $m = [\beta] + 1$:

1. $D^\beta I^\beta f(t) = f(t)$.

2. $I^\beta D^\beta f(t) = f(t) - \sum_{i=0}^{m-1} f^{(i)}(0^+) \left(\frac{t^i}{i!}\right)$.

3. If f is continuous then $D^\beta D^\gamma f(x) = D^{\beta+\gamma} f(t)$, $t > 0$.

4. $D^\beta C = 0$, where C is constant.

5. $D^\beta x^\alpha = \begin{cases} 0, & \alpha < \beta, \alpha \in 0, 1, 2, \dots, \\ \frac{\alpha(\alpha-1)}{\alpha(\alpha-\beta+1)} t^{\alpha-\beta}, & \text{otherwise.} \end{cases}$

$$6. D^\beta \left(\sum_{j=0}^n C_j f_j(n) \right) = \sum_{j=0}^n C_j D^\beta f_j(t), \quad \text{where } C_1, C_2, \dots, C_n \text{ are constants.}$$

On the other hand, Weyl(1917) introduced the Weyl fractional integral of order β by

$${}_x w_\infty^{-\beta} f(x) = \frac{1}{\Gamma(\beta)} \int_x^\infty (t-x)^{\beta-1} f(t) dt, \quad \text{Re}\beta > 0. \quad (1.1.17)$$

The main difference between this definition and the Riemann-Liouville definition is the limitation of integration, with the kernel in this definition being $(t-x)^{\beta-1}$.

The Weyl fractional derivative of f of order β is thus defined by

$$W^\beta f(x) = E^n \left[\frac{1}{\Gamma(n-\beta)} \int_x^\infty (t-x)^{n-\beta-1} f(t) dt \right]. \quad (1.1.18)$$

Here $\beta > 0$ and n is the smallest integer greater than β .

Grunwald(1867) introduced the concept of fractional derivative as the limit of a sum given by

$$D^\beta f(x) = \lim_{h \rightarrow 0} \frac{1}{h^\beta} \sum_{r=0}^n (-1)^r \frac{\Gamma(\beta+1) f(x-rh)}{\Gamma(r+1)\Gamma(\beta-r+1)}. \quad (1.1.19)$$

In contrast, Marchaud (1927) developed the fractional derivative of any order β in the form

$$D^\beta f(x) = \frac{f(x)}{\Gamma(1-\beta)x^\beta} + \frac{\beta}{\Gamma(1-\beta)} \int_0^x \frac{f(x)-f(t)}{(x-t)^{\beta+1}} dt, \quad (1.1.20)$$

where $0 < \beta < 1$.

Many researchers have pointed out in recent decades that fractional derivatives and integrals are particularly suited to describing the properties of various real materials, such as polymers [9], memory and hereditary properties [70], optimal control

problems [3], signal process [19], fluid mechanics [40], pharmacokinetics [64], diffusion processes [24].

Fractional calculus has a long and rich history but was unknown to applied scientists until recently. This is due to its inherent difficulty, the evident self-adequacy of classical calculus, and the lack of a meaningful geometric or physical interpretation for fractional derivatives. Physical and geometric interpretations for physical operators have been attempted on several occasions. These interpretations, however, are limited to a very few particular fractional derivatives and integrals in the context of genetic effects and self-similarity. As a result, its applications in different fields of engineering and research have been postponed.

1.2 Fractional differential equations

Fractional differential equations have become more significant in modelling the unique dynamics of many processes associated to complex systems across a wide range of scientific and engineering fields. However, even the most valuable literature on fractional derivatives and integrals lacks good general procedures for solving them. Orthogonal wavelet bases have recently gained popularity for numerical solutions of differential equations because of their useful properties, including their ability to identify singularities, orthogonality, flexibility to represent a function at different levels of resolution, and compact support.

On the other hand, the most of fractional differential equations lack analytical solutions. Because these equations have so many various applications, there has been a lot of interest in creating numerical methods to solve fractional different equations. Variational iteration method [73], Adomian decomposition method [44], Homotopy analysis method [16, 43], Homotopy perturbation method [31, 35] are among them.

In addition to these numerical techniques, several researchers have investigated a new numerical method based on wavelets for analysing problems of high computational complexity, proving that wavelets are effective tools for exploring novel approaches in fractional differential equations.

For many researchers in various fields of science and technology, fractional differential equations have been the focus of interest in recent years. As a result, finding solutions to fractional differential equations is an essential part of scientific research.

There have been several methods for solving fractional differential equations with variable coefficients. These types of problems have been studied by many authors using different methods [10, 25].

To solve fractional differential equations, operational matrices of fractional order integrations for Haar wavelets [71, 53], Chebyshev wavelets [23, 11], Second kind Chebyshev wavelets [66], Legendre wavelets [12], Bernoulli wavelets [34, 54], Ultra spherical wavelets [1, 18], Third kind Chebyshev wavelets [72], CAS wavelets [67] and Euler wavelets [62, 69] have recently been proposed.

1.3 Integral transforms

The development of integral transforms of scientific problem-solving can be traced back to P.S. Laplace's (1749-1827) work on probability theory in the 1780s as well as to J.B. Fourier's (1768-1830) dissertation "La Theorie Analytique de La Chaleur" published in 1822 [15]. Researchers have been interested in the creation and development of new integral transforms with various modifications since that time. There has been a lot of interest in developing integral transforms for the solutions of fractional differential equations because of the increasing applications. The most effective mathematical methods for solving differential equations, partial differential equations, integro-differential equations, partial integro-differential equations, delay differential equations and population growth problems are integral transforms. In many sectors of science and engineering, integral transformations are employed. Integral transforms are commonly employed to solve fractional order differential equations, and numerous studies have been conducted on the theory and applications of the Laplace, Fourier and Mellin transforms. The Laplace transform is the most often used integral transform with an exponential type kernel. In engineering and applied scientific applications, the Laplace transform has demonstrated its dominance.

Fractional integral transforms have recently been proposed as generalization of classical integral transforms. They are used to solve fractional differential equations in science and engineering. The fractional fourier transform, for instance, can be used

to analyze optical difficulties.

1.4 Wavelets

Wavelets trace back to Alfred Haar's construction of an orthonormal system of functions on the unit interval $[0,1]$ in 1910, which resulted in the development of a collection of rectangular basis functions [58]. In the past, J. Morlet, a French geophysical engineer, and Grossmen first explicitly established the idea of wavelets at the beginning of the 1980s as a family of functions created by translation and dilation of a single function known as the Mother wavelet [45, 55]. They used the name *ondelette*, which means small wave in French. The mathematical analysis of wavelets by Stromberg, Grossmen, Morlet and Meyer has led to the present growth of wavelet research. Soon, it was translated to English as "wavelet" by changing the word "ondo" to "wave". The Fourier series models a signal's frequency, but it does not adequately model its localised properties, which led to the discovery of wavelets. This is so because the sine and cosine functions, which serve as the foundation of the Fourier series, are constantly repeating periodic waves.

Because of the wavelet theory's extensive mathematical capability and various scientific and engineering applications, it has attracted a significant lot of interest from scientists work in a wide range of field. In many scientific and engineering gatherings nowadays, "wavelets" has been a hot topic of discussion. Recently, mathematical

scientists across fields have paid a lot of attention to the topic of wavelet analysis. Two very simple procedures, binary dilations and integral translations, are used to describe the wavelet series in terms of a single function, referred to as a “wavelet”. The integral wavelet transform (IWT) is defined as the convolution with respect to the dilation of the reflection of some function, called a “basic wavelet”. There are integral wavelet transforms (IWT) and wavelet series (WS), which are comparable Fourier analysis. WS and IWT are closely related in wavelet analysis. The coefficients for the wavelet series representation of a function on the real line are determined by the IWT of that function when it is evaluated at specific locations in the time-scale domain. As the polynomial spline functions are the simplest functions for both computational and implementation purposes, they are most attractive for analyzing and constructing wavelets.

Wavelets are seen in different ways by different people. Some see them as a new basis for describing functions, while others see them as a method for time-frequency analysis. Since the idea of “wavelets” is a versatile tool with extremely rich mathematical content and a lot of application potential, of course all of them are correct. It is surely too early to make a comprehensive presentation, though, as this topic is still in its development.

Wavelets can be used in signal analysis for a range of tasks, including wave form segmentation and demonstration, diagnostics, time frequency analysis, geophysical

signal processing, statistical analysis, pattern recognition, and fast algorithms with simple implementation. The wavelet analysis may be a useful technique for solving a variety of problems in engineering, physics, and image processing. Wavelet technique is specifically used in scanning and disease diagnostics to help doctors in performing their duties precisely in this sensitive field of human care. In the field of telecommunications, it can also help in encoding audio and video signals. In addition, there are additional helpful applications that can effectively help intelligence agencies in identifying even the tiniest details of human bodies for security reasons, in the event of terrorist attacks, the crash of an aeroplane or ship, or for other human verification uses. For example, the US Federal Bureau of Investigation employs wavelet technique to identify and verify the fingerprints of millions of people. Mathematical wavelet technology is predicted to have hundreds of uses in the future, with a primary focus on healthcare and human welfare to produce the greatest results possible [28, 61, 41, 29]. Wave propagation, the detection of aircraft and submarines, data compression, image processing, pattern recognition, computer graphics, improvements in CAT scans, and other improvements in medical technology are some of the contemporary applications of the wavelet method. The wavelet method is an innovative approach for solving difficult problems in engineering, physics, and mathematics. Furthermore, wavelet techniques have been applied to create precise and fast algorithms for solving fractional order integral and differential equations, particularly those whose solutions are

extremely localized in terms of scale and position. Even if wavelets are becoming popular in these areas, researchers are always looking into new possibilities.

We can break down a complex function using wavelet techniques and analyze each component separately. This property, together with the fast wavelet algorithm, makes these techniques particularly appealing for analysis and synthesis. To more accurately represent non-stationary signals, wavelet analysis uses bases that are localised in time frequency as compared to Fourier-based analyses, which use global (non-local) sine and cosine functions as bases. As a result, a wavelet representation is substantially more compact and easier to implement. A function can be represented as a finite sum of components at several resolutions using the powerful multiresolution analysis, enabling each component to be processed adaptively depending on the application's objectives. The main advantage of wavelet analysis is its capacity to compactly express functions at various levels of resolution. The unknown solution can be represented by wavelets with different resolutions while solving partial differential equations numerically, yielding a multigrid representation. Using wavelet-based thresholding techniques, the dense matrix produced by an integral operator can be sparsified to achieve any level of solution accuracy. Wavelets enable accurate description of a wide range of operators and functions. A defining feature of wavelets is their ability to convert the given differential and integral equations into a set of algebraic equations, either linear or nonlinear, that can be solved numerically. This

section aims to present an overview of wavelets and to provide a detailed description of several wavelet techniques.

In order to address various problems with dynamic systems, orthogonal functions and polynomial series have drawn a lot of attention. The main feature of this method is that it greatly simplifies problems by converting them into ones that can be solved by solving a set of algebraic equations. In this thesis, particular attention has been put on applications of Euler wavelets, Bernoulli wavelets, and Chebyshev wavelets.

A family of two parameter functions called $\psi_{a,b}(t)$ is constructed by dilation and translation of a single function called a wavelet, $\psi(t)$, and is defined as follows.

$$\psi_{a,b}(x) = \frac{1}{\sqrt{|a|}}\psi\left(\frac{x-b}{a}\right), \quad a, b \in \mathbb{R}, a \neq 0, \quad (1.4.1)$$

where a is the dilation parameter and b is the translation parameter. Higher frequencies are represented by $\psi_{a,b}$, which is a compressed form of the mother wavelet if $|a| < 1$. On the other hand, lower frequencies are represented by the wavelet $\psi_{a,b}$ for $|a| > 1$. Wavelets are defined as follows more precisely:

Definition 1.4.1. A function $\psi \in L^2(\mathbb{R})$ is admissible as a wavelet if and only if

$$A_\psi = \int_{-\infty}^{\infty} \frac{|\hat{\psi}(\omega)|^2}{|\omega|} d\omega < \infty, \quad (1.4.2)$$

where $\hat{\psi}(\omega)$ is the Fourier transform of ψ .

In order to satisfy the admissibility requirement, A_ψ must be finite, which means

that $\hat{\psi}(0) = 0$, or the mean value of ψ , should vanish;

$$\int_{-\infty}^{\infty} \psi(s) ds = 0 \quad (1.4.3)$$

For a large number of practical applications, continuous wavelets are not useful. They do not serve as a basis, in particular. In order to discretize wavelets, the positive constants $a_0 > 1$, $b_0 > 0$ are fixed, and $a = a_0^{-k}$, $b = nb_0 a_0^{-k}$ are set where $n, k \in \mathbb{N}$. As a result, the following family of discrete wavelets is defined as

$$\psi_{k,n}(x) = |a_0|^{\frac{1}{2}} \psi(a_0^k x - nb_0). \quad (1.4.4)$$

Usually a_0 is chosen to be 2 and $b = 1$. For wavelet theory, Ingrid Daubechies gave strong foundations. By constructing an orthonormal wavelet system with compact support in [40], she made a major breakthrough.

In contrast to harmonic waves, wavelets must terminate at zero as $x \rightarrow \pm\infty$. Small waves $\psi(x)$ that oscillate at least a few times are what are meant by wavelets. The wavelets that die out to identical zero after a few oscillations on a finite interval, i.e., outside the interval, are those that have $\psi(x) = 0$. The “support” or “compact support” of the specified (basic) wavelet $\psi(x)$ is a special interval that is used in wavelet analysis. The reason we use the term “basic wavelet” is because it will have two parameters, scale a and translation b , which together form the “family” of wavelets $\psi(\frac{x-b}{a})$. Basic wavelets are built using the “building blocks” or “scaling functions” $\phi(x)$ that are associated with them. The scaling relation, often known as

the “recurrence relation” is the equation that governs the latter. In wavelet analysis, a single sequence of scaling functions is often employed to produce an approximation of the input signal. A new series of the associated wavelets is added to the first to further improve it. The signal is satisfactorily represented as a result. Finding scaling functions leads to the easy computation of building the corresponding basic wavelets. The scaling functions, or “building blocks” are of utmost importance while studying wavelet analysis in this chapter.

Now, we examine at the space $L^2(\mathbb{R})$ of measurable functions f , defined on the real line \mathbb{R} , satisfying

$$\int_{-\infty}^{\infty} |f(t)|^2 dt \leq \infty.$$

We actually search for such “waves” that produce $L^2(\mathbb{R})$; these waves should degenerate to zero at $\pm\infty$, and for all kinds of reasons, the decay should occur very quickly. That is, we look for small waves, or “wavelets”, to generate $L^2(\mathbb{R})$. For this purpose, we prefer a single function ψ that generates all of $L^2(\mathbb{R})$. Since, ψ is very fast decay, to cover whole real line, we shift ψ along \mathbb{R} . For computational efficiency, we have used integral powers of 2 for frequency partitioning. That is, consider the small waves

$$\psi(2^j t - k), \quad j, k \in \mathbb{Z}.$$

$\psi(2^j t - k)$ is obtained from a single wavelet function $\psi(t)$ by a binary dilation (dilation by 2^j) and a dyadic translation (of $\frac{k}{2^j}$). Any wavelet function $\psi \in L^2(\mathbb{R})$ has two

arguments as $\psi_{j,k}$ and it is defined by

$$\psi_{j,k}(t) = 2^{\frac{j}{2}}\psi(2^j t - k), \quad j, k \in \mathbb{Z},$$

where the quantity $2^{\frac{j}{2}}$ is for normality.

Definition 1.4.2. When the family $\psi_{j,k}$ is an orthonormal basis of $L^2(\mathbb{R})$, the wavelet $\psi \in L^2(\mathbb{R})$ is referred to as an orthogonal wavelet; in other words,

$$\langle \psi_{j,k}, \psi_{l,m} \rangle = \delta_{j,l} \delta_{k,m}, \quad j, k, l, m \in \mathbb{Z}.$$

Definition 1.4.3. The term “semi-orthogonal wavelet” refers to a wavelet $\psi \in L^2(\mathbb{R})$ if the family $\psi_{j,k}$ satisfies the requirements given below.

$$\langle \psi_{j,k}, \psi_{l,m} \rangle = 0, j \neq l, \quad j, k, l, m \in \mathbb{Z}.$$

1.4.1 Multiresolution Analysis

In 1988 [14], I. Daubechies introduced the first orthonormal bases of compactly supported wavelets. He used multiresolution analysis to prove that for any non negative integer n , there exists an orthogonal wavelet with compact supports that contains all derivatives up to order n .

Mallat [49] and Meyer [50] proposed the concept of multiresolution analysis. The fundamental concept of MRA is to consider of a function as a set of successive approximations, each of which is a smoother version of the original. As a formal way to generate orthogonal wavelet bases using a definite set of rules, multiresolution analysis is named after the consecutive approximations that correspond to different

resolutions. Additionally, it enables the development of “functions” and “scaling filters” which are then used to create wavelets and fast numerical algorithms. It is a useful mathematical framework that consists of a sequence of \mathbb{R} function spaces to decompose a signal or image into components of various scales.

A direct sum decomposition of $L^2(\mathbb{R})$ is generated by any wavelet, whether it is orthogonal or semi-orthogonal. Let's consider the closed subspaces for each $j \in \mathbb{Z}$

$$u_j = \dots \oplus w_{j-2} \oplus w_{j-1}, \quad j \in \mathbb{Z}$$

of $L^2(\mathbb{R})$. A set of subspaces $u_{j \in \mathbb{Z}}$ is said to be MRA of $L^2(\mathbb{R})$ if it possess the following properties:

$$1. u_j \subset u_{j+1}, \quad \forall j \in \mathbb{Z}.$$

$$2. \bigcup_{j \in \mathbb{Z}} u_j \text{ is dense in } L^2(\mathbb{R}).$$

$$3. \bigcap_{j \in \mathbb{Z}} u_j = \{0\}.$$

$$4. u_{j+1} = u_j \oplus w_j.$$

$$5. f(t) \in u_j \Leftrightarrow f(2t) \in u_{j+1}, \quad j \in \mathbb{Z}.$$

The nested sequence of subspaces $u_{j \in (\mathbb{Z})}$ effectively covers $L^2(\mathbb{R})$ according to properties (2) through (5). That is to say, a function belonging to at least one of the subspaces u_j can be used to approximate any square integrable function as closely as needed. If a function $\phi \in L^2(\mathbb{R})$ provides the nested sequence of subspaces u_j and

satisfies the dilation equation, which is

$$\phi(x) = \sum_j p_j \phi(ax - j),$$

then it is referred to as a scaling function, where $p_j \in (L^2)$ and a is any rational number.

Since $u_j \subset u_{j+1}$, each scale j has a unique orthogonal complementary subspace w_j of u_j in u_{j+1} . The equation $\psi_{j,k} = \psi(2^j t - k)$, where $\psi \in L^2$ is referred to as the wavelet, results in this subspace, u_j , which is referred to as the wavelet subspace.

From the above discussion, these results follow easily

$$1. u_{j1} \cap u_{j2} = u_{j2}, \quad j1 > j2.$$

$$2. w_{j1} \cap w_{j2} = 0, \quad j1 \neq j2.$$

$$3. u_{j1} \cap w_{j2} = 0, \quad j1 \leq j2.$$

1.4.2 Advantages of wavelet theory

1. Wavelets' greatest advantage is their ability to provide simultaneous localization in the time and frequency domains.
2. Often, it can de-noise or compress a signal without appreciably degrading it.
3. Data features including trends, breakdown points, discontinuities in higher derivatives, and self similarity can be revealed via wavelet theory.
4. A signal can be divided down into its component wavelets using a wavelet transform.

5. When compared to the Fourier transform, the great achievement of wavelet theory is the frequent ability to obtain a good approximation of the given function f by utilising only a few coefficients.
6. The ability to distinguish the fine details in a signal is a major benefit of wavelets. While extremely big wavelets can be used to identify coarse details in a signal, very small wavelets can be used to isolate very fine details in a signal.
7. The speedy wavelet transform is the next advantage of wavelets.

1.4.3 Comparison of wavelet transform with Fourier transform

1. Wavelet and Fourier transforms are mainly different in the domains of time and frequency. Wavelets are well localized in time and frequency, while Fourier application in such domains is standardized in localizing them. Both have positive effects on localized time and frequency, but wavelet exhibits greater representation according to wavelet multi-resolution analysis [28, 61, 41].
2. The Fourier transform is effective in some areas outside of traditional signal processing. The mathematical design of wavelets, however, is more broader than the Fourier transform, and to be more specific, the mathematics of wavelets includes the Fourier transform [28, 61].

3. For the analysis of a collection of stationary signals, the Fourier transform is an effective tool (a signal with no change in the properties). The Fourier transform is used, for example, to process sine and cosine (sinusoid signals). However, the application of Fourier is less effective for the analysis of non-stationary signals (where the change in properties occurs). The wavelet transform, on the other hand, works with both stationary and non-stationary signals [28, 61].

4. The Fourier transform uses a single scaled function $\psi(x)$, however the wavelet transform has the capacity to move the function and generate the two-parameter functions $\psi_{a,b}(x)$ defined in [61, 41].

Chapter 2

Numerical solutions of fractional differential equations using Aboodh Transform method and a generalized fractional integral transform with exponential type kernel

2.1 Introduction

This chapter gives a brief overview of the Aboodh transform method and a generalized fractional integral transform with an exponential type kernel for solving fractional differential equations. Integral transforms are important to solve real problems. Appropriate choice of integral transforms helps to convert differential equations in terms of an algebraic equation that can be solved easily. Aboodh transform which was recently introduced by Khalid Aboodh is a new transform derived from the

Fourier transform and similar to Laplace transform. Aboodh transform is defined for a function of exponential order in the time domain $t \geq 0$. Typically, Fourier, Laplace, Elzaki and Sumudu transforms are the essential mathematical tools for solving differential equations. The generalized fractional integral transform with exponential type kernel is a very powerful tool because it allows us to choose whether to use the generalized fractional integral transform with exponential type kernel or any other existing or non-existing fractional integral transforms, depending on our needs and problem situation. The existence of many fractional integral transforms is ensured by sufficient conditions for the existence of the generalized fractional integral transform with exponential type kernel. The generalized fractional integral transform with exponential type kernel is an effective and beneficial approach for solving fractional differential equations.

2.2 Aboodh transform method

Definition 2.2.1.

$$\text{Let } A = \{f(t) : \exists M, k_1, k_2 > 0, |f(t)| < Me^{-vt}\}, \quad (2.2.1)$$

where M is finite and k_1 and k_2 may be finite or infinite. The Aboodh transform for a function $f(t)$ belonging to the class A is defined as

$$A[f(t)](v) = K(v) = \frac{1}{v} \int_0^\infty f(t)e^{-vt} dt, \quad t \geq 0, k_1 \leq v \leq k_2 \quad (2.2.2)$$

In this transform, the variable v is used to factor the variable t in the function f 's argument. This transform is more closely related to the Laplace transform.

Definition 2.2.2. The inverse Aboodh transform of a function $f(t)$ denoted by $A[f(t)] = k(v)$ then

$$f(t) = A^{-1}[k(v)]. \quad (2.2.3)$$

Definition 2.2.3. Two parameters Mittag-Leffler function is defined by

$$E_{\alpha,\beta} = \sum_{k=0}^{\infty} \frac{z^k}{\Gamma(\alpha k + \beta)}, \quad (z, \alpha, \beta \in \mathbb{C}, \text{Re}(\alpha) > 0). \quad (2.2.4)$$

Definition 2.2.4. The simplest wright function is defined by

$$\phi(\alpha, \beta; z) = \sum_{k=0}^{\infty} \frac{1}{\Gamma(\alpha k + \beta)} \frac{z^k}{k!}, \quad (z, \alpha, \beta \in \mathbb{C}). \quad (2.2.5)$$

2.2.1 Properties of Aboodh transform

1. $A[f^{(n)}(t)](v) = v^n k(v) - \sum_{k=0}^{n-1} \frac{f^{(k)}(0)}{v^{2-n+k}}$.
2. $A[t^n](v) = \frac{n!}{v^{n+2}}$.
3. $A[x^\beta] = \frac{\Gamma(\beta + 1)}{v^{\beta+2}}$.
4. $A[f^{(n)}(x)] = v^n k(v) - v^{n-2} f(0) - v^{n-3} f^{(1)}(0) - \dots - \frac{f^{(n-1)}(0)}{v}$.
5. $A\left[\int_0^t f(t) dt\right] = \frac{k(v)}{v}$.
6. $A\left[\int_0^x f(x-t)g(t) dt\right] = vk(v)g(v)$.
7. The binomial coefficients are defined by $\binom{\lambda}{n} = \frac{\lambda!}{\lambda!(\lambda-n)!}$ where λ and n are integers.

Note that $0! = 1$, then

$$\begin{aligned} \binom{\lambda}{0} = 1, \binom{\lambda}{\lambda} = 1 \quad \text{and} \quad (1-z)^{-\lambda} &= \sum_{r=0}^{\infty} \frac{(\lambda_r)}{r!} z^r \\ &= \sum_{r=0}^{\infty} \binom{\lambda+r-1}{r} z^r. \end{aligned}$$

Lemma 2.2.1. *Aboodh transformation of Riemann-Liouville fractional integral operator of order $\alpha > 0$ can be written in the form*

$$A[J^\alpha f(x)] = \frac{k(v)}{v^\alpha} \quad (2.2.6)$$

Proof. Aboodh transform of Riemann-Liouville fractional integral operator $\alpha > 0$ is

$$\begin{aligned} A[J^\alpha f(x)] &= A\left[\frac{1}{\Gamma(\alpha)} \int_0^x (x-a)^{(\alpha-1)} f(t) dt\right]. \\ &= \frac{1}{\Gamma(\alpha)} vk(v)g(v) \\ &= \frac{k(v)}{v^\alpha} \end{aligned}$$

$$\text{where } g(v) = A[x^{\alpha-1}] = \frac{\Gamma(\alpha)}{v^{\alpha+1}}.$$

□

Lemma 2.2.2. *Aboodh transformation of Caputo fractional derivative of*

$$\alpha > 0, m - 1 < \alpha \leq m, m \in \mathbb{N}$$

can be written in the form

$$A[D^\alpha f(x)] = \frac{1}{v^{m-\alpha}} [v^m K(v) - v^{m-2} f(0) - v^{m-3} f^{(1)}(0) - \dots - \frac{f^{(m-1)}(0)}{v}]. \quad (2.2.7)$$

Proof.

$$A[D^\alpha f(x)] = A[J^{m-\alpha} f^{(m)}(x)] = \frac{A[f^{(m)}(x)]}{v^{m-\alpha}} \quad (2.2.8)$$

By use of Property (4), the desired result follows. □

2.2.2 Solutions of Fractional Differential Equations using Aboodh transform method

In this section, we apply the Aboodh transform of the fractional derivative and the expansion coefficients of binomial series to derive solutions of some families of

fractional differential equations. Throughout this section, we let $y(t)$ be such that for some value of the parameter v , the Aboodh transform $A[f(t)](v)$ converges.

Theorem 2.2.3. *Let $0 < \alpha \leq 1$ and $b \in \mathbb{R}$. The solution to the fractional differential equation*

$$y^\alpha(t) - by(t) = 0 \quad (2.2.9)$$

with the initial condition $y(0) = c_0$ is

$$y(t) = c_0 \sum_{k=0}^{\infty} \frac{(bt^\alpha)^k}{\Gamma(\alpha k + 1)} = E_{\alpha,1}(bt^\alpha). \quad (2.2.10)$$

Proof. Applying Aboodh transform to (2.2.9),

$$[v^\alpha k(v) - \frac{y(0)}{v^{2-\alpha}}] - bk(v) = 0$$

$$k(v)[v^\alpha - b] - \frac{c_0}{v^{2-\alpha}} = 0$$

$$k(v)[v^\alpha - b] = c_0 v^{\alpha-2}$$

$$k(v) = c_0 \sum_{k=0}^{\infty} b^k v^{-\alpha k - 2}.$$

Applying inverse Aboodh transform,

$$\begin{aligned} &= c_0 \sum_{k=0}^{\infty} \frac{b^k t^{\alpha k}}{\Gamma(\alpha k + 1)} \\ y(t) &= c_0 \sum_{k=0}^{\infty} \frac{(bt^\alpha)^k}{\Gamma(\alpha k + 1)} \\ &= c_0 E_{\alpha,1}(bt^\alpha). \end{aligned}$$

□

Theorem 2.2.4. *Let $1 < \alpha < 2$ and $a, b \in \mathbb{R}$. The solution to the fractional differential equation*

$$y''(t) + ay^{(\alpha)}(t) + by(t) = 0 \quad (2.2.11)$$

with the initial conditions $y(0) = c_0$ and $y'(0) = c_1$ is

$$\begin{aligned}
y(t) &= c_0 \sum_{k=0}^{\infty} \frac{(-b)^k t^{(2k)}}{k!} \sum_{r=0}^{\infty} \frac{\Gamma(r+k+1)(-at^{(2-\alpha)})^r}{\Gamma[(2-\alpha)r+2k+1]r!} \\
&+ c_1 \sum_{k=0}^{\infty} \frac{(-b)^k t^{(2k+1)}}{k!} \sum_{r=0}^{\infty} \frac{\Gamma(r+k+1)(-at^{(2-\alpha)})^r}{\Gamma[(2-\alpha)r+2k+2]r!} \\
&+ ac_0 \sum_{k=0}^{\infty} \frac{(-b)^k t^{(2k-\alpha+2)}}{k!} \sum_{r=0}^{\infty} \frac{\Gamma(r+k+1)(-at^{(2-\alpha)})^r}{\Gamma[(2-\alpha)r+2k+3]r!} \\
&+ ac_1 \sum_{k=0}^{\infty} \frac{(-b)^k t^{(2k-\alpha+3)}}{k!} \sum_{r=0}^{\infty} \frac{\Gamma(r+k+1)(-at^{(2-\alpha)})^r}{\Gamma[(2-\alpha)r+2k+4]r!}
\end{aligned} \tag{2.2.12}$$

Proof. Applying Aboodh transform to equation (2.2.11),

$$\begin{aligned}
[v^2 k(v) - y(0) - \frac{y'(0)}{v}] + a[v^\alpha k(v) - \frac{y(0)}{v^{2-\alpha}} - \frac{y'(0)}{v^{3-\alpha}}] + bk(v) &= 0 \\
k(v)[v^2 + av^\alpha + b] - c_0 - \frac{c_1}{v} - \frac{ac_0}{v^{2-\alpha}} - \frac{ac_1}{v^{3-\alpha}} &= 0
\end{aligned}$$

$$k(v) = \frac{c_0 + c_1 v^{-1} + ac_0 v^{\alpha-2} + ac_1 v^{\alpha-3}}{v^2 + av^\alpha + b} \tag{2.2.13}$$

$$\begin{aligned}
\text{Now } \frac{1}{v^2 + av^\alpha + b} &= \frac{1}{(v^2 + av^\alpha)[1 + \frac{b}{v^2 + av^\alpha}]} \\
&= \frac{1}{v^2 + av^\alpha} \left[1 + \frac{b}{v^2 + av^\alpha}\right]^{-1} \\
&= \frac{1}{v^2 + av^\alpha} \sum_{k=0}^{\infty} \left(\frac{-b}{v^2 + av^\alpha}\right)^k \\
&= \sum_{k=0}^{\infty} \frac{(-b)^k}{(v^2 + av^\alpha)^{k+1}} \\
&= \sum_{k=0}^{\infty} \frac{(-b)^k}{(v^2)^{k+1} [1 + av^{\alpha-2}]^{k+1}} \\
&= \sum_{k=0}^{\infty} (-b)^k v^{-2k-2} \sum_{r=0}^{\infty} \binom{k+r}{r} (-av^{\alpha-2})^r \\
&= \sum_{k=0}^{\infty} (-b)^k \sum_{r=0}^{\infty} \binom{k+r}{r} (-a)^r v^{(\alpha-2)r-2k-2}
\end{aligned}$$

From (2.2.13),

$$\begin{aligned}
k(v) &= c_0 \sum_{k=0}^{\infty} (-b)^k \sum_{r=0}^{\infty} \binom{k+r}{r} (-a)^r v^{[(2-\alpha)r+2k]-2} \\
&+ c_1 \sum_{k=0}^{\infty} (-b)^k \sum_{r=0}^{\infty} \binom{k+r}{r} (-a)^r v^{[(2-\alpha)r+2k]-1-1+1} \\
&+ ac_0 \sum_{k=0}^{\infty} (-b)^k \sum_{r=0}^{\infty} \binom{k+r}{r} (-a)^r v^{[(2-\alpha)r+2k]+\alpha-4} \\
&+ ac_1 \sum_{k=0}^{\infty} (-b)^k \sum_{r=0}^{\infty} \binom{k+r}{r} (-a)^r v^{[(2-\alpha)r+2k]+\alpha-5}
\end{aligned}$$

Applying inverse Aboodh transform, we have

$$\begin{aligned}
y(t) &= c_0 \sum_{r=0}^{\infty} \frac{(-b)^k \Gamma(k+r+1) (-a)^r t^{(2-\alpha)r+2k}}{k! \Gamma[(2-\alpha)r+2k+1] r!} \\
&+ c_1 \sum_{r=0}^{\infty} \frac{(-b)^k \Gamma(k+r+1) (-a)^r t^{(2-\alpha)r+2k+1}}{k! \Gamma[(2-\alpha)r+2k+2] r!} \\
&+ ac_0 \sum_{r=0}^{\infty} \frac{(-b)^k \Gamma(k+r+1) (-a)^r t^{(2-\alpha)r+2k-\alpha+2}}{k! \Gamma[(2-\alpha)r+2k-\alpha+3] r!} \\
&+ ac_1 \sum_{r=0}^{\infty} \frac{(-b)^k \Gamma(k+r+1) (-a)^r t^{(2-\alpha)r+2k-\alpha+3}}{k! \Gamma[(2-\alpha)r+2k-\alpha+4] r!}
\end{aligned}$$

Thus we will get the desired solution (2.2.12). □

Theorem 2.2.5. *Let $1 < \alpha < 2$ and $a, b \in \mathbb{R}$. The solution to the fractional differential equation*

$$y^{(\alpha)}(t) + ay'(t) + by(t) = 0 \tag{2.2.14}$$

with the initial condition $y(0) = c_0$ and $y'(0) = c_1$ is

$$\begin{aligned}
y(t) &= c_0 \sum_{k=0}^{\infty} \frac{(-b)^k}{k!} \sum_{r=0}^{\infty} \frac{\Gamma(r+k+1)(-a)^r t^{(\alpha-1)r+\alpha k}}{\Gamma[(\alpha-1)r+\alpha k]r!} \\
&+ c_1 \sum_{k=0}^{\infty} \frac{(-b)^k}{k!} \sum_{r=0}^{\infty} \frac{\Gamma(r+k+1)(-a)^r t^{(\alpha-1)r+\alpha k+1}}{\Gamma[(\alpha-1)r+\alpha k+2]r!} \\
&+ ac_0 \sum_{k=0}^{\infty} \frac{(-b)^k}{k!} \sum_{r=0}^{\infty} \frac{\Gamma(r+k+1)(-a)^r t^{(\alpha-1)r+\alpha k+\alpha+1}}{\Gamma[(\alpha-1)r+\alpha k+\alpha]r!}
\end{aligned} \tag{2.2.15}$$

Proof. Applying Aboodh transform to equation (2.2.14),

$$\begin{aligned}
[v^\alpha k(v) - \frac{y(0)}{v^{2-\alpha}} - \frac{y'(0)}{v^{3-\alpha}}] + a[vk(v) - \frac{y(0)}{v}] + bk(v) &= 0 \\
k(v)[v^\alpha + av + b] - \frac{c_0}{v^{2-\alpha}} - \frac{c_1}{v^{3-\alpha}} - \frac{ac_0}{v} &= 0 \\
k(v)[v^\alpha + av + b] &= c_0 v^{\alpha-2} + c_1 v^{\alpha-3} + ac_0 v^{-1} \\
k(v) &= \frac{c_0 v^{\alpha-2} + c_1 v^{\alpha-3} + ac_0 v^{-1}}{v^\alpha + av + b}
\end{aligned} \tag{2.2.16}$$

$$\begin{aligned}
\text{Since } \frac{1}{v^\alpha + av + b} &= \frac{1}{(v^\alpha + av)[1 + \frac{b}{v^\alpha + av}]} \\
&= \frac{1}{v^\alpha + av} \left[1 + \frac{b}{v^\alpha + av}\right]^{-1} \\
&= \frac{1}{v^\alpha + av} \sum_{k=0}^{\infty} \left(\frac{-b}{v^\alpha + av}\right)^k \\
&= \sum_{k=0}^{\infty} \frac{(-b)^k}{(v^\alpha + av)^{k+1}} \\
&= \sum_{k=0}^{\infty} \frac{(-b)^k}{(v^\alpha)^{k+1} (1 + av^{1-\alpha})^{k+1}} \\
&= \sum_{k=0}^{\infty} (-b)^k v^{-\alpha k - \alpha} \sum_{r=0}^{\infty} \binom{k+r}{r} (-av^{1-\alpha})^r \\
&= \sum_{k=0}^{\infty} (-b)^k \sum_{r=0}^{\infty} \binom{k+r}{r} (-a)^r v^{-(\alpha-1)r - \alpha k - \alpha}
\end{aligned}$$

From (2.2.16),

$$\begin{aligned}
k(v) &= c_0 \sum_{k=0}^{\infty} (-b)^k \sum_{r=0}^{\infty} \binom{k+r}{r} (-a)^r v^{-(\alpha-1)r-\alpha k-2} \\
&\quad + c_1 \sum_{k=0}^{\infty} (-b)^k \sum_{r=0}^{\infty} \binom{k+r}{r} (-a)^r v^{-(\alpha-1)r-\alpha k-3} \\
&\quad + a c_0 \sum_{k=0}^{\infty} (-b)^k \sum_{r=0}^{\infty} \binom{k+r}{r} (-a)^r v^{-(\alpha-1)r-\alpha k-\alpha-1}
\end{aligned}$$

Applying inverse Aboodh transform, we have

$$\begin{aligned}
k(v)) &= c_0 \sum_{k=0}^{\infty} \frac{(-b)^k}{k!} \sum_{r=0}^{\infty} \frac{\Gamma(r+k+1)(-a)^r t^{(\alpha-1)r+\alpha k}}{\Gamma[(\alpha-1)r+\alpha k]r!} \\
&\quad + c_1 \sum_{k=0}^{\infty} \frac{(-b)^k}{k!} \sum_{r=0}^{\infty} \frac{\Gamma(r+k+1)(-a)^r t^{(\alpha-1)r+\alpha k+1}}{\Gamma[(\alpha-1)r+\alpha k+2]r!} \\
&\quad + a c_0 \sum_{k=0}^{\infty} \frac{(-b)^k}{k!} \sum_{r=0}^{\infty} \frac{\Gamma(r+k+1)(-a)^r t^{(\alpha-1)r+\alpha k+\alpha+1}}{\Gamma[(\alpha-1)r+\alpha k+\alpha]r!}
\end{aligned}$$

Thus we will get the desired solution (2.2.15).

□

Remark 2.2.1. If $a=0$ in equation (2.2.14), then the the solution to the equation

$$y^\alpha(t) + by(t) = 0, 1 < \alpha \leq 2 \quad (2.2.17)$$

with the initial conditions $y(0) = c_0$ and $y'(0) = c_1$ is

$$\begin{aligned}
y(t) &= c_0 \sum_{k=0}^{\infty} \frac{(-bt^\alpha)^k}{\Gamma(\alpha k + 1)} + c_1 t \sum_{k=0}^{\infty} \frac{(-bt^\alpha)^k}{\Gamma(\alpha k + 2)} \\
&= c_0 E_{\alpha,1}(-bt^\alpha) + c_1 t E_{\alpha,2}(-bt^\alpha)
\end{aligned} \quad (2.2.18)$$

2.3 A generalized fractional integral transform with exponential type kernel

Many integral transformations with exponential type kernels have been introduced in the last few years.

Definition 2.3.1. Let $f(x)$ be sectionally continuous on the interval $0 \leq x \leq T$ for any $T > 0$ and $|f(x)| \leq me^{bx}$ when $x \geq \mathbb{N}$ for any $b \in \mathbb{R}$ and $m, N \in \mathbb{R}^+$. We define Sadik transform of $f(x)$ as [60]

$$U[f(x)] = F(v^{\alpha, \beta}) = \frac{1}{v^\beta} \int_0^\infty e^{-xv^\alpha} f(x) dx \quad (2.3.1)$$

where v is a complex variable, $\alpha > 0$ and $\beta \in \mathbb{R}$.

The function $f(x)$ used in (2.3.1) is normally continuous and continuously differentiable; the question is what happens when it is continuous but only has a fractional derivative of order α , $0 < \alpha < 1$. There are two possibilities. $f(x)$ has both a continuous and a fractional derivative in the first instance. $f(x)$ has a derivative of order α in the second instance, but none in the first. We must discover an alternative in the second instance. This chapter's main objective is to present a possible method to this option.

The following table explores various integral transforms with exponential type kernel.

The transforms in table 2.1 are all special instances of the Sadik transform.

The Sadik transform can be converted into the Laplace, Sumudu, Elzaki, Tarig,

S.No	Name of the integral transform	Kernel
1	Laplace transform(1749-1827)[32]	$k(x, v) = e^{-vx}$
2	Sumudu transform(1993)	$k(x, v) = \frac{1}{v}e^{-\frac{x}{v}}$
3	Laplace-Carson transform (1886-1940)	$k(x, v) = ve^{-vx}$
4	N-transform(2008)[36],zz-transform(2016)[48]	$k(x, s, v) = \frac{1}{v}e^{-\frac{x}{v}}; s = 1$
5	Elzaki transform(2011)[21]	$k(x, v) = ve^{-\frac{x}{v}}$
6	Tarig transform(2013)[22],New integral transform(2013)[33, 13]	$k(x, v) = \frac{1}{v}e^{-\frac{x}{v^2}}$
7	Aboodh transform(2016)[2]	$k(x, v) = \frac{1}{v}e^{-vx}$
8	Kamal transform(2016),Yang transform(2018)	$k(x, v) = e^{-\frac{x}{v}}$
9	Mahgoub transform((2018)[39],New transform(2018)[30]	$k(x, v) = ve^{-vx}$

Table 2.1: Integral transforms with exponential type kernel

Kamal, Laplace-Carson, and Aboodh transforms by changing the values of α and β . It can also be changed into integral transforms that are not mentioned in the literature.

The following table demonstrates how the Sadik transform is converted into other integral transforms by fixing α and β values.

S.No	Values of α and β	Sadik transform converts into
1	$\beta = 0$ and $\alpha = 1$	Laplace transform
2	$\beta = 1$ and $\alpha = -1$	Sumudu transform
3	$\beta = -1$ and $\alpha = 1$	Laplace-Carson transform
4	$\beta = 1$ and $\alpha = -1$	N-transform, zz-transform
5	$\beta = -1$ and $\alpha = -1$	Elzaki transform
6	$\beta = 1$ and $\alpha = -2$	Tarig transform, New integral transform
7	$\beta = 1$ and $\alpha = 1$	Aboodh transform
8	$\beta = 0$ and $\alpha = -1$	Kamal transform, Yang transform
9	$\beta = -1$ and $\alpha = 1$	Mahgoub transform, New transform

Table 2.2: Conversion of Sadik transform to various integral transforms

Definition 2.3.2. Let $f(x)$ be a function that vanishes when t is negative. Its generalized integral transform of fractional order α , $0 < \alpha < 1$, with exponential type

kernel is defined as follows:

$$\begin{aligned}
 S_\alpha\{f(x)\} = A_\alpha(v^{\beta,\gamma}) &= \left(\frac{1}{v^\beta}\right)^\alpha \int_0^\infty E_\alpha(-xv^\gamma)^\alpha f(x)(dx)^\alpha \\
 &= \lim_{M \uparrow \infty} \left(\frac{1}{v^\beta}\right)^\alpha \int_0^M E_\alpha(-xv^\gamma)^\alpha f(x)(dx)^\alpha
 \end{aligned} \tag{2.3.2}$$

where v is a complex variable, γ is any non-zero real number, β is any real number and $E_\alpha(u)$ is the Mittag-Leffler function $\sum \frac{u^k}{(k\alpha)!}$

The table below shows how to convert the generalized fractional integral transform with exponential type kernel into fractional order integral transform by applying certain β and γ values.

Table 2.3: Conversion of the generalized fractional integral transform with exponential type kernel into existing fractional integral transforms

S.No	Values of β and γ	The generalized fractional integral transform with exponential type kernel converts into
1	$\beta = 0$ and $\gamma = 1$	Fractional Laplace transform
2	$\beta = 1$ and $\gamma = -1$	Fractional Sumudu transform [38]
3	$\beta = 1$ and $\gamma = -1$	Fractional Natural transform [52]
4	$\beta = -1$ and $\gamma = -1$	Fractional Elzaki transform

2.3.1 Sufficient conditions for the existence of the generalized fractional integral transform with exponential type kernel

Theorem 2.3.1. *For each positive real constant A , let $f(x)$ be sectionally continuous in each finite subinterval of the intervals $0 \leq x \leq A$ and $x > A$. The generalized fractional integral transform with exponential type kernel of $f(x)$ occurs if $f(x)$ has fractional exponential order α .*

Proof. For any $A > 0$,

$$S_\alpha\{f(x)\} = \left(\frac{1}{v^\beta}\right)^\alpha \int_0^A E_\alpha(-xv^\gamma)^\alpha f(x)(dx)^\alpha + \left(\frac{1}{v^\beta}\right)^\alpha \int_A^\infty E_\alpha(-xv^\gamma)^\alpha f(x)(dx)^\alpha \quad (2.3.3)$$

The first integral in (2.3.3) exists because $f(x)$ is sectionally continuous in $0 \leq x \leq A$

$$\begin{aligned} \text{Now, } \left| \int_A^\infty E_\alpha(-xv^\gamma)^\alpha f(x)(dx)^\alpha \right| &\leq \int_A^\infty |E_\alpha(-xv^\gamma)^\alpha f(x)|(dx)^\alpha \\ &\leq \int_0^\infty E_\alpha(-xv^\gamma)^\alpha |f(x)|(dx)^\alpha \\ &\leq \int_0^\infty E_\alpha(-xv^\gamma)^\alpha M E_\alpha(xc^\gamma)^\alpha (dx)^\alpha \\ \left| \int_A^\infty E_\alpha(-xv^\gamma)^\alpha f(x)(dx)^\alpha \right| &\leq \int_0^\infty M E_\alpha(-x(v^\gamma - c^\gamma))^\alpha (dx)^\alpha \end{aligned}$$

Taking $t = x(v^\gamma - c^\gamma)$ and using $\Gamma_\alpha(x) = \frac{1}{\Gamma(\alpha + 1)} \int_0^\infty E_\alpha(-t)^\alpha t^{(x-1)\alpha} (dt)^\alpha$, we have

$$\begin{aligned} \left| \int_A^\infty E_\alpha(-xv^\gamma)^\alpha f(x)(dx)^\alpha \right| &\leq \frac{M}{(v^\gamma - c^\gamma)^\alpha} \Gamma_\alpha(1) \Gamma(\alpha + 1) \\ &= \frac{M}{(v^\gamma - c^\gamma)^\alpha} \Gamma(\alpha + 1). \end{aligned}$$

As a result, the second integral in (2.3.3) occurs, and the generalized fractional transform of $f(x)$ defined by (2.3.2) exists as well. \square

2.3.2 Duality relation between the fractional Laplace transform and the generalized fractional integral transform with exponential type kernel

Theorem 2.3.2. *Let $F_\alpha(v)$ be the Laplace transform of fractional order α of a function $f(x)$ and $A_\alpha(v^{\beta,\gamma})$ be the generalized integral transform of fractional order α with*

exponential type kernel of the same function $f(x)$. Then

$$A_\alpha(v^{\beta,\gamma}) = \left(\frac{1}{v^\beta}\right)^\alpha F_\alpha(v^\gamma).$$

Proof. Let $f(x) \in \mathcal{A}$. By the generalized fractional integral transform with exponential type kernel, we have

$$A_\alpha(v^{\beta,\gamma}) = \left(\frac{1}{v^\beta}\right)^\alpha \int_0^\infty E_\alpha(-xv^\gamma)^\alpha f(x)(dx)^\alpha = \left(\frac{1}{v^\beta}\right)^\alpha F_\alpha(v^\gamma).$$

□

2.3.3 Operational Properties of generalized fractional integral transform with exponential type kernel

$$(i). \quad S_\alpha\{t^n\} = \frac{1}{(v^\beta)^\alpha} \frac{1}{(v^\gamma)^{(n+\alpha)}} \Gamma_\alpha\left(\frac{n}{\alpha} + 1\right) \Gamma(\alpha + 1).$$

Proof.

$$S_\alpha\{t^n\} = \left(\frac{1}{v^\beta}\right)^\alpha \int_0^\infty E_\alpha(-tv^\gamma)^\alpha t^n (dt)^\alpha$$

By taking $tv^\gamma = x$, and using

$$\Gamma_\alpha(x) = \frac{1}{\Gamma(\alpha + 1)} \int_0^\infty E_\alpha(-t)^\alpha t^{(x-1)\alpha} (dt)^\alpha, \quad (2.3.4)$$

$$\text{we have } S_\alpha\{t^n\} = \frac{1}{(v^\beta)^\alpha} \frac{1}{(v^\gamma)^{(n+\alpha)}} \Gamma_\alpha\left(\frac{n}{\alpha} + 1\right) \Gamma(\alpha + 1).$$

□

$$(ii). \quad S_\alpha\{t^{n\alpha}\} = \left(\frac{1}{v^\beta}\right)^\alpha \frac{1}{(v^\gamma)^{(n+1)\alpha}} \Gamma^{(n+1)}(\alpha + 1) \Gamma(n + 1).$$

Proof.

$$S_\alpha\{t^{n\alpha}\} = \left(\frac{1}{v^\beta}\right)^\alpha \int_0^\infty E_\alpha(-tv^\gamma)^\alpha t^{n\alpha} (dt)^\alpha$$

By taking $tv^\gamma = x$, and using (2.3.4), we have

$$S_\alpha\{t^{n\alpha}\} = \left(\frac{1}{v^\beta}\right)^\alpha \frac{1}{(v^\gamma)^{(n+1)\alpha}} \Gamma_\alpha(n+1) \Gamma(\alpha+1).$$

Since $\Gamma_\alpha(n+1) = \Gamma^n(\alpha+1) \Gamma(n+1)$, $n \in \mathbb{N}$, we have

$$S_\alpha\{t^{n\alpha}\} = \left(\frac{1}{v^\beta}\right)^\alpha \frac{1}{(v^\gamma)^{(n+1)\alpha}} \Gamma^{(n+1)}(\alpha+1) \Gamma(n+1).$$

□

$$(iii). \quad S_\alpha\{f(ax)\} = \frac{1}{a^{2\alpha}} A_\alpha(v^{\gamma,\beta}).$$

Proof.

$$S_\alpha\{f(ax)\} = \left(\frac{1}{v^\beta}\right)^\alpha \int_0^\infty E_\alpha(-xv^\gamma)^\alpha f(ax) (dx)^\alpha$$

$$S_\alpha\{f(ax)\} = \alpha \left(\frac{1}{v^\beta}\right)^\alpha \lim_{M \uparrow \infty} \int_0^M [M-x]^{\alpha-1} E_\alpha(-xv^\gamma)^\alpha f(ax) (dx)$$

By taking $ax = u$, we have

$$\begin{aligned} S_\alpha\{f(ax)\} &= \alpha \left(\frac{1}{v^\beta}\right)^\alpha \lim_{M \uparrow \infty} \int_0^{aM} \left[M - \frac{u}{a}\right]^{\alpha-1} E_\alpha\left(-\frac{u}{a}v^\gamma\right)^\alpha f(u) \frac{du}{a} \\ &= \left(\frac{1}{a^{2\alpha}}\right) \left(\frac{1}{v^\beta}\right)^\alpha \lim_{M \uparrow \infty} \int_0^{aM} E_\alpha(-uv^\gamma)^\alpha f(u) (du)^\alpha \end{aligned}$$

$$S_\alpha\{f(ax)\} = \frac{1}{a^{2\alpha}} S_\alpha\{f(x)\}.$$

□

$$(iv). \quad S_\alpha\{f(x-b)\} = E_\alpha(-b^\alpha v^{\gamma\alpha}) S_\alpha\{f(u)\}.$$

Proof.

$$\begin{aligned} S_\alpha\{f(x-b)\} &= \left(\frac{1}{v^\beta}\right)^\alpha \int_0^\infty E_\alpha(-xv^\gamma)^\alpha f(x-b) (dx)^\alpha \\ &= \alpha \left(\frac{1}{v^\beta}\right)^\alpha \lim_{M \uparrow \infty} \int_0^M E_\alpha(-xv^\gamma)^\alpha (M-x)^{\alpha-1} f(x-b) dx \end{aligned}$$

By taking $x - b = u$, we have

$$S_\alpha\{f(x - b)\} = \alpha \left(\frac{1}{v^\beta}\right)^\alpha \lim_{M \uparrow \infty} \int_0^{M-b} (M - b - u)^{\alpha-1} E_\alpha(-(v^\gamma)^\alpha (b + u)^\alpha) f(u) du$$

$$S_\alpha\{f(x - b)\} = E_\alpha(-b^\alpha v^{\gamma\alpha}) S_\alpha\{f(u)\}.$$

□

$$(v). \quad S_\alpha\{E_\alpha(-c^\alpha x^\alpha) f(x)\} = S_\alpha\{f(x)\}_{(v^\gamma \rightarrow c + v^\gamma)}.$$

Proof.

$$S_\alpha\{E_\alpha(-c^\alpha x^\alpha) f(x)\} = \left(\frac{1}{v^\beta}\right)^\alpha \int_0^\infty E_\alpha(-xv^\gamma)^\alpha E_\alpha(-c^\alpha x^\alpha) f(x) (dx)^\alpha$$

$$= \left(\frac{1}{v^\beta}\right)^\alpha \int_0^\infty E_\alpha(-x(v^\gamma + c))^\alpha f(x) (dx)^\alpha$$

$$S_\alpha\{E_\alpha(-c^\alpha x^\alpha) f(x)\} = S_\alpha\{f(x)\}_{(v^\gamma \rightarrow c + v^\gamma)}.$$

□

$$(vi). \quad S_\alpha\{f^{(\alpha)}(x)\} = (v^\gamma)^\alpha S_\alpha\{f(x)\} - \left(\frac{1}{v^\beta}\right)^\alpha \Gamma(1 + \alpha) f(0).$$

Proof.

$$S_\alpha\{f^{(\alpha)}(x)\} = \left(\frac{1}{v^\beta}\right)^\alpha \int_0^\infty E_\alpha(-xv^\gamma)^\alpha f^{(\alpha)}(x) (dx)^\alpha$$

By integration by parts and using

$$D_x^\alpha\{E_\alpha(\lambda x^\alpha)\} = \lambda E_\alpha(\lambda x^\alpha), \text{ we have}$$

$$S_\alpha\{f^{(\alpha)}(x)\} = \left(\frac{1}{v^\beta}\right)^\alpha \left\{ \Gamma(1 + \alpha) [f(x) E_\alpha(-xv^\gamma)^\alpha]_0^\infty + v^{\gamma\alpha} \int_0^\infty E_\alpha(-xv^\gamma)^\alpha f(x) (dx)^\alpha \right\}$$

$$= - \left(\frac{1}{v^\beta}\right)^\alpha \Gamma(1 + \alpha) f(0) + \frac{v^{\gamma\alpha}}{(v^\beta)^\alpha} \int_0^\infty E_\alpha(-xv^\gamma)^\alpha f(x) (dx)^\alpha$$

$$S_\alpha\{f^{(\alpha)}(x)\} = (v^\gamma)^\alpha S_\alpha\{f(x)\} - \left(\frac{1}{v^\beta}\right)^\alpha \Gamma(1 + \alpha)f(0). \quad (2.3.5)$$

□

$$(vii). \quad S_\alpha\left\{\int_0^x f(x)(dx)^\alpha\right\} = v^{-\gamma\alpha}\Gamma(\alpha + 1)S_\alpha\{f(x)\}.$$

Proof.

$$\text{From (2.3.5), } (v^\gamma)^\alpha S_\alpha\{f(x)\} = S_\alpha\{f^{(\alpha)}(x)\} + \left(\frac{1}{v^\beta}\right)^\alpha \Gamma(1 + \alpha)f(0)$$

Let $g(x) = \int_0^x f(x)(dx)^\alpha$. Then $g(0) = 0$

$$\begin{aligned} (v^\gamma)^\alpha S_\alpha\left\{\int_0^x f(x)(dx)^\alpha\right\} &= S_\alpha\{g^{(\alpha)}(x)\} \\ &= S_\alpha\left\{D_x^\alpha \int_0^x f(x)(dx)^\alpha\right\} \\ &= S_\alpha\{\Gamma(\alpha + 1)f(x)\} \\ &= \Gamma(\alpha + 1)S_\alpha\{f(x)\} \end{aligned}$$

$$S_\alpha\left\{\int_0^x f(x)(dx)^\alpha\right\} = v^{-\gamma\alpha}\Gamma(\alpha + 1)S_\alpha\{f(x)\}.$$

□

2.3.4 Convolution theorem using generalized fractional integral transform with exponential type kernel

Theorem 2.3.3. *If the convolution of order α of the two functions $f(x)$ and $g(x)$ is given by the expression*

$$(a(x) * b(x))_\alpha = \int_0^x a(x - u)b(u)(du)^\alpha$$

*then one has the equality $S_\alpha\{a(x) * b(x)\} = (v^\beta)^\alpha S_\alpha\{a(x)\}S_\alpha\{b(x)\}$*

Proof.

$$\begin{aligned} S_\alpha\{(a * b)_\alpha\} &= \left(\frac{1}{v^\beta}\right)^\alpha \int_0^\infty E_\alpha(-x^\alpha v^{\gamma\alpha}) \int_0^x a(x-u)b(u)(du)^\alpha(dx)^\alpha \\ &= \left(\frac{1}{v^\beta}\right)^\alpha \int_0^\infty E_\alpha(-v^{\gamma\alpha}(x-u)^\alpha) E_\alpha(-v^{\gamma\alpha}u^\alpha) \int_0^x a(x-u)b(u)(du)^\alpha(dx)^\alpha \end{aligned}$$

We obtain by modifying the variables $x - u = t$, $u = s$,

$$\begin{aligned} S_\alpha\{(a * b)_\alpha\} &= \left(\frac{1}{v^\beta}\right)^\alpha \int_0^\infty E_\alpha(-v^{\gamma\alpha}t^\alpha) a(t)(dt)^\alpha \int_0^\infty E_\alpha(-v^{\gamma\alpha}s^\alpha) b(s)(ds)^\alpha \\ &= (v^\beta)^\alpha S_\alpha\{a(t)\} S_\alpha\{b(s)\}. \end{aligned}$$

□

2.3.5 Inversion theorem using generalized fractional integral transform with exponential type kernel

Theorem 2.3.4. *For $0 < \alpha < 1$, the generalized fractional integral transform with exponential type kernel*

$$A_\alpha(v^{\beta,\gamma}) = \left(\frac{1}{v^\beta}\right)^\alpha \int_0^\infty E_\alpha(-xv^\gamma)^\alpha f(x)(dx)^\alpha$$

has the inversion formula,

$$f(x) = \frac{1}{(M_\alpha)^\alpha} \int_{-i\infty}^{+i\infty} (v^\beta)^\alpha E_\alpha(v^{\gamma\alpha}x^\alpha) A_\alpha(v^{\beta,\gamma})(dv)^\alpha,$$

where M_α is the period of the complex-valued Mittag-Leffler function defined by the equality $E_\alpha(i(M_\alpha)^\alpha) = 1$

Proof. The Laplace transform of fractional order α of $f(x)$, i.e.,

$$F_\alpha(v) = \int_0^\infty E_\alpha(-v^\alpha x^\alpha) f(x) (dx)^\alpha, 0 < \alpha < 1$$

has the inversion formula

$$f(x) = \frac{1}{(M_\alpha)^\alpha} \int_{-i\infty}^{+i\infty} E_\alpha(v^\alpha x^\alpha) F_\alpha(v) (dv)^\alpha.$$

We arrive at the necessary inversion formula by using the duality relationship between the fractional order laplace transform and generalized fractional integral transform with exponential type kernel.

□

2.3.6 Solutions of fractional differential equations using generalized fractional integral transform with exponential type kernel

2.3.7 Example 1

Suppose $A_\alpha(v^{\beta,\gamma})$ is the generalized fractional integral transform with exponential type kernel of a function $f(x)$. Then the solution of fractional differential equation

$$y^{(\alpha)} + \lambda y = f(x), y(0) = 0, 0 < \alpha < 1 \quad (2.3.6)$$

is given by

$$y(x) = \frac{1}{(M_\alpha)^\alpha} \int_{-i\infty}^{+i\infty} \frac{(v^\beta)^\alpha}{\lambda + (v^\gamma)^\alpha} E_\alpha(v^{\gamma\alpha} x^\alpha) A_\alpha(v^{\beta,\gamma}) f(dv)^\alpha \quad (2.3.7)$$

where λ is a constant.

Now we solve (2.3.6). By taking the generalized fractional integral transform with exponential type kernel on the both sides of (2.3.6), we get

$$(v^\gamma)^\alpha A_\alpha\{v^{\beta,\gamma}\}_y + \lambda A_\alpha\{v^{\beta,\gamma}\}_y = A_\alpha\{v^{\beta,\gamma}\}_f$$

$$A_\alpha\{v^{\beta,\gamma}\}_y = \frac{1}{\lambda + (v^\gamma)^\alpha} A_\alpha\{v^{\beta,\gamma}\}_f \quad (2.3.8)$$

By substituting (2.3.8) in the inversion formula of the generalized fractional integral transform with exponential type kernel, we arrive the required solution (2.3.7).

2.3.8 Example 2

The equation governs the current in a circuit with inductance L , resistance R , and capacitance C with an applied voltage $E(t)$.

$$L \frac{dI}{dt} + RI + \frac{1}{C} \int_0^t I dt = E(t),$$

where L, R and C are constants and $I(t)$ is the current, and

$$I(t) = \frac{dQ}{dt} \text{ represents the accumulated charge } Q \text{ on the condenser at time } t \text{ is } Q(t) = \int_0^t I(t) dt$$

Let us consider the fractional equation of current in the circuit, that is,

$$LI^{(\alpha)}(t) + RI + \frac{1}{C} \int_0^t I(t)(dt)^\alpha = E(t), \quad (2.3.9)$$

with $t = 0$, $I(0) = 0$, $Q(0) = 0$ and $0 < \alpha < 1$

Now we solve (2.3.9). By taking the generalized fractional integral transform with exponential type kernel on both sides of (2.3.9), we get,

$$A_\alpha(v^{\beta,\gamma})_I = \frac{1}{\frac{v^{2\gamma\alpha}\Gamma(\alpha+1)}{c} + Rv^\alpha + L} A_\alpha(v^{\beta,\gamma})_E \quad (2.3.10)$$

where $A_\alpha(v^{\beta,\gamma})_I$ and $A_\alpha(v^{\beta,\gamma})_E$ are the generalized fractional integral transforms of $I(t)$ and $E(t)$ respectively. Then characteristic equation of (2.3.10) is given by

$$v^{2\gamma\alpha} + \frac{R}{L}v^{\gamma\alpha} + \frac{\Gamma(\alpha+1)}{CL} = 0$$

The roots of the above characteristic equation are $v^{\gamma\alpha} = -k \pm in$, where $k = \frac{R}{2L}$ and $n^2 = \frac{\Gamma(\alpha+1)}{CL} - \frac{R^2}{4L^2}$ is the negative real part. This demonstrates the system's stability. We may now get at (2.3.10) by inserting it into the inversion formula of the generalized integral formula with exponential type kernel.

Now by substituting (2.3.10) in the inversion formula of the generalized fractional integral transform with exponential type kernel, we arrive

$$I(t) = \frac{1}{L(M_\alpha)^\alpha} \int_{-i\infty}^{+i\infty} \frac{(v^\beta)^\alpha E_\alpha(x^\alpha v^{\gamma\alpha})}{v^{2\gamma\alpha} + \frac{R}{L}v^{\gamma\alpha} + \frac{\Gamma(\alpha+1)}{CL}} A_\alpha(v^{\beta,\gamma})_E(dv)^\alpha$$

as a solution of (2.3.9).

Chapter 3

Numerical solutions of fractional differential equations by Euler wavelet method

3.1 Introduction

In this chapter, we discuss the numerical solutions of some fractional differential equations using Euler wavelet based numerical scheme. Euler wavelets are the types of wavelets constructed from Euler polynomials as their basis functions. It is commonly known that when it comes to approximating arbitrary functions, Euler polynomials provide many advantages over Legendre polynomials. First, there are less terms in the Euler polynomials than in the Legendre polynomials. Therefore, utilising Euler polynomials rather than Legendre polynomials saves processing time when approximating arbitrary functions. Second, employing Euler polynomials for function approximation reduces computational errors. Thus, there is a reason for

us to believe that Euler wavelets inherit these benefits from Euler polynomials. In order to solve the fractional differential equations, the major goal of this chapter is to introduce the Euler wavelet operational matrix. We then utilize this resulting Euler wavelet operational matrix to reduce the fractional differential equation into a system of algebraic equations to get the required Euler coefficients, which are computed by using Matlab. The convergence analysis of the Euler wavelets is also given. It not only simplifies the problem, but also speeds up the computation. What is more, the numerical examples demonstrate that Euler wavelet performs better in approximating an arbitrary function compared to many other numerical methods. Euler wavelet based numerical scheme (EWM) yields fruitful results in terms of accuracy. The comparison shows that, when compared to other methods, the current method has the best accuracy. This methods can be implemented easily, effectively, and conveniently to get the numerical solutions to fractional differential equations. For the analysis of the numerical results, the corresponding graphs and tables are provided.

3.2 Euler wavelet based numerical scheme

Wavelets are a family of functions generated by dilation and translation of a single function $\psi(x)$, termed the mother wavelet. We get the following family of continuous

wavelets if the dilation and translation parameters c and d change continuously.

$$\psi_{cd}(x) = |c|^{-\frac{1}{2}} \psi\left(\frac{x-d}{c}\right), c, d \in (\mathbb{R}), c \neq 0.$$

If the translation and dilation parameters are chosen to have discrete values, that is, $c = c_0^{-p}, d = qd_0c_0^{-p}, c_0 > 1, d_0 > 0$ and $p, q \in \mathbb{Z}$, then we have the following family of discrete wavelets,

$$\psi_{pq}(x) = |c_0|^{\frac{p}{2}} \psi(c_0^p x - qd_0),$$

where the functions ψ_{pq} form a wavelet basis for $L^2(\mathbb{R})$. In particular, if $c_0 = 2$ and $d_0 = 1$, we can attain an orthonormal basis from $\psi_{pq}(x)$ for $L^2(\mathbb{R})$.

The Euler wavelets are defined on the interval $[0,1)$ as

$$\psi_{mn}(x) = \begin{cases} 2^{\frac{j-1}{2}} \widetilde{E}_n(2^{j-1}x - m + 1), & \frac{m-1}{2^{j-1}} \leq x < \frac{m}{2^{j-1}} \\ 0, & \text{otherwise} \end{cases}$$

for $m = 1, 2, \dots, 2^{j-1}, n = 0, 1, \dots, M-1$ and $j, M \in \mathbb{N}$,

$$\text{where } \widetilde{E}_n(x) = \begin{cases} 1, & n = 0 \\ \frac{1}{\sqrt{\left(\frac{2(-1)^{n-1}(n!)^2}{(2n)!}\right) E_{2n+1}(0)}} E_n(x), & n > 0 \end{cases}$$

the co-efficient

$$\frac{1}{\sqrt{\left(\frac{2(-1)^{n-1}(n!)^2}{(2n)!}\right) E_{2n+1}(0)}}$$

is for normality, the dilation parameter is $2^{-(j-1)}$ and the translation parameter is $(m-1)2^{-(j-1)}$. Here, $E_n(x)$ denote Euler polynomials of degree n which can be

defined by the generating functions

$$\frac{2e^{xs}}{e^s + 1} = \sum_{n=0}^{\infty} E_n(x) \frac{s^n}{n!}, \quad |s| < \pi.$$

We can also define the first kind Euler polynomials by the relation,

$$\sum_{j=0}^n \binom{n}{j} E_j(x) + E_n(x) = 2x^n$$

where $\binom{n}{j}$ is a binomial co-efficient.

The first few Euler polynomials are

$$E_0(x) = 1, E_1(x) = x - \frac{1}{2}, E_2(x) = x^2 - x, E_3(x) = x^3 - \frac{2}{3}x^2 + \frac{1}{4}, \dots\dots\dots$$

These polynomials satisfy the following formula,

$$\int_0^1 E_n(x) E_m(x) dx = (-1)^{m-1} \frac{n!(m+1)!}{(n+m+1)!} E_{n+m+1}(0), \quad n, m \geq 1$$

and the Euler polynomials form a complete basis for $L^2(\mathbb{R})$.

3.3 Function approximation by Euler wavelets

A function $f(x) \in L^2[0, 1)$ can be expressed in terms of the Euler wavelets as

$$f(x) = \sum_{m=0}^{\infty} \sum_{n \in \mathbb{Z}} C_{mn} \psi_{mn}(x) \tag{3.3.1}$$

where the coefficients C_{mn} are given by

$$C_{mn} = \langle f(x), \psi_{mn} \rangle = \int_0^1 f(x) \psi_{mn}(x) dx$$

By truncating the infinite series in (3.3.1), $f(x)$ is approximated as

$$\widetilde{f}(x) \approx \sum_{m=1}^{2^{j-1}} \sum_{n=0}^{M-1} C_{mn} \psi_{mn}(x) = C^T \psi(x)$$

where the coefficient vector C and the Euler function vector $\psi(x)$ are $2^{j-1}M \times 1$ matrices, given by

$$C = [C_{10}, C_{11}, \dots, C_{1(M-1)}, C_{20}, \dots, C_{2(M-1)}, \dots, C_{2^{j-1}0}, \dots, C_{2^{j-1}(M-1)}]^T$$

and

$$\psi(x) = [\psi_{10}, \psi_{11}, \dots, \psi_{1(M-1)}, \psi_{20}, \dots, \psi_{2(M-1)}, \dots, \psi_{2^{j-1}0}, \dots, \psi_{2^{j-1}(M-1)}]^T \quad (3.3.2)$$

We define the Euler wavelet coefficient matrix $\phi_{k \times k}$, $k = 2^{j-1}M$ at the collocation points $x_i = \frac{2i-1}{2k}$, $i = 1, 2, \dots, k$ as

$$\phi_{k \times k} = \left[\psi\left(\frac{1}{2k}\right), \psi\left(\frac{3}{2k}\right), \dots, \psi\left(\frac{2k-1}{2k}\right) \right]$$

Specifically, the Euler wavelet coefficient matrix for $j = 2$, $M = 3$ becomes

$$\phi_{6 \times 6} = \begin{pmatrix} 1.4142 & 1.4142 & 1.4142 & 0 & 0 & 0 \\ -0.9428 & 0 & 0.9428 & 0 & 0 & 0 \\ -0.4811 & -0.8660 & -0.4811 & 0 & 0 & 0 \\ 0 & 0 & 0 & 1.4142 & 1.4142 & 1.4142 \\ 0 & 0 & 0 & -0.9428 & 0 & 0.9428 \\ 0 & 0 & 0 & -0.4811 & -0.8660 & -0.4811 \end{pmatrix}$$

Correspondingly, we have

$$\widetilde{f}_k = [\widetilde{f}(x_1), \widetilde{f}(x_2), \dots, \widetilde{f}(x_k)] = C^T \phi_{k \times k}$$

Since the Euler wavelet coefficient matrix $\phi_{k \times k}$ is invertible, the Euler wavelet coefficient vector C^T can be attained by

$$C^T = \tilde{f}_k \phi_{k \times k}^{-1}$$

3.4 Error analysis for the Euler wavelet bases

We now establish the error analysis for the Euler wavelets expansion in the following Theorem.

Theorem 3.4.1. *If the function $f : [0, 1) \rightarrow \mathbb{R}$ is $n + 1$ times continuously differentiable and $f \in C^{n+1}[0, 1)$, then $\tilde{f}(x) = C^T \psi(x)$ approximates $f(x)$ with mean error bounded*

$$\|f(x) - \tilde{f}(x)\|_2 \leq \frac{\sqrt{2}\tilde{M}}{2^{(j-1)(n+1)}(n+1)!\sqrt{(2n+3)}}, \text{ where } \tilde{M} = \max_{x \in [0,1)} |f^{(n+1)}(x)|$$

Proof. We first divide the interval $[0,1)$ into subintervals $I_{j,m} = [\frac{m-1}{2^{j-1}}, \frac{m}{2^{j-1}}], m = 1, 2, \dots, 2^{j-1}, j \in \mathbb{N}$ with the restriction that $\tilde{f}(x)$ is a polynomial of degree less than $n + 1$ that approximates f with minimum mean error. Using Lemma 3 [68], we attain

$$\begin{aligned} \|f(x) - \tilde{f}(x)\|_2^2 &= \int_0^1 [f(x) - \tilde{f}(x)]^2 dx \\ &= \sum_m \int_{I_{j,m}} [f(x) - \tilde{f}(x)]^2 dx \\ &\leq \sum_m \left[\frac{\sqrt{(2)}\tilde{M}_m \left(\frac{1}{2^{j-1}}\right)^{\frac{2n+3}{2}}}{(n+1)!\sqrt{(2n+3)}} \right]^2 \\ &\leq \frac{2\tilde{M}^2}{2^{(j-1)(2n+2)}[(n+1)!]^2(2n+3)} \end{aligned}$$

$$\text{where } \tilde{M}_m = \max_{x \in I_{j,m}} |f^{(n+1)}(x)|$$

We get the upper bound by taking the square roots. As a result, the error of the approximation $\tilde{f}(x)$ of $f(x)$ decays like $2^{-(n+1)(j-1)}$. Meanwhile, we notice that the number of wavelets is $k = 2^{j-1}M$, where M denotes the degree of the Euler polynomials, which is usually small in computation. When M is fixed, the numerical results improve as j increasing, and we may conclude that the approximate solutions converge to the exact solution. \square

3.5 Operational matrix of the fractional integration of Euler wavelets

We now explore the basic idea of finding the fractional integration operational matrix of the Euler wavelets.

A k -set of Block pulse functions(BPFs) over the interval $[0,1]$ is defined as

$$b_i(x) = \begin{cases} 1, & (i-1)/k \leq x < i/k \\ 0, & otherwise \end{cases}$$

where $i=1,2,3\dots k$, $k \in \mathbb{N}$, For $x \in [0, 1)$,

$$b_i(x)b_j(x) = \begin{cases} 0, & i \neq j \\ b_i(x), & i = j \end{cases}$$

and

$$\int_0^1 b_i(x)b_j(x) = \begin{cases} 0, & i \neq j \\ \frac{1}{k}, & i = j \end{cases}$$

It is known that any square integrable function $f(x)$ defined over $[0,1)$ can be expanded in terms of BPFs as

$$f(x) \simeq \sum_{i=1}^k f_i b_i(x) = f^T B_k(x)$$

where $f = [f_1, f_2, \dots, f_k]^T$, $f_i = \frac{1}{k} \int_{(i-1)/k}^{i/k} f(x) b_i(x) dx$ and $B_k(x) = [b_1(x), b_2(x), \dots, b_k(x)]^T$

The block pulse functions and Euler wavelets have a relationship,

$$\psi(x) = \phi_{k \times k} B_k(x) \tag{3.5.1}$$

The block pulse operational matrix of the fractional integration F^α , $\alpha \geq 0$ is defined as in [37], that is,

$$(I^\alpha B_k)(x) \approx F^\alpha B_k(x) \tag{3.5.2}$$

where

$$F^\alpha = \frac{1}{k^\alpha} \frac{1}{\Gamma(\alpha + 2)} \begin{pmatrix} 1 & \xi_1 & \xi_2 & \xi_3 & \dots & \xi_{k-1} \\ 0 & 1 & \xi_1 & \xi_2 & \dots & \xi_{k-2} \\ 0 & 0 & 1 & \xi_1 & \dots & \xi_{k-3} \\ \vdots & \vdots & \ddots & \ddots & \vdots & \vdots \\ 0 & 0 & \dots & 0 & 1 & \xi_1 \\ 0 & 0 & \dots & 0 & 0 & 1 \end{pmatrix}$$

with $\xi_s = (s + 1)^{\alpha+1} - 2s^{\alpha+1} + (s - 1)^{\alpha+1}$

The fractional integration of the vector $\psi(x)$ defined in (3.3.2) with order $\alpha \geq 0$, can be approximated as

$$(I^\alpha \psi)(x) \approx P_{k \times k}^\alpha \psi(x) \tag{3.5.3}$$

where $P_{k \times k}^\alpha$ is called Euler wavelet operational matrix of order $\alpha \geq 0$. Using (3.5.1) and (3.5.2), we attain

$$(I^\alpha \psi)(x) \approx (I^\alpha \phi_{k \times k} B_k)(x) = \phi_{k \times k} (I^\alpha B_k)(x) \approx \phi_{k \times k} F^\alpha B_k(x) \quad (3.5.4)$$

Thus combining (3.5.3) and (3.5.4), we attain

$$P_{k \times k}^\alpha \psi(x) \approx (I^\alpha \psi)(x) \approx \phi_{k \times k} F^\alpha B_k(x) = \phi_{k \times k} F^\alpha \phi_{k \times k}^{-1} \psi(x) \text{ and so}$$

$$P_{k \times k}^\alpha \approx \phi_{k \times k} F^\alpha \phi_{k \times k}^{-1}$$

For $j = 2$, $M = 3$ and $\alpha = 0.5$, the Euler wavelet operational matrix of the fractional integration yields,

$$P_{6 \times 6}^{0.5} = \begin{pmatrix} 0.4616 & 0.3150 & -0.1631 & 0.5012 & -0.1509 & 0.1404 \\ 0.0878 & 0.2243 & 0.4203 & 0.0717 & -0.0449 & 0.0626 \\ -0.1305 & -0.1591 & 0.2354 & -0.2110 & 0.0615 & -0.0545 \\ 0 & 0 & 0 & 0.4616 & 0.3150 & -0.1631 \\ 0 & 0 & 0 & 0.0878 & 0.2243 & 0.4203 \\ 0 & 0 & 0 & -0.1305 & -0.1591 & 0.2354 \end{pmatrix}$$

Because the operational matrix $P_{6 \times 6}^{0.5}$ contains a large number of zeros, this phenomenon allows for quick computations.

3.6 Numerical Examples

To show the efficiency of the numerical approach based on Euler wavelets, we describe some numerical examples.

3.6.1 Example 3

Consider

$$AD^\alpha y(x) + BD^\beta y(x) + Cy(x) = g(x), \text{ with } y(0) = y_0, y'(0) = y_1, 0 < \beta < \alpha \leq 2, 0 \leq x < 1 \quad (3.6.1)$$

where $A \neq 0, B, C \in \mathbb{R}, g(x) \in L^2[0, 1)$ and the solution to be determined in [63] is $y(x)$.

Eq.(3.6.1) reduces to the Bagley-Torvik equation for $\alpha = 2, \beta = \frac{3}{2}$, which obtains when modelling the motion of a rigid plate immersed in a Newtonian fluid.

Table 3.1: Comparisons between numerical solutions attained by Euler wavelet based numerical scheme(EWM) for M=3 and various numerical methods

x	y_{exact}	$y_{EWM}(j=9)$	$y_{FDM}[6]$	$y_{ADM}[51]$	$y_{FDTM}[6]$	$y_{VIM}[51]$	$y_{LWM}(j=10)$ [63]
0.0	0.000000	0.000000	0.000000	0.000000	0.000000	0.000000	0.000000
0.1	0.039750	0.039750	0.039473	0.039874	0.039750	0.039874	0.039750
0.2	0.157036	0.157036	0.157703	0.158512	0.157036	0.158512	0.157035
0.3	0.347370	0.347370	0.352402	0.353625	0.347370	0.353625	0.347370
0.4	0.604695	0.604695	0.620435	0.622083	0.604695	0.622083	0.604695
0.5	0.921768	0.921768	0.957963	0.960047	0.921768	0.960047	0.921767
0.6	1.290457	1.290456	1.360551	1.363093	1.290457	1.363093	1.290456
0.7	1.702008	1.702008	1.823267	1.826257	1.702008	1.826257	1.702007
0.8	2.147287	2.147286	2.340749	2.344224	2.147287	2.344224	2.147286
0.9	2.617001	2.617000	2.907324	2.911278	2.617001	2.911278	2.617000

$$\text{Suppose } D^\alpha y(x) \simeq C^T \psi(x) \text{ and } g(x) \simeq F^T \psi(x) \quad (3.6.2)$$

$$\text{Then } D^\beta y(x) = I^{\alpha-\beta}(D^\alpha y)(x) = C^T P_{k \times k}^{\alpha-\beta} \psi(x) \quad (3.6.3)$$

and

$$y(x) = C^T P_{k \times k}^\alpha \psi(x) + y_0 + y_1 x \quad (3.6.4)$$

Using (3.6.2), (3.6.3) and (3.6.4) in (3.6.1), we have the following system of algebraic equations

$$AC^T \psi(x) + BC^T P_{k \times k}^{\alpha-\beta} \psi(x) + C[C^T P_{k \times k}^\alpha \psi(x) + y_0 + y_1(x)] = F^T \psi(x)$$

Table 3.1 compares the numerical solutions of (3.6.1) obtained by the proposed numerical method based on Euler wavelets(EWM) with the numerical solutions obtained by Finite Difference Method(FDM), Adomian Decomposition Method(ADM), Finite Difference Transform Method(FDTM), Variational Iteration Method(VIM) and Legendre Wavelet Method(LWM) when $\alpha = 2, \beta = \frac{1}{2}, A = B = C = 1, g(x) = 8$ and $y_0, y_1 = 0$. Clearly, the numerical scheme based on Euler wavelets is superior to the numerical schemes stated above, as seen by the comparisons of numerical solutions in Table 3.1.

3.6.2 Example 4

In Example 3.6.1, suppose $A=B=C=1$,

$$\alpha = 2, 0 \leq \beta \leq 1, y_0 = 0, y_1 = 0 \quad \text{and} \quad g(x) = 6x^3 \left(\frac{x^{-\alpha}}{\Gamma(4-\alpha)} - \frac{x^{-\beta}}{\Gamma(4-\beta)} \right)$$

Table 3.2: Comparisons of maximum absolute errors for different values of k and β

β	EWM		LWM		HWM	
	$k = 32$	$k = 128$	$k = 24$	$k = 96$	$k = 32$	$k = 128$
0.25	1.4205×10^{-5}	5.1634×10^{-6}	8.546×10^{-4}	5.343×10^{-5}	4.807×10^{-4}	3.005×10^{-5}
0.50	1.0680×10^{-4}	5.3760×10^{-7}	7.963×10^{-4}	4.978×10^{-5}	4.479×10^{-4}	2.800×10^{-5}
0.75	1.0605×10^{-4}	1.1484×10^{-5}	7.405×10^{-4}	4.631×10^{-5}	4.166×10^{-4}	2.605×10^{-5}
1.00	6.8563×10^{-5}	4.1935×10^{-5}	6.946×10^{-4}	4.341×10^{-5}	3.907×10^{-4}	2.442×10^{-5}

$y(x) = x^3$ is the exact solution. The absolute errors obtained by the proposed numerical scheme(EWM), Legendre wavelet method(LWM) and Haar wavelet method(HWM), are shown in Table 3.2. Table 3.2 shows that as k increases, the absolute errors become smaller and smaller. Table 3.2 further illustrates that the proposed numerical scheme exceeds Legendre and Haar wavelets in terms of accuracy, when compared to the results obtained by the Legendre and Haar wavelet schemes, this demonstrates that the numerical results obtained by the Euler wavelet based numerical scheme are in good agreement with the exact solution.

3.6.3 Example 5

Consider the fractional differential equation(3.6.5) for an Electrical Circuit with charged capacitor of capacitance C farads and resistor of resistance R ohms, as shown below

$$D^\beta Q(x) + \kappa Q(x) = 0, \quad \beta \in (0, 1], x \in [0, 1) \quad (3.6.5)$$

with initial state $Q(0) = Q_0$, where $\kappa = \frac{1}{RC}$,

The exact solution of (3.6.5) for $\beta = 1$ is $Q(x) = Q_0 e^{-\kappa x}$

Table 3.3: Comparisons between numerical solutions attained by Euler wavelet based numerical scheme and Legendre wavelet method

x	$\beta = 0.50$		$\beta = 0.75$		$\beta = 0.999$		<i>Exact</i> ($\beta = 1$)
	EWM	LWM	EWM	LWM	EWM	LWM	
0.1	19.3564	19.3481	19.6378	19.6340	19.8017	19.8012	19.8010
0.2	19.0219	19.0500	19.3599	19.3717	19.6042	19.6039	19.6040
0.3	18.8214	18.8163	19.1422	19.1413	19.4091	19.4086	19.4089
0.4	18.6545	18.6471	18.9462	19.9428	19.2165	19.2154	19.2158
0.5	18.4927	18.4976	18.7530	18.7573	19.0238	19.0242	19.0246
0.6	18.3680	18.3669	18.5861	18.5854	18.8359	18.8349	18.8353
0.7	18.2432	18.2450	18.4193	18.4207	18.6480	18.6475	18.6479
0.8	18.1312	18.1319	18.2623	18.2630	18.4625	18.4620	18.4623
0.9	18.0285	18.0275	18.1131	18.1124	18.2793	18.2784	18.2786

$$\text{Suppose } D^\beta Q(x) \simeq C^T \psi(x) \tag{3.6.6}$$

$$\text{Then } Q(x) = C^T P^\beta \psi(x) + Q_0 \tag{3.6.7}$$

Thus, using (3.6.6) and (3.6.7) in (3.6.5), we attain

$$C^T \psi(x) + \kappa [C^T P^\beta \psi(x) + Q_0] = 0 \tag{3.6.8}$$

The coefficients vector C may be obtained by solving the matrix equation(3.6.8).

Table 3.3 displays the numerical solutions to (3.6.5) obtained using EWM and LWM for $R = 10$, $C = 1$, $Q_0 = 20$ and various β values. The numerical method on Euler wavelets clearly outperforms the Legendre wavelet method, as shown in table 3.3.

3.6.4 Example 6

Consider the multi-term fractional differential equation [17, 42]

$$D^2 y(x) + 3Dy(x) + 2D^{q_2} y(x) + D^{q_1} y(x) + 5y(x) = f(x), \tag{3.6.9}$$

where $0 < q_1 < q_2 < 1$, $0 \leq x < 1$ and

$$f(x) = 1 + 3x + \frac{2}{\Gamma(3 - q_2)} x^{2-q_2} + \frac{1}{\Gamma(3 - q_1)} x^{2-q_1} + 5(1 + 0.5x^2)$$

with the initial states $y(0) = 1$, $y'(0) = 0$.

If $q_1 = 0.0159$ and $q_2 = 0.1379$, then the exact solution of (3.6.9) is given by

$$y(x) = 1 + 0.5x^2.$$

Table 3.4: Absolute errors for $M = 3$ and different values of j

x	j=3	j=5	j=7	j=9	j=11
0.1	2.7746e-04	1.7346e-05	1.0839e-06	6.7737e-08	4.2335e-09
0.2	2.4925e-04	1.5530e-05	9.7013e-07	6.0625e-08	3.7889e-09
0.3	2.1031e-04	1.3092e-05	8.1761e-07	5.1091e-08	3.1930e-09
0.4	1.6732e-04	1.0390e-05	6.4872e-07	4.0535e-08	2.5332e-09
0.5	1.2436e-04	7.6988e-06	4.8055e-07	3.0024e-08	1.8763e-09
0.6	8.4086e-05	5.2128e-06	3.2527e-07	2.0321e-08	1.2699e-09
0.7	4.9432e-05	3.0575e-06	1.9067e-07	1.1909e-08	7.4420e-10
0.8	2.1033e-05	1.2979e-06	8.0809e-08	5.0447e-09	3.1518e-10
0.9	7.3449e-07	4.8261e-08	3.2143e-09	2.0522e-10	1.2910e-11

Table 3.5: Comparison of maximum absolute errors for Euler wavelet based numerical scheme with $j = 3$, $M = 3$ and Adams-type Predictor-Corrector method

Step size	Maximum Absolute errors	
	EWM	Adams-type Predictor-Corrector Method
0.1	7.3449e-07	0.051115750000
0.01	7.3449e-07	0.004546523000
0.001	1.1577e-08	0.000409626200

$$\text{Suppose } D^2 y(x) \simeq C^T \psi(x) \text{ and } f(x) \simeq F^T \psi(x) \quad (3.6.10)$$

$$\text{Then } Dy(x) = C^T P_{k \times k} \psi(x) \quad (3.6.11)$$

$$D^{q_2} y(x) = C^T P_{k \times k}^{2-q_2} \psi(x) \quad (3.6.12)$$

$$D^{q_1} y(x) = C^T P_{k \times k}^{2-q_1} \psi(x) \quad (3.6.13)$$

and

$$y(x) = C^T P_{k \times k}^2 \psi(x) + 1 \quad (3.6.14)$$

Using (3.6.10)-(3.6.14) in (3.6.9), we arrive

$$\begin{aligned} C^T \psi(x) + 3C^T P_{k \times k} \psi(x) + 2C^T P_{k \times k}^{2-q_2} \psi(x) + C^T P_{k \times k}^{2-q_1} \psi(x) \\ + 5[C^T P_{k \times k}^2 \psi(x) + [1, 1, \dots, 1] \phi_{k \times k}^{-1} \psi(x)] = F^T \psi(x) \end{aligned} \quad (3.6.15)$$

Solving the system of algebraic equations (3.6.15), we can attain the coefficients vector C^T and so we can get the approximate output response $y(x)$. Table 3.4 shows that the absolute errors attained by the Euler wavelet based numerical scheme with $M=3$ and the values of j increasing, become smaller and smaller. From table 3.4, we also infer that the approximate solutions converge to the exact solution. Table 3.5 shows that the EWM can reach a higher degree of accuracy than Adams-type Predictor-Corrector Method.

3.6.5 Example 7

Consider the linear fractional differential equation

$$D^\alpha y(x) + y(x) = 0 \text{ with } 0 < \alpha \leq 2, 0 \leq x < 1, \text{ and } y(0) = 1, y'(0) = 0. \quad (3.6.16)$$

The second initial condition is only for $1 < \alpha \leq 2$. The exact solution of (3.6.16) is

$$y(x) = E_\alpha(-x^\alpha), \text{ where } E_\alpha(z) = \sum_0^\infty \frac{z^k}{\Gamma(\alpha k + 1)} \text{ is the Mittag-Leffler function of order } \alpha$$

Table 3.6: Absolute errors for different values of k and for $\alpha = 1.5$

x	$k = 12$	$k = 24$	$k = 48$	$k = 96$	$k = 192$	$k = 384$
0.1	6.8808e-04	6.9051e-05	2.2513e-05	7.0231e-06	1.7455e-06	4.156e-07
0.2	7.9552e-05	3.5316e-05	1.3415e-05	3.3178e-06	7.608e-07	1.911e-07
0.3	9.4834e-05	2.2910e-05	2.9444e-06	7.7780e-07	2.384e-07	5.91e-08
0.4	1.0088e-04	8.0418e-06	2.1604e-06	8.1000e-07	1.974e-07	4.58e-08
0.5	3.6805e-04	6.4931e-05	1.2401e-05	2.5924e-06	5.859e-07	1.4209e-07
0.6	1.6556e-04	5.2566e-05	1.3004e-05	3.0970e-06	7.968e-07	2.225e-07
0.7	2.7243e-04	6.6998e-05	1.5649e-05	4.0075e-06	1.1023e-06	3.5728e-07
0.8	2.8032e-04	7.0973e-05	1.9028e-05	5.0157e-06	1.5096e-06	6.49e-07
0.9	3.4727e-04	8.0723e-05	2.1038e-05	6.1479e-06	2.316e-06	1.3906e-06

Table 3.7: Comparison of maximum absolute errors for $\alpha = 1.5$, $M = 3$ and different values of j

	$j = 4$	$j = 5$	$j = 8$
EWM	8.042e-06	2.160e-06	4.58e-08
LWM	1.178e-05	2.948e-06	4.605e-08

$$\text{Suppose } D^\alpha y(x) \simeq C^T \psi(x) \tag{3.6.17}$$

$$\text{Then } y(x) = C^T P_{k \times k}^\alpha \psi(x) + 1 \tag{3.6.18}$$

Using (3.6.17) and (3.6.18) in (3.6.16), we arrive

$$C^T \psi(x) + C^T P_{k \times k}^\alpha \psi(x) + 1 = 0 \tag{3.6.19}$$

We can obtain the Euler coefficients vector C^T by solving the system (3.6.19) at the collocation points. The exact solution of (3.6.16) for $\alpha = 1$ is $y(x) = e^{-x}$, while for $\alpha = 2$, the exact solution of (3.5.16) is $y = \cos x$. Table 3.6 shows that as the value of k increases, the absolute errors achieved by the EWM become smaller and smaller. We can also deduce from Table 3.6 that approximate solutions converge to exact solutions. The maximum absolute errors achieved by the proposed numerical scheme and Legendre wavelet method(LWM) for $\alpha = 1.5, M = 3$ and various values of

j are shown in table 3.7. The numerical approach based on Euler wavelets is clearly superior to the Legendre wavelets method, as shown in table 3.7.

Chapter 4

Numerical solutions of fractional differential equations with variable coefficients by Bernoulli wavelet method

4.1 Introduction

This chapter addresses the numerical solutions of fractional differential equations with variable coefficients using Bernoulli wavelet based numerical scheme(BWM). The numerical scheme based on Bernoulli wavelets is simple and straight forward. The new technique is based upon Bernoulli polynomials, Bernoulli numbers and Bernoulli wavelet approximations. The properties of Bernoulli wavelets and Bernoulli polynomials are first presented. We then present the operational matrix of fractional integration of Bernoulli wavelets. We use this resulting Bernoulli wavelet operational matrix to reduce the fractional differential equation with variable coefficients into a

system of algebraic equations to get the required Bernoulli coefficients, which are computed by using Matlab. The numerical solutions of fractional differential equations by using BWM are compared with exact solutions and the comparison shows that BWM has the higher degree of accuracy. Convergence analysis of the BWM has been discussed in this Chapter. Some illustrative examples demonstrate the applicability and accuracy of Bernoulli wavelet based numerical scheme.

4.2 Bernoulli wavelet based numerical scheme

Wavelets are a family of functions generated by dilation and translation of a single function $\psi(x)$, termed the mother wavelet. We get the following family of continuous wavelets if the dilation and translation parameters c and d change continuously.

$$\psi_{cd}(x) = |c|^{-\frac{1}{2}}\psi\left(\frac{x-d}{c}\right), c, d \in (\mathbb{R}), c \neq 0.$$

If the translation and dilation parameters are chosen to have discrete values, that is, $c = c_0^{-p}, d = qd_0c_0^{-p}, c_0 > 1, d_0 > 0$ and $p, q \in \mathbb{Z}$, then we have the following family of discrete wavelets,

$$\psi_{pq}(x) = |c_0|^{\frac{p}{2}}\psi(c_0^p x - qd_0),$$

where the functions ψ_{pq} form a wavelet basis for $L^2(\mathbb{R})$. In particular, if $c_0 = 2$ and $d_0 = 1$, we can attain an orthonormal basis from $\psi_{pq}(x)$ for $L^2(\mathbb{R})$.

The Bernoulli wavelets are defined on $[0,1)$ as

$$\psi_{mn}(x) = \begin{cases} 2^{\frac{j-1}{2}} \widetilde{E}_n(2^{j-1}x - m + 1), & \frac{m-1}{2^{j-1}} \leq x < \frac{m}{2^{j-1}}, \\ 0, & \text{otherwise,} \end{cases} \quad (4.2.1)$$

for $m = 1, 2, \dots, 2^{j-1}$, $n = 0, 1, \dots, N - 1$ and $j, N \in \mathbb{N}$, where

$$\widetilde{E}_n(x) = \begin{cases} 1, & n = 0, \\ \frac{1}{\sqrt{\binom{(-1)^{n-1}(n!)^2}{(2n)!} \beta_{2n}}} E_n(x), & n > 0, \end{cases}$$

the coefficient $\frac{1}{\sqrt{\binom{(-1)^{n-1}(n!)^2}{(2n)!} \beta_{2n}}}$ is used for normality, the dilation parameter is $2^{-(j-1)}$ and the translation parameter is $(m - 1)2^{-(j-1)}$. Here $E_n(x)$, $n = 0, 1, \dots, N - 1$, denote Bernoulli polynomials of order n which can be defined by the relation

$$E_n(x) = \sum_{r=0}^n \binom{n}{r} \beta_r x^{n-r}, \quad (4.2.2)$$

where β_r , ($r = 0, 1, 2, \dots, n$) are Bernoulli numbers. Bernoulli numbers can be defined by the following generating function

$$\frac{x}{e^x - 1} = \sum_{r=0}^{\infty} \beta_r \frac{x^r}{r!}. \quad (4.2.3)$$

The first few Bernoulli numbers are

$$\beta_0 = 1, \beta_1 = -\frac{1}{2}, \beta_2 = \frac{1}{6}, \beta_4 = -\frac{1}{30}, \dots, \quad (4.2.4)$$

with $\beta_{2r+1} = 0$, $r = 1, 2, 3, \dots$

The first few Bernoulli polynomials are

$$E_0(x) = 1, E_1(x) = x - \frac{1}{2}, E_2(x) = x^2 - x + \frac{1}{6}, E_3(x) = x^3 - \frac{3}{2}x^2 + \frac{1}{2}x, \dots \quad (4.2.5)$$

4.3 Properties of Bernoulli polynomials and Bernoulli wavelets

The properties of Bernoulli polynomials and Bernoulli wavelets have been discussed in [65].

Moreover,

$$\int_0^1 E_m(x)E_n(x)dx = (-1)^{m-1} \frac{n!m!}{(n+m)!} \beta_{m+n}, \quad n, m \geq 1, \quad (4.3.1)$$

and

$$\int_0^1 |E_n(x)|dx \leq 16 \frac{n!}{(2\pi)^{n+1}}, \quad n \geq 0. \quad (4.3.2)$$

Let $\psi(x) = [\psi_1(x), \psi_2(x), \dots, \psi_k(x)]^T$, where $\psi_i(x) = \psi_{mn}(x)$, $i = N(m-1)+n+1$, $k = 2^{j-1}N$, $m = 1, 2, \dots, 2^{j-1}$, $n = 0, 1, \dots, N-1$ and $j, N \in \mathbb{N}$. Then Bernoulli wavelets have the following orthonormality properties.

$$\langle \psi_r(x), \psi_s(x) \rangle = \int_0^1 \psi_r(x)\psi_s(x)dx = \begin{cases} 1, & r = s, \\ 0, & r \neq s, \end{cases} \quad (4.3.3)$$

and

$$\int_0^1 \Psi(x)\Psi^T(x)dx = E, \quad (4.3.4)$$

where $\langle \cdot, \cdot \rangle$ denotes the inner product and E indicates identity matrix.

4.4 Function approximation by Bernoulli wavelets

A function $h(x) \in L^2[0, 1)$ can be expressed in terms of Bernoulli wavelets as

$$h(x) = \sum_{m=0}^{\infty} \sum_{n \in \mathbb{Z}} a_{mn} \psi_{mn}(x), \quad (4.4.1)$$

where the coefficients a_{mn} are given by

$$a_{mn} = \langle h(x), \psi_{mn}(x) \rangle = \int_0^1 h(x) \psi_{mn}(x) dx.$$

By truncating the infinite series in Equation (4.4.1), $h(x)$ is approximated as

$$\widetilde{h}(x) \approx \sum_{m=1}^{2^{j-1}} \sum_{n=0}^{N-1} a_{mn} \psi_{mn}(x). \quad (4.4.2)$$

For simplicity, Equation (4.4.2) is written as

$$\widetilde{h}(x) = \sum_{i=1}^k a_i \psi_i(x) = A^T \Psi(x), \quad (4.4.3)$$

$$\text{where } a_i = a_{mn}, \psi_i = \psi_{mn}, k = 2^{j-1}N, A = [a_1, a_2, \dots, a_k]^T, \quad (4.4.4)$$

and

$$\Psi(x) = [\psi_1(x), \psi_2(x), \dots, \psi_k(x)]^T. \quad (4.4.5)$$

The index i is determined by the relation $i = N(m - 1) + n + 1$.

We define the Bernoulli wavelet coefficient matrix $\phi_{k \times k}$, $k = 2^{j-1}N$, at the collocation points $x_r = \frac{2r-1}{2k}$, $r = 1, 2, \dots, k$ as

$$\phi_{k \times k} = \left[\Psi \left(\frac{1}{2k} \right), \Psi \left(\frac{3}{2k} \right), \dots, \Psi \left(\frac{2k-1}{2k} \right) \right]. \quad (4.4.6)$$

Specifically, the Bernoulli wavelet coefficient matrix for $j = 2$ and $N = 3$ becomes

$$\phi_{6 \times 6} = \begin{pmatrix} 1.4142 & 1.4142 & 1.4142 & 0 & 0 & 0 \\ -1.6330 & 0 & 1.6330 & 0 & 0 & 0 \\ 0.5270 & -1.5811 & 0.5270 & 0 & 0 & 0 \\ 0 & 0 & 0 & 1.4142 & 1.4142 & 1.4142 \\ 0 & 0 & 0 & -1.6330 & 0 & 1.6330 \\ 0 & 0 & 0 & 0.5270 & -1.5811 & 0.5270 \end{pmatrix}. \quad (4.4.7)$$

Here, we have

$$\tilde{h}_k = [\tilde{h}(x_1), \tilde{h}(x_2), \dots, \tilde{h}(x_k)] = A^T \phi_{k \times k}.$$

Since the Bernoulli wavelet coefficient matrix $\phi_{k \times k}$ is invertible, it is possible to obtain the Bernoulli wavelet coefficient vector A^T by $\tilde{h}_k \phi_{k \times k}^{-1}$.

4.5 Operational matrix of fractional order integration of Bernoulli wavelets

In this section, we explore the basic idea of finding the operational matrix of fractional order integration for the Bernoulli wavelets.

A k -set of Block pulse functions (BPFs) over the interval $[0,1)$ is defined as

$$b_r(x) = \begin{cases} 1, & (r-1)/k \leq x < r/k, \\ 0, & \text{otherwise,} \end{cases} \quad (4.5.1)$$

where $r = 1, 2, 3, \dots, k$.

It is known that any square integrable function $h(x)$ defined on the interval $[0,1)$ can

be extended in terms of BPFs, and by using orthogonality of BPFs as

$$h(x) \simeq \sum_{r=1}^k h_r b_r(x) = h^T B_k(x), \quad (4.5.2)$$

where $h = [h_1, h_2, \dots, h_k]^T$, h_r for $r = 1, 2, \dots, k$ are given by

$$h_r = \frac{1}{k} \int_{(r-1)/k}^{r/k} h(x) b_r(x) dx, \text{ and } B_k(x) = [b_1(x), b_2(x), \dots, b_k(x)]^T.$$

There is a connection between the block pulse functions and Bernoulli wavelets, which is,

$$\Psi(x) = \phi_{k \times k} B_k(x). \quad (4.5.3)$$

The block pulse operational matrix H^β , $\beta \geq 0$ of fractional integration of order $\beta \geq 0$ is defined as,

$$(I^\beta B_k)(x) \approx H^\beta B_k(x), \quad (4.5.4)$$

where

$$H^\beta = \frac{1}{k^\beta} \frac{1}{\Gamma(\beta + 2)} \begin{pmatrix} 1 & \zeta_1 & \zeta_2 & \zeta_3 & \dots & \zeta_{k-1} \\ 0 & 1 & \zeta_1 & \zeta_2 & \dots & \zeta_{k-2} \\ 0 & 0 & 1 & \zeta_1 & \dots & \zeta_{k-3} \\ \vdots & \vdots & \ddots & \ddots & \vdots & \vdots \\ 0 & 0 & \dots & 0 & 1 & \zeta_1 \\ 0 & 0 & \dots & 0 & 0 & 1 \end{pmatrix},$$

$$\text{with } \zeta_j = (j+1)^{\beta+1} - 2j^{\beta+1} + (j-1)^{\beta+1}.$$

The fractional integration of order $\beta \geq 0$ of the vector $\Psi(x)$ defined in Equation (4.4.5) can be approximated as

$$(I^\beta \Psi)(x) \approx P_{k \times k}^\beta \Psi(x), \quad (4.5.5)$$

where $P_{k \times k}^\beta$ is called Bernoulli wavelet operational matrix of order $\beta \geq 0$.

Using Equations (4.5.3) and (4.5.4), we attain

$$(I^\beta \Psi)(x) \approx (I^\beta \phi_{k \times k} B_k)(x) = \phi_{k \times k} (I^\beta B_k)(x) \approx \phi_{k \times k} H^\beta B_k(x). \quad (4.5.6)$$

Thus combining Equations (4.5.5) and (4.5.6), we attain

$$P_{k \times k}^\beta \Psi(x) \approx (I^\beta \Psi)(x) \approx \phi_{k \times k} H^\beta B_k(x) = \phi_{k \times k} H^\beta \phi_{k \times k}^{-1} \Psi(x), \quad \text{and so} \quad (4.5.7)$$

$$P_{k \times k}^\beta \approx \phi_{k \times k} H^\beta \phi_{k \times k}^{-1}. \quad (4.5.8)$$

For example, the Bernoulli wavelet operational matrix of the fractional order integration for $j = 2$, $N = 3$ and $\beta = 0.5$ yields

$$P_{6 \times 6}^{0.5} = \begin{pmatrix} 0.5282 & 0.1819 & -0.0298 & 0.4438 & -0.0871 & 0.0256 \\ -0.1452 & 0.2243 & 0.1329 & 0.0799 & -0.0449 & 0.0198 \\ -0.0598 & -0.0964 & 0.1688 & -0.0417 & -1.8589e - 04 & 0.0029 \\ 0 & 0 & 0 & 0.5282 & 0.1819 & -0.0298 \\ 0 & 0 & 0 & -0.1452 & 0.2243 & 0.1329 \\ 0 & 0 & 0 & -0.0598 & -0.0964 & 0.1688 \end{pmatrix}. \quad (4.5.9)$$

Since the operational matrix $P_{6 \times 6}^{0.5}$ contains several zeros, the proposed technique reduces the computation greatly.

4.6 Convergence Analysis

In the following theorem, we establish the convergence of the Bernoulli wavelets expansion [57].

Theorem 4.6.1. *If $h(x) \in L^2[0, 1)$ is a continuous function and $|h(x)| \leq \eta$, $\eta \in \mathbb{R}$, then the Bernoulli wavelets expansion of $h(x)$ defined in Equation (4.3.1) converges uniformly and also*

$$|a_{m,n}| < \eta \frac{F}{2^{\frac{j-1}{2}}} \frac{16n!}{(2\pi)^{n+1}}, \quad (4.6.1)$$

where

$$F = \frac{1}{\sqrt{\left(\frac{(-1)^{n-1}(n!)^2}{(2n)!}\right)\beta_{2n}}}.$$

Proof. Any function $h(x) \in L^2[0, 1)$ can be approximated in terms of Bernoulli wavelets as

$$h(x) \simeq \sum_{m=1}^{2^{j-1}} \sum_{n=0}^{N-1} a_{mn} \psi_{mn}(x), \quad (4.6.2)$$

Here

$$\begin{aligned} a_{mn} &= \int_0^1 h(x) \psi_{mn}(x) dx \\ &= \sum_m \int_{I_{j,m}} h(x) \psi_{mn}(x) dx, \text{ where } I_{j,m} = \left[\frac{m-1}{2^{j-1}}, \frac{m}{2^{j-1}} \right), m = 1, 2, \dots, 2^{j-1}, \end{aligned} \quad (4.6.3)$$

$$= 2^{\frac{j-1}{2}} F \sum_m \int_{I_{j,m}} h(x) E_n(2^{j-1}x - m + 1) dx, \text{ where } F = \frac{1}{\sqrt{\left(\frac{(-1)^{n-1}(n!)^2}{(2n)!}\right)\beta_{2n}}}. \quad (4.6.4)$$

Using $2^{j-1}x - m + 1 = t$, we have

$$a_{mn} = \frac{F}{2^{j-1}} \sum_m \int_{I_{j,m}} h\left(\frac{t+m-1}{2^{j-1}}\right) E_n(t) dt, \quad (4.6.5)$$

and so

$$|a_{mn}| = \left| \frac{F}{2^{\frac{j-1}{2}}} \sum_m \int_{I_{j,m}} h\left(\frac{t+m-1}{2^{j-1}}\right) E_n(t) dt \right| \leq \frac{F\eta}{2^{\frac{j-1}{2}}} \int_0^1 |E_n(t)| dt < \frac{F\eta}{2^{\frac{j-1}{2}}} 16 \frac{n!}{(2\pi)^{n+1}}. \quad (4.6.6)$$

Thus the series $\sum_{m=1}^{2^{j-1}} \sum_{n=0}^{N-1} a_{mn}$ is absolutely convergent, and so the series

$\sum_{m=1}^{2^{j-1}} \sum_{n=0}^{N-1} a_{mn} \psi_{mn}(x)$ is uniformly convergent. \square

4.7 Algorithm for the Bernoulli wavelet based numerical scheme

- Step 1:** Assign the values for j and N for step size $k = 2^{j-1}N$ in Equation (4.4.4).
- Step 2:** Compute Bernoulli wavelet coefficient matrix $\phi_{k \times k}$ at the collocation points $x_r = \frac{2r-1}{2k}$, $r = 1, 2, \dots, k$ from Equation (4.4.6).
- Step 3:** Compute the block pulse operational matrix H^β from Equation (4.5.4).
- Step 4:** Construct Bernoulli wavelet operational matrix $P_{k \times k}^\beta$ of order $\beta \geq 0$ using Equation (4.5.8).
- Step 5:** Dispersing the coefficients of the given fractional differential equations at the collocation points, construct diagonal matrices.
- Step 6:** Express all Caputo fractional derivatives in the given fractional differential equations in terms of Bernoulli wavelets.
- Step 7:** Solve the system of algebraic equations using MATLAB2015a to compute the unknown vector.
- Step 8:** Compute the solution using the unknown vector and the Bernoulli wavelet operational matrix.

4.8 Numerical Examples

To show the applicability and the effectiveness of the Bernoulli wavelet based numerical scheme, we consider here some fractional differential equations with variable coefficients.

4.8.1 Example 8

Consider the following fractional order linear differential equation with variable coefficients

$$r[D^2h(x)] + s(x)[D^{\gamma_2}h(x)] + t(x)[Dh(x)] + u(x)[D^{\gamma_1}h(x)] + v(x)h(x) = w(x), \quad (4.8.1)$$

with $0 \leq x < 1, 0 < \gamma_1 \leq 1, 1 < \gamma_2 \leq 2, h(0) = 2$ and $h'(0) = 0$,

where $r \in \mathbb{R}, s(x), t(x), u(x), v(x), h(x), w(x) \in L^2[0, 1)$,

$$w(x) = -r - \frac{s(x)}{\Gamma(3 - \gamma_2)}x^{2-\gamma_2} - t(x)x - \frac{u(x)}{\Gamma(3 - \gamma_2)}x^{2-\gamma_2} + v(x)\left(2 - \frac{1}{2}x^2\right).$$

Suppose

$$D^2h(x) \simeq A^T\Psi(x) \text{ where } A = [a_1, a_2, \dots, a_k]^T, \text{ and} \quad (4.8.2)$$

$$w(x) \simeq W^T\Psi(x) \text{ where } W = [w_1, w_2, \dots, w_k].$$

$$\text{Then } D^{\gamma_2}h(x) = A^T P_{k \times k}^{2-\gamma_2}\Psi(x), \quad (4.8.3)$$

$$D^{\gamma_1}h(x) = A^T P_{k \times k}^{2-\gamma_1}\Psi(x), \quad (4.8.4)$$

$$Dh(x) = A^T P_{k \times k}\Psi(x), \quad (4.8.5)$$

$$\text{and } h(x) = A^T P_{k \times k}^2\Psi(x) + 2. \quad (4.8.6)$$

Using Equations (4.8.2) - (4.8.6) in (4.8.1), we attain

$$\begin{aligned} [rA^T]\Psi(x) + [A^T P_{k \times k}^{2-\gamma_2}]\Psi(x)s(x) + [A^T P_{k \times k}]\Psi(x)t(x) + [A^T P_{k \times k}^{2-\gamma_1}]\Psi(x)u(x) \\ + [A^T P_{k \times k}^2]\Psi(x)v(x) + 2v(x) = W^T \Psi(x). \end{aligned} \quad (4.8.7)$$

Dispersing the coefficients $s(x), t(x), u(x), v(x)$ at the collocation points, construct the following matrices.

$$\begin{aligned} S &= \begin{pmatrix} s(x_1) & 0 & \dots & 0 \\ 0 & s(x_2) & \dots & 0 \\ \vdots & \ddots & \ddots & \vdots \\ 0 & \dots & 0 & s(x_k) \end{pmatrix}, \quad T = \begin{pmatrix} t(x_1) & 0 & \dots & 0 \\ 0 & t(x_2) & \dots & 0 \\ \vdots & \ddots & \ddots & \vdots \\ 0 & \dots & 0 & t(x_k) \end{pmatrix}, \\ U &= \begin{pmatrix} u(x_1) & 0 & \dots & 0 \\ 0 & u(x_2) & \dots & 0 \\ \vdots & \ddots & \ddots & \vdots \\ 0 & \dots & 0 & u(x_k) \end{pmatrix}, \quad V = \begin{pmatrix} v(x_1) & 0 & \dots & 0 \\ 0 & v(x_2) & \dots & 0 \\ \vdots & \ddots & \ddots & \vdots \\ 0 & \dots & 0 & v(x_k) \end{pmatrix}. \end{aligned}$$

Discretizing Equation (4.8.7), we can achieve

$$\begin{aligned} rA^T \phi_{k \times k} + A^T P^{2-\gamma_2} \phi_{k \times k} \cdot S + A^T P \phi_{k \times k} \cdot T + A^T P^{2-\gamma_1} \phi_{k \times k} \cdot U \\ + [A^T P^2 \phi_{k \times k} + Y] \cdot V = W^T \phi_{k \times k}, \end{aligned} \quad (4.8.8)$$

where $Y = [2, 2, \dots, 2]_{1 \times k}$. At the collocation points $x_i = (2i-1)/2k$, $i = 1, 2, \dots, k$, we transform Equation (4.8.8) into a system of algebraic equations. Solving this system of algebraic equations using MATLAB2015a, we can easily obtain A^T .

Suppose

$$r = 1, s(x) = x^{1/2}, t(x) = x^{1/3}, u(x) = x^{1/4}, v(x) = x^{1/5}, \gamma_1 = 0.333, \gamma_2 = 1.234.$$

Then the exact solution of Equation (4.8.1) for $\gamma_1 = 0.333$ and $\gamma_2 = 1.234$ is

Table 4.1: Maximum absolute errors for various choices of j and N .

k	48	96	192	384	768
	$(j = 3, N = 3)$	$(j = 4, N = 3)$	$(j = 5, N = 3)$	$(j = 6, N = 3)$	$(j = 7, N = 3)$
The proposed method	1.5100e-05	3.8168e-06	9.6282e-07	2.4249e-07	6.0990e-08

Table 4.2: Adams type Predictor-Corrector method [20].

Step size	Maximum absolute errors
0.1	0.023658990000
0.01	0.000986218500
0.001	0.000043988230

$$h(x) = 2 - \frac{1}{2}x^2.$$

In Tables 4.1 and 4.2, the maximum absolute error obtained using Adams type Predictor-Corrector method is $4.40\text{e-}05$ in 1000^{th} step, while the maximum absolute error using the Bernoulli wavelet based numerical scheme is $1.51\text{e-}05$ in 48^{th} step. We also see clearly from Table 4.1 that the numerical solutions are in perfect agreement with the exact solutions for larger values of k . Numerical results of this problem demonstrate that the Bernoulli wavelet based numerical scheme converges rapidly and is more efficient than the Adams type predictor-corrector method [20]. Also from Figure 4.1, we see clearly that the numerical solutions are in perfect agreement with the exact solutions.

4.8.2 Example 9

Consider the following fractional differential equation

$$D^{1/3}h(x) + x^{1/3}h(x) = w(x), \quad x \in [0, 4], \quad (4.8.9)$$

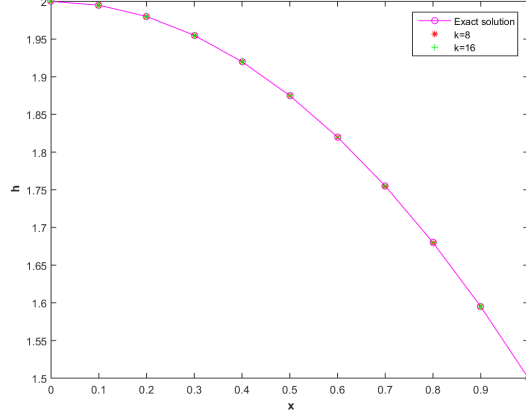


Figure 4.1: Comparison of Numerical solutions of Example 5.1 for $k = 8$ ($j = 3, N = 2$) and $k = 16$ ($j = 4, N = 2$) with the Exact solutions.

with the initial state $h(0) = 0$ and $w(x) = \frac{3}{2\Gamma(2/3)}x^{2/3} + x^{4/3}$. The exact solution of Equation (4.8.9) is $h(x) = x$.

Let $t = x/4$. Then $x = 4t, t \in [0, 1)$.

Thus

$$D^{1/3}h(4t) + (4t)^{1/3}h(4t) = v(t), \quad (4.8.10)$$

where

$$v(t) = w(4t) = \frac{3 \cdot 2^{1/3}}{\Gamma(2/3)}t^{2/3} + (4t)^{4/3}, \quad t \in [0, 1).$$

Approximating

$$D^{1/3}h(4t) \text{ as } A^T \Psi(t) \text{ where } A = [a_1, a_2, \dots, a_k]^T, \quad (4.8.11)$$

we have

$$h(4t) = A^T P^{1/3} \Psi(t). \quad (4.8.12)$$

Table 4.3: Absolute errors for various choices of j and for $N = 2$.

x	$k = 8$		$k = 16$		$k=32$	
	$(j = 3, N = 2)$		$(j = 4, N = 2)$		$(j = 5, N = 2)$	
	BWM	HWM	BWM	HWM	BWM	HWM
0.25	3.4042e-02	4.6972e-02	1.0979e-02	2.5554e-02	1.6860e-03	6.3723e-03
0.75	5.2261e-03	1.8818e-02	1.7086e-03	7.7490e-03	4.8561e-04	2.6655e-03
1.25	2.9291e-03	1.2333e-02	9.1120e-04	4.9465e-03	2.7618e-04	1.7841e-03
1.75	1.8933e-03	9.2464e-03	5.9425e-04	3.6780e-03	1.8461e-04	1.3549e-03
2.25	1.3507e-03	7.4107e-03	4.2765e-04	3.2651e-03	1.3471e-04	1.3549e-03
2.75	1.0238e-03	6.1850e-03	3.2668e-04	2.6691e-03	1.0387e-04	1.0953e-03
3.25	8.0889e-04	5.3060e-03	2.5985e-04	2.0961e-03	8.3183e-05	9.1997e-04
3.75	6.5879e-04	4.6437e-03	2.1286e-04	1.8332e-03	6.8503e-05	6.9676e-04

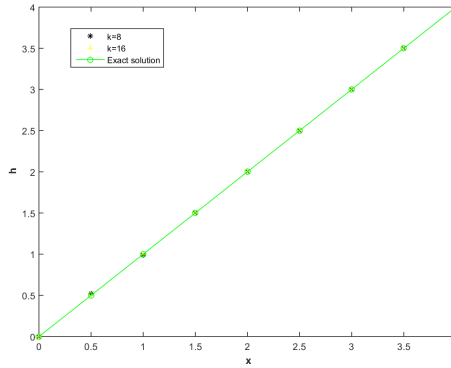


Figure 4.2: Comparison of Numerical solutions of Example 5.2 for $k = 8$ ($j = 3, N = 2$) and $k = 16$ ($j = 4, N = 2$) with the Exact solutions.

Similarly, $v(t)$ can be approximated by the Bernoulli wavelet functions as

$$v(t) = V^T \Psi(t), \text{ where } V = [v_1, v_2, \dots, v_k]^T. \quad (4.8.13)$$

Using Equations (4.8.11), (4.8.12) and (4.8.13) in Equation (4.8.10), we have

$$A^T \Psi(t) + (4t)^{1/3} A^T P^{1/3} \Psi(t) = V^T \Psi(t). \quad (4.8.14)$$

Dispersing the coefficient $(4t)^{1/3}$ of Equation (4.8.14) at the collocation points, construct the following matrix.

$$R = \begin{pmatrix} (4t_1)^{(1/3)} & 0 & \dots & 0 \\ 0 & (4t_2)^{(1/3)} & \dots & 0 \\ \vdots & \ddots & \ddots & \vdots \\ 0 & \dots & 0 & (4t_k)^{(1/3)} \end{pmatrix}.$$

Discretizing Equation (4.8.14), we get

$$A^T \phi_{k \times k} + A^T P^{1/3} \phi_{k \times k} \cdot R = V^T \phi_{k \times k}. \quad (4.8.15)$$

We convert Equation (4.8.15) into a system of algebraic equations at the collocation points $t_i = \frac{2i-1}{2^j N}$, $i = 1, 2, \dots, 2^{j-1}N$. Solving this system of algebraic equations using MATLAB2015a, we can easily obtain the coefficients vector A^T . Then we get the numerical solutions $h(4t)$ of Equation (4.8.10). The numerical solutions $h(x)$ of Equation (4.8.9) are obtained by $h(x) = A^T P^{1/3} \psi(x/4)$.

The numerical results for $k = 8$ ($j = 3, N = 2$) and $k = 16$ ($j = 4, N = 2$) are shown in Figure 4.2. The numerical solutions are in good agreement with the exact solutions, as can be seen from Figure 4.2. Table 4.3 displays the absolute errors for various k values. We also see from Table 4.3 that as k increases, the errors become smaller and the Bernoulli wavelet based numerical scheme is more accurate compared with the Haar wavelets method.

Chapter 5

Numerical solutions of multi-order fractional differential equations by Chebyshev wavelet method

5.1 Introduction

The motivation of the present chapter is to solve multi-order fractional differential equations using the Chebyshev wavelet based numerical scheme. A fractional derivative is employed in accordance with the Caputo definition. Chebyshev wavelets are the types of wavelets constructed from Chebyshev polynomials as their basis functions. They have very excellent interpolating properties and give better accuracy for numerical approximations. Chebyshev wavelet-based techniques have drawn a lot of interest over the past ten years. The existence of four different types of Chebyshev polynomials is well known. The first and second types of Chebyshev polynomials are specific examples of symmetric Jacobi polynomials, whereas the third and fourth types are particular examples of non-symmetric Jacobi polynomials. The first and

second types of Chebyshev polynomials and their numerous applications have received a lot of attentions. However, there aren't many publications that focus on the wavelets that can be used in fractional partial differential equations when they are shaped by these two kinds of Chebyshev polynomials. Our curiosity in such wavelets is motivated by this.

The use of Chebyshev wavelets approximations based on collocation spectral method has a number of benefits. First, it is currently common for them to be characterized by the use of exponentially decaying errors, contrary to the majority of numerical methods. Second, while wavelet approximations successfully handle the problem's singularities, other numerical approaches perform poorly when used close to singularities. In the end, Chebyshev wavelet-based numerical schemes do not experience the instability problems pertaining with other numerical approaches because of their result oriented. In this chapter, one of our goals is to extend the applications of the third kind Chebyshev wavelets. Several wavelet functions with unknown coefficients are used to estimate the solution. The numerical simulations are performed by using Chebyshev wavelet method. The comparison shows that Chebyshev wavelet based numerical scheme has good accuracy.

5.2 Chebyshev wavelet based numerical scheme

Wavelets are a family of functions generated by dilation and translation of a single function $\psi(x)$, termed the mother wavelet. We get the following family of continuous wavelets if the dilation and translation parameters c and d change continuously.

$$\psi_{cd}(x) = |c|^{-\frac{1}{2}} \psi\left(\frac{x-d}{c}\right), c, d \in (\mathbb{R}), c \neq 0.$$

If the translation and dilation parameters are chosen to have discrete values, that is, $c = c_0^{-p}, d = qd_0c_0^{-p}, c_0 > 1, d_0 > 0$ and $p, q \in \mathbb{Z}$, then we have the following family of discrete wavelets,

$$\psi_{pq}(x) = |c_0|^{\frac{p}{2}} \psi(c_0^p x - qd_0),$$

where the functions ψ_{pq} form a wavelet basis for $L^2(\mathbb{R})$. In particular, if $c_0 = 2$ and $d_0 = 1$, we can attain an orthonormal basis from $\psi_{pq}(x)$ for $L^2(\mathbb{R})$.

A family of Chebyshev wavelets over the interval $[0,1)$ is defined by

$$\psi_{mn}(t) = \begin{cases} 2^{\frac{j}{2}} \widetilde{U}_n(2^j t - 2m + 1), & \frac{m-1}{2^{j-1}} \leq t < \frac{m}{2^{j-1}}, \\ 0, & \text{otherwise,} \end{cases}$$

where $m = 1, 2, \dots, 2^{j-1}, n = 0, 1, \dots, M-1, j, M \in \mathbb{N}, \widetilde{U}_n(t) = \frac{1}{\sqrt{\pi}} U_n(t)$ and $U_n(t)$'s

denote the Chebyshev polynomials of third kind of degree n , which are mutually orthogonal with respect to the weight function $\omega(t) = \frac{\sqrt{(1+t)}}{\sqrt{(1-t)}}$ on the interval $[-1,1]$ and satisfy the following recursive formula $U_0(t) = 1, U_1(t) = 2t - 1, U_{n+1}(t) = 2tU_n(t) - U_{n-1}(t)$.

5.3 Function approximation by Chebyshev wavelets

The Chebyshev wavelets can be used to expand any function $f(t) \in L^2[0, 1)$ as

$$f(t) = \sum_{m=0}^{\infty} \sum_{n=0}^{\infty} d_{mn} \psi_{mn}(t), \quad (5.3.1)$$

where $d_{mn} = \langle f(t), \psi_{mn}(t) \rangle = \int_0^1 f(t) \psi_{mn}(t) \omega_m(t) dt$, and $\langle \cdot, \cdot \rangle$ denotes the

inner product on $L_{\omega_m}^2[0, 1)$.

By truncating the infinite series in (5.3.1), $f(t)$ is approximated as

$$f(t) \approx \sum_{m=1}^{2^{j-1}} \sum_{n=0}^{M-1} a_{mn} \psi_{mn}(t) = A^T \Psi(t), \quad (5.3.2)$$

where A and $\Psi(t)$ are $2^{j-1}M \times 1$ matrices, given by

$$A = [a_{10}, a_{11}, \dots, a_{1(M-1)}, a_{20}, \dots, a_{2(M-1)}, \dots, a_{2^{j-1}0}, \dots, a_{2^{j-1}(M-1)}]^T \text{ and} \quad (5.3.3)$$

$$\Psi(t) = [\psi_{10}, \psi_{11}, \dots, \psi_{1(M-1)}, \psi_{20}, \dots, \psi_{2(M-1)}, \dots, \psi_{2^{j-1}0}, \dots, \psi_{2^{j-1}(M-1)}]^T. \quad (5.3.4)$$

We define the Chebyshev wavelet matrix $\phi_{\hat{n} \times \hat{n}}$ at the collocation points

$$t_i = \frac{2i-1}{2^j M}, i = 1, 2, \dots, 2^{j-1}M \text{ as } \phi_{\hat{n} \times \hat{n}} = \left[\Psi \left(\frac{1}{2\hat{n}} \right), \Psi \left(\frac{3}{2\hat{n}} \right), \dots, \Psi \left(\frac{2\hat{n}-1}{2\hat{n}} \right) \right],$$

where $\hat{n} = 2^{j-1}M$. Specifically, for $j = 2$ and $M = 3$, the Chebyshev wavelet matrix

becomes

$$\phi_{6 \times 6} = \begin{pmatrix} 1.1284 & 1.1284 & 1.1284 & 0 & 0 & 0 \\ -2.6329 & -1.1284 & 0.3761 & 0 & 0 & 0 \\ 2.3821 & -1.1284 & -0.6269 & 0 & 0 & 0 \\ 0 & 0 & 0 & 1.1284 & 1.1284 & 1.1284 \\ 0 & 0 & 0 & -2.6329 & -1.1284 & 0.3761 \\ 0 & 0 & 0 & 2.3821 & -1.1284 & -0.6269 \end{pmatrix}.$$

5.4 The Chebyshev wavelet Operational matrix of fractional integration

In this section, we explore the basic idea of finding the fractional integration operational matrix of the Chebyshev wavelets.

An \hat{n} set of Block pulse functions(BPFs) is defined as

$$b_i(t) = \begin{cases} 1, & (i-1)/\hat{n} \leq t < i/\hat{n}, \\ 0, & \text{otherwise,} \end{cases} \quad \text{where } i = 1, 2, 3, \dots, \hat{n}.$$

$$\text{For } t \in [0, 1), \quad b_i(t)b_j(t) = \begin{cases} 0, & i \neq j, \\ b_i(t), & i = j, \end{cases} \quad \text{and} \quad \int_0^1 b_i(\tau)b_j(\tau)d\tau = \begin{cases} 0, & i \neq j, \\ \frac{1}{\hat{n}}, & i = j. \end{cases}$$

In terms of \hat{n} set of BPFs, any function $f(t) \in L^2[0, 1)$ can be expanded as follows:

$$f(t) = \sum_{i=1}^{\hat{n}} f_i b_i(t) = f^T B_{\hat{n}}(t),$$

$$\text{where } f = [f_1, f_2, \dots, f_{\hat{n}}]^T, \quad f_i = \frac{1}{\hat{n}} \int_{(i-1)/\hat{n}}^{i/\hat{n}} f(t)b_i(t)dt \quad \text{and} \quad B_{\hat{n}}(t) = [b_1(t), b_2(t), \dots, b_{\hat{n}}(t)]^T.$$

The Chebyshev wavelet matrix can be expressed as

$$\Psi(t) = \phi_{\hat{n} \times \hat{n}} B_{\hat{n}}(t). \tag{5.4.1}$$

The block pulse operational matrix F^β of fractional integration I^β is defined as

$$(I^\beta B_{\hat{n}})(t) \approx F^\beta B_{\hat{n}}(t), \quad (5.4.2)$$

$$\text{where } F^\beta = \frac{1}{\hat{n}^\beta} \frac{1}{\Gamma(\beta+2)} \begin{pmatrix} 1 & \zeta_1 & \zeta_2 & \zeta_3 & \dots & \zeta_{\hat{n}-1} \\ 0 & 1 & \zeta_1 & \zeta_2 & \dots & \zeta_{\hat{n}-2} \\ 0 & 0 & 1 & \zeta_1 & \dots & \zeta_{\hat{n}-3} \\ \vdots & \vdots & \ddots & \ddots & \vdots & \vdots \\ 0 & 0 & \dots & 0 & 1 & \zeta_1 \\ 0 & 0 & \dots & 0 & 0 & 1 \end{pmatrix},$$

$$\text{with } \xi_j = (j+1)^{\beta+1} - 2j^{\beta+1} + (j-1)^{\beta+1}.$$

The fractional integration of order $\beta \geq 0$ of the vector $\Psi(t)$ defined in (5.3.4) can be expressed as

$$(I^\beta \Psi)(t) \approx P_{\hat{n} \times \hat{n}}^\beta \Psi(t), \quad (5.4.3)$$

where $P_{\hat{n} \times \hat{n}}^\beta$ is called the Chebyshev wavelet operational matrix of order $\beta \geq 0$. Using (5.4.1) and (5.4.2), we obtain,

$$(I^\beta \Psi)(t) \approx (I^\beta \phi_{\hat{n} \times \hat{n}} B_{\hat{n}})(t) = \phi_{\hat{n} \times \hat{n}} (I^\beta B_{\hat{n}})(t) \approx \phi_{\hat{n} \times \hat{n}} F^\beta B_{\hat{n}}(t) \quad (5.4.4)$$

Moreover, from (5.4.3) and (5.4.4), we have

$$P_{\hat{n} \times \hat{n}}^\beta \Psi(t) \approx (I^\beta \Psi)(t) \approx \phi_{\hat{n} \times \hat{n}} F^\beta B_{\hat{n}}(t). \quad (5.4.5)$$

Thus by considering (5.4.1) and (5.4.5), we attain

$$P_{\hat{n} \times \hat{n}}^\beta \approx \phi_{\hat{n} \times \hat{n}} F^\beta \phi_{\hat{n} \times \hat{n}}^{-1}. \quad (5.4.6)$$

In particular, the Chebyshev wavelet operational matrix of the fractional integration for $j = 2$, $M = 3$ and $\beta = 0.5$ yields

$$P_{6 \times 6}^{0.5} = \begin{pmatrix} 0.6691 & 0.1325 & -0.0250 & 0.3827 & -0.0539 & 0.0215 \\ -0.5266 & 0.2205 & 0.1537 & -0.3226 & 0.0282 & -0.0023 \\ 0.0221 & -0.2396 & 0.0318 & 0.0194 & 0.0104 & -0.0091 \\ 0 & 0 & 0 & 0.6691 & 0.1325 & -0.0250 \\ 0 & 0 & 0 & -0.5266 & 0.2205 & 0.1537 \\ 0 & 0 & 0 & 0.0221 & -0.2396 & 0.0318 \end{pmatrix}.$$

As $P_{\hat{n} \times \hat{n}}^\beta$ contains many zeros, the proposed technique will have faster simulations. $P_{\hat{n} \times \hat{n}}^\beta$ is done once and is utilized to solve fractional order differential equations just as integer order differential equations.

5.5 Numerical Examples

In this section, some numerical examples are given to illustrate the efficiency and the reliability of the Chebyshev wavelet based numerical technique and all the numerical calculations are performed by MATLAB.

5.5.1 Example 10

Consider the multi-order fractional differential equation [27]

$$D^\gamma u(t) = y_0 D^{\gamma_0} u(t) + y_1 D^{\gamma_1} u(t) + y_2 D^{\gamma_2} u(t) + y_3 D^{\gamma_3} u(t) + f(t), \quad t \in [0, 1), \quad (5.5.1)$$

where $y_0, y_1, y_2, y_3 \in \mathbb{R}$, $f(t)$ is a known function, $m - 1 < \gamma \leq m$, $m \in \mathbb{Z}^+$,

$\gamma_0, \gamma_1, \gamma_2, \gamma_3 \leq \gamma$ with the initial states

$$u^{(j)}(0) = c_j \in \mathbb{R}, j = 0, 1, \dots, m - 1. \quad (5.5.2)$$

Approximating $D^\gamma u(t)$ as $A^T \Psi(t)$, we have (5.5.3)

$$D^{\gamma_0} u(t) = A^T P^{\gamma - \gamma_0} \Psi(t), \quad (5.5.4)$$

$$D^{\gamma_1} u(t) = A^T P^{\gamma - \gamma_1} \Psi(t), \quad (5.5.5)$$

$$D^{\gamma_2} u(t) = A^T P^{\gamma - \gamma_2} \Psi(t), \quad (5.5.6)$$

$$D^{\gamma_3} u(t) = A^T P^{\gamma - \gamma_3} \Psi(t) \text{ and} \quad (5.5.7)$$

$$u(t) = A^T P^\gamma \Psi(t) + \sum_{j=0}^{m-1} u^{(j)}(0) \frac{t^j}{j!}. \quad (5.5.8)$$

Similarly, the function $f(t)$ may be expanded by the Chebyshev wavelets as

$$f(t) = F^T \Psi(t), \quad (5.5.9)$$

where F^T is a known constant vector.

Using Equations 5.5.3-5.5.7 and 5.5.9) in Equation 5.5.1, we attain

$$\begin{aligned} A^T \Psi(t) = & y_0 A^T P^{\gamma - \gamma_0} \Psi(t) + y_1 A^T P^{\gamma - \gamma_1} \Psi(t) + y_2 A^T P^{\gamma - \gamma_2} \Psi(t) \\ & + y_3 A^T P^{\gamma - \gamma_3} \Psi(t) + F^T \Psi(t), \end{aligned}$$

Since $\Psi(t) = \phi_{\hat{n} \times \hat{n}} B_{\hat{n}}(t)$, we have

$$\begin{aligned} A^T \phi_{\hat{n} \times \hat{n}} B_{\hat{n}}(t) = & y_0 A^T P^{\gamma - \gamma_0} \phi_{\hat{n} \times \hat{n}} B_{\hat{n}}(t) + y_1 A^T P^{\gamma - \gamma_1} \phi_{\hat{n} \times \hat{n}} B_{\hat{n}}(t) \\ & + y_2 A^T P^{\gamma - \gamma_2} \phi_{\hat{n} \times \hat{n}} B_{\hat{n}}(t) + y_3 A^T P^{\gamma - \gamma_3} \phi_{\hat{n} \times \hat{n}} B_{\hat{n}}(t) + F^T \phi_{\hat{n} \times \hat{n}} B_{\hat{n}}(t). \end{aligned} \quad (5.5.10)$$

Table 5.1: Absolute errors of example 10 for various values of \widehat{n}

t	$\widehat{n} = 24$ ($j = 4, M = 3$)	$\widehat{n} = 48$ ($j = 5, M = 3$)	$\widehat{n} = 96$ ($j = 6, M = 3$)	$\widehat{n} = 192$ ($j = 7, M = 3$)
0.1	5.6757e-04	1.4109e-04	3.5200e-05	8.7901e-06
0.2	5.2023e-04	1.2917e-04	3.2520e-05	8.0929e-06
0.3	4.7091e-04	1.0846e-04	2.4930e-05	6.1988e-06
0.4	1.6459e-05	4.3184e-05	9.2216e-06	1.5083e-06
0.5	5.5512e-03	5.7762e-04	8.1605e-05	1.4377e-05
0.6	1.2675e-03	5.6763e-04	1.4110e-04	3.1709e-05
0.7	5.6379e-03	1.4022e-03	2.9665e-04	7.5132e-05
0.8	8.3151e-03	2.2370e-03	6.5392e-04	1.6275e-04
0.9	2.2315e-02	4.3762e-03	1.1157e-03	2.9777e-04

The Equation 5.5.10 can be transformed into a system of algebraic equations at the collocation points $t_i = \frac{2i-1}{2^j M}$, $i = 1, 2, \dots, 2^{j-1}M$. Solving this system, we can obtain the Chebyshev wavelet co-efficient vector A^T . Then using Equation 5.5.8, we get the approximate output response $u(t)$.

In particular, if we choose $\gamma = 2, c_0 = c_1 = 0, y_0 = y_2 = -1, y_1 = 2, y_3 = 0, \gamma_0 = 0, \gamma_1 = 1, \gamma_2 = \frac{1}{2}$ and $f(t) = t^7 + \frac{2048}{429\sqrt{\pi}}t^{6.5} - 14t^6 + 42t^5 - t^2 - \frac{8}{3\sqrt{\pi}}t^{1.5} + 4t - 2$, then the exact solution of Equation 5.5.1 is $u(t) = t^7 - t^2$. The absolute errors in Table 5.1 confirm the convergency and the reliability of the Chebyshev wavelet based numerical technique.

5.5.2 Example 11

In the above example, suppose $\gamma = 2, c_0 = c_1 = 0, y_0 = y_2 = -1,$

$$y_1 = 0, y_3 = 2, \gamma_0 = 0, \gamma_2 = \frac{2}{3} \in (0, 1), \gamma_3 = \frac{5}{3} \in (1, 2),$$

and
$$f(t) = t^3 + 6t - \frac{12}{\Gamma(\frac{7}{3})}t^{4/3} + \frac{6}{\Gamma(\frac{10}{3})}t^{7/3}.$$

The exact solution in this case is $u(t) = t^3$. Table 5.2 shows that the absolute

Table 5.2: Absolute errors of example 11 for various values of \hat{n}

t	$\hat{n} = 24$ ($j = 4, M = 3$)	$\hat{n} = 48$ ($j = 5, M = 3$)	$\hat{n} = 96$ ($j = 6, M = 3$)	$\hat{n} = 192$ ($j = 7, M = 3$)
0.1	1.3231e-03	1.0852e-03	1.0218e-03	1.0057e-03
0.2	9.0992e-03	8.2858e-03	8.0759e-03	8.0200e-03
0.3	2.9622e-02	2.7704e-02	2.7186e-02	2.7049e-02
0.4	6.9620e-02	6.5489e-02	6.4395e-02	6.4103e-02
0.5	1.3600e-01	1.2792e-01	1.2577e-01	1.2520e-01
0.6	2.3717e-01	2.2155e-01	2.1746e-01	2.1638e-01
0.7	3.8203e-01	3.5317e-01	3.4568e-01	3.4370e-01
0.8	5.8250e-01	5.3030e-01	5.1681e-01	5.1326e-01
0.9	8.5504e-01	7.6151e-01	7.3754e-01	7.3123e-01

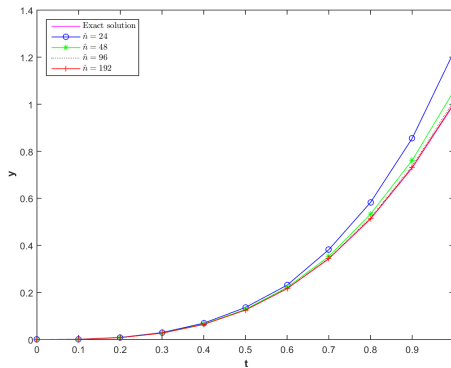


Figure 5.1: Comparison of the numerical and exact solutions for example 11

errors attained by the Chebyshev wavelet based numerical technique with $M = 3$ and

the values of j increasing become smaller and smaller. Figure 5.1 also depicts the convergency and the reliability of the Chebyshev wavelet based numerical technique.

5.5.3 Example 12

Consider the non-homogeneous multi-order fractional differential equation [63]

$$aD^\alpha u(t) + bD^\beta u(t) + cu(t) = g(t), \quad t \in [0, 1), \quad (5.5.11)$$

where $a \neq 0$, $b, c \in \mathbb{R}$, $g(t)$ is a known function, $m - 1 < \alpha \leq m$, $m \in \mathbb{Z}^+$, $\beta \leq \alpha$ with the initial states $u^{(j)}(0) = u_j \in \mathbb{R}$, $j = 0, 1, \dots, m - 1$.

Now, suppose $\alpha = 2$, $\beta = 0.5$, $a = b = c = 1$, $g(t) = 6t^3 \left(\frac{t^{-\alpha}}{\Gamma(4-\alpha)} - \frac{t^{-\beta}}{\Gamma(4-\beta)} \right)$ and $u_0 = u_1 = 0$. Using the Chebyshev wavelet based numerical technique, we arrive

$$A^T \Psi(t) + A^T P_{\hat{n} \times \hat{n}}^{0.5} \Psi(t) + A^T P_{\hat{n} \times \hat{n}}^2 \Psi(t) = G^T \Psi(t).$$

Since $\Psi(t) = \phi_{\hat{n} \times \hat{n}} B_{\hat{n}}(t)$, we have

$$A^T \phi_{\hat{n} \times \hat{n}} B_{\hat{n}}(t) + A^T P_{\hat{n} \times \hat{n}}^{0.5} \phi_{\hat{n} \times \hat{n}} B_{\hat{n}}(t) + A^T P_{\hat{n} \times \hat{n}}^2 \phi_{\hat{n} \times \hat{n}} B_{\hat{n}}(t) = G^T \phi_{\hat{n} \times \hat{n}} B_{\hat{n}}(t). \quad (5.5.12)$$

Table 5.3: Maximum absolute errors of example 12 for various values of \hat{n}

β	Legendre		Haar		Chebyshev	
	$\hat{n}=24$	$\hat{n}=96$	$\hat{n}=32$	$\hat{n}=128$	$\hat{n}=32$	$\hat{n}=128$
0.25	8.546×10^{-4}	5.343×10^{-5}	4.807×10^{-4}	3.005×10^{-5}	1.4205×10^{-5}	5.1634×10^{-6}
0.50	7.963×10^{-4}	4.978×10^{-5}	4.479×10^{-4}	2.800×10^{-5}	1.0680×10^{-4}	5.3760×10^{-7}
0.75	7.405×10^{-4}	4.631×10^{-5}	4.166×10^{-4}	2.605×10^{-5}	1.0605×10^{-4}	1.1484×10^{-5}

The equation Equation 5.5.12 can be transformed into a system of algebraic equations at the collocation points. Solving this system, we can attain the co-efficient

vector A^T . Maximum absolute errors attained by Legendre wavelets, Haar wavelets and the Chebyshev wavelets are compared in Table 5.3. Also Table 5.3 shows that the Chebyshev wavelet based numerical technique gives better results compared to Haar and Legendre wavelets.

Chapter 6

Applications of Bernoulli wavelets

6.1 Introduction

In this chapter, numerical solutions of fractional electrical circuits, namely LC(Inductor-Capacitor) circuit, RL(Resistor-Inductor) circuit, RC(Resistor-Capacitor) circuit and RLC(Resistor-Inductor-Capacitor) circuit are obtained using a numerical method based on Bernoulli wavelets.

Fractional models for electrical circuits have already been proposed in [4]. In this regard, Gomez et al. [26] have obtained solutions of RL and RC circuits involving caputo derivatives using numerical Laplace transform. Besides, they have also studied RLC circuit in time domain and found solution with respect to the Mittag-Leffler function. Shah et al. [59] considered the Laplace transform of fractional derivatives in the caputo sense to get the solutions of RL electrical circuit described by a fractional differential equation of the order $0 < \beta \leq 1$.

Atangana et al. [8] investigated the RLC circuit model utilising the fractional

derivative without singular kernel. To study fractional electrical circuits, Legendre wavelet has been applied by Arora and Chauhan [7]. Sahar Altaf and Sumaira Yousuf Khan [5])recently made the discovery of the numerical solutions of fractional circuits defined by fractional derivatives.

The numerical solutions to the corresponding problems that were obtained using the Bernoulli wavelet method are then compared with the classical solutions. The comparison demonstrates that Bernoulli wavelet based numerical scheme has good accuracy.

6.2 Applications

This section deals with the applicability and the simplicity of the numerical method based on Bernoulli wavelets for solving fractional differential equations of the electrical circuits LC, RL, RC and RLC.

6.2.1 Example 13

Consider the fractional differential equation of an LC Circuit with charged capacitor and inductor,

$$D^\beta R(t) + \rho_0^2 R(t) = 0, \quad \beta \in [1, 2], \text{ where } \rho_0^2 = \frac{1}{LC} \quad (6.2.1)$$

with $R(0) = R_0$ and $R'(0) = 0$.

$$\text{The classical solution for } \beta = 2 \text{ is } R(t)_{LC} = R_0 \cos(\rho_0 t). \quad (6.2.2)$$

Table 6.1: Numerical results of LC circuit($L = 1, C = 1, R_0 = 0.01$ and for $\beta = 2$)

t	$u = 2, Q = 2$	$u = 3, Q = 2$	$u = 4, Q = 2$	CS
1/16	1.0050×10^{-3}	9.9740×10^{-3}	9.9740×10^{-3}	9.9805×10^{-3}
3/16	9.7439×10^{-3}	9.8186×10^{-3}	9.8184×10^{-3}	9.8247×10^{-3}
5/16	9.4378×10^{-3}	9.5101×10^{-3}	9.5096×10^{-3}	9.5157×10^{-3}
7/16	9.1317×10^{-3}	9.0535×10^{-3}	9.0525×10^{-3}	9.0581×10^{-3}
9/16	8.5201×10^{-3}	8.4557×10^{-3}	8.4542×10^{-3}	8.4592×10^{-3}
11/16	7.6764×10^{-3}	7.7262×10^{-3}	7.7240×10^{-3}	7.7283×10^{-3}
13/16	6.8327×10^{-3}	6.8762×10^{-3}	6.8733×10^{-3}	6.8769×10^{-3}
15/16	5.9890×10^{-3}	5.9191×10^{-3}	5.9154×10^{-3}	5.9181×10^{-3}

Approximating $D^\beta R(t)$ as $C^T \psi(t)$, we have (6.2.3)

$$R(t) = C^T P^\beta \psi(t) + tR'(0) + R(0) \quad (6.2.4)$$

Using the initial conditions, $R(t) = C^T P^\beta \psi(t) + R_0$ (6.2.5)

$$\text{Thus } C^T \psi(t) + \rho_0^2 [C^T P^\beta \psi(t) + R_0] = 0 \quad (6.2.6)$$

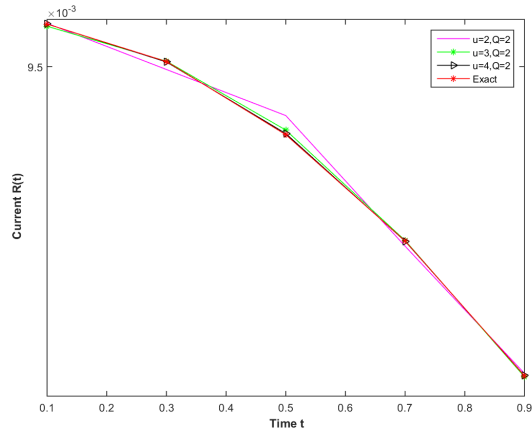


Figure 6.1: Current versus Time graph ($L = 1, C = 1, R_0 = 0.01$ and $\beta = 2$)

Solving the Equation 6.2.6 at the collocation points, we get the Bernoulli coefficient vector C^T . The numerical solutions of the LC circuit for $\beta = 2$ and various values of q' are given in Table 6.1. Also, from Fig 6.1, it is graphically shown that the Bernoulli wavelet based numerical approach reaches a higher precision of accuracy.

6.2.2 Example 14

Consider the fractional differential equation of an RL Circuit with only charged capacitor and resistor

$$D^\beta Q(t) + \kappa Q(t) = \rho, \quad \beta \in (0, 1], \quad (6.2.7)$$

with the initial state $Q(0) = Q_0$, where $\kappa = \frac{R}{L}$, $\rho = \frac{V}{L}$

The classical solution for $\beta = 1$ is

$$Q(t) = \left[Q_0 - \frac{VL}{R} \right] e^{-\kappa t} + \frac{VL}{R} \quad (6.2.8)$$

Table 6.2: Numerical results of RL circuit($R = 10, L = 1, Q_0 = 0.01, V = 10$ and for $\beta = 1$)

t	$u = 2, Q = 2$	$u = 3, Q = 2$	$u = 4, Q = 2$	CS
1/16	4.3778×10^{-1}	3.9077×10^{-1}	4.2531×10^{-1}	4.7009×10^{-1}
3/16	6.8222×10^{-1}	8.5941×10^{-1}	8.423×10^{-1}	8.4818×10^{-1}
5/16	9.2667×10^{-1}	9.6756×10^{-1}	9.5674×10^{-1}	9.5650×10^{-1}
7/16	11.7111	9.9251×10^{-1}	9.8813×10^{-1}	9.8754×10^{-1}
9/16	9.9306×10^{-1}	9.9827×10^{-1}	9.9674×10^{-1}	9.9643×10^{-1}
11/16	9.9607×10^{-1}	9.9960×10^{-1}	9.9911×10^{-1}	9.9898×10^{-1}
13/16	9.9909×10^{-1}	9.9991×10^{-1}	9.9975×10^{-1}	9.9971×10^{-1}
15/16	10.0212	9.9998×10^{-1}	9.9993×10^{-1}	9.9992×10^{-1}

Approximating $D^\beta Q(t)$ as $C^T \psi(t)$, we have (6.2.9)

$$Q(t) = C^T P^\beta \psi(t) + Q(0) \quad (6.2.10)$$

Using the initial conditions, we attain

$$Q(t) = C^T P^\beta \psi(t) + Q_0 \quad (6.2.11)$$

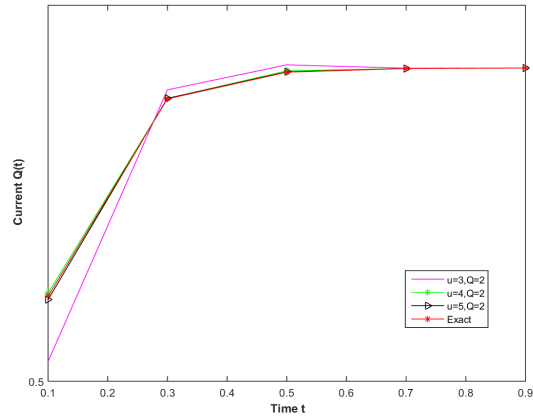


Figure 6.2: Current versus Time graph ($R = 10, L = 1, Q_0 = 0.01, V = 10$ and $\beta = 1$)

$$\text{Thus } C^T \psi(t) + \kappa[C^T P^\beta \psi(t) + Q_0] = \rho \quad (6.2.12)$$

By solving the above matrix equation at the collocation points, we obtain Bernoulli coefficient vector C^T . The Table 6.2 shows the numerical solutions of the RL circuit for $\beta = 1$ and various values of q' . As it is clearly seen in Fig. 6.2, the fractional RL circuit exhibits similar graphical behaviour to the classical solution for $\beta = 1$.

6.2.3 Example 15

Consider the fractional differential equation of an RC circuit with resistance and charged capacitance

$$D^\beta Q(t) + \mu Q^\beta(t) = 0, \quad \beta \in [0, 1] \quad (6.2.13)$$

with the condition $Q(0) = Q_0$, where $\mu = \frac{1}{RC}$.

The classical solution for $\beta = 1$ is $Q(t) = Q_0 e^{-\mu t}$ (6.2.14)

Table 6.3: Numerical results of RC circuit ($R = 10, C = 1, Q_0 = 20$ and for $\beta = 1$)

t	$u = 3, Q = 2$	$u = 4, Q = 2$	$u = 5, Q = 2$	CS
1/16	19.8758	19.8756	19.8753	19.8754
3/16	19.6289	19.6287	19.6284	19.6285
5/16	19.3850	19.3849	19.3846	19.3847
7/16	19.1443	19.1440	19.1438	19.1439
9/16	18.9064	18.9062	18.9060	18.9061
11/16	18.6715	18.6714	18.6711	18.6712
13/16	18.4396	18.4394	18.4392	18.4394
15/16	18.2105	18.2104	18.2102	18.2102

Approximating $D^\beta Q(t)$ as $C^T \psi(t)$, we have (6.2.15)

$$Q(t) = C^T P^\beta \psi(t) + Q(0) \quad (6.2.16)$$

Using the initial condition, we attain

$$Q(t) = C^T P^\beta \psi(t) + Q_0 \quad (6.2.17)$$

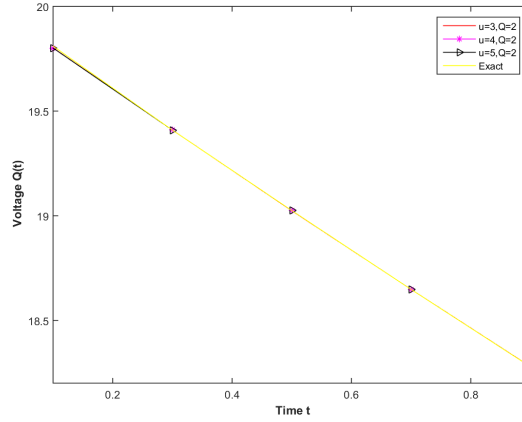


Figure 6.3: Voltage versus Time graph ($R = 10, C = 1, Q_0 = 20$ and $\beta = 1$)

$$\text{Thus } C^T \psi(t) + \mu[C^T P^\beta \psi(t) + Q_0] = 0 \quad (6.2.18)$$

Solving this system at the collocation points, we obtain Bernoulli coefficient vector C^T . In Table 6.3, the numerical solutions for the RC circuit with $\beta = 1$ and various values of q' are provided. In Fig. 6.3, graphical analysis for various values of q' is also displayed. As seen in Fig. 6.3, the graphical behaviour of the fractional RC circuit resembles that of the classical solution for $\beta = 1$.

6.2.4 Example 16

Consider the fractional differential equation of an RLC circuit with resistance, inductance and charged capacitance

$$D^{2\beta} Q(t) + \rho Q^\beta(t) + \eta Q(t) = 0, \quad \beta \in [1/2, 1] \quad (6.2.19)$$

with the conditions $Q(0) = Q_0$ and $Q'(0) = 0$, where $\eta = \frac{1}{LC}$ and $\rho = \frac{R}{L}$.

The classical solution for $\beta = 1$ is

$$Q(t) = \frac{Q_0}{k_1 - k_2} [-k_2 e^{k_1 t} + k_1 e^{k_2 t}], \quad (6.2.20)$$

$$\text{where } k_1 = \frac{-\rho + \sqrt{\rho^2 - 4\eta}}{2}, k_2 = \frac{-\rho - \sqrt{\rho^2 - 4\eta}}{2}.$$

Table 6.4: Numerical results of RLC circuit (R=10, L=10, C=10, $Q_0 = 0.01$ and for $\beta = 1$)

t	$u = 2, Q = 2$	$u = 3, Q = 2$	$u = 4, Q = 2$	CS
0.1	0.01096	0.01093	0.01095	0.0099991
0.2	0.01174	0.01181	0.0118	0.0099981
0.3	0.01253	0.01259	0.01259	0.0099959
0.4	0.01331	0.01328	0.01329	0.0099930
0.5	0.01409	0.01396	0.01393	0.0099989
0.6	0.01451	0.01449	0.01450	0.0099953
0.7	0.01498	0.01502	0.01501	0.010006
0.8	0.01545	0.01548	0.01547	0.010005
0.9	0.01592	0.01589	0.01590	0.010009

Approximating $D^{2\beta}Q(t)$ as $C^T \psi(t)$, we have (6.2.21)

$$D^\beta Q(t) = C^T P^\beta \psi(t) + Q(0) \quad (6.2.22)$$

$$Q(t) = C^T P^{2\beta} \psi(t) + Q(0) \frac{t^\beta}{\Gamma(\beta + 1)} + Q_0 \quad (6.2.23)$$

$$\text{Thus } C^T \psi(t) + \rho[C^T P^\beta \psi(t) + Q_0] + \eta[C^T P^{2\beta} \psi(t) + Q(0) \frac{t^\beta}{\Gamma(\beta + 1)} + Q_0] = 0 \quad (6.2.24)$$

Solving the Equation 6.2.24 at the collocation points, we obtain Bernoulli coefficient vector C^T . In Table 6.4, the numerical solutions for the RLC circuit for $\beta = 1$ and

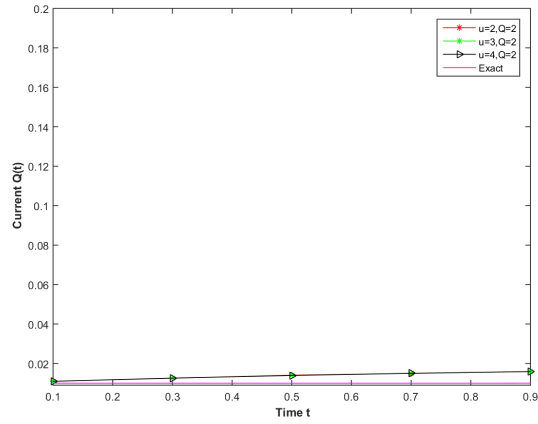


Figure 6.4: Current versus Time graph ($R = 10, L = 10, C = 10, Q_0 = 0.01$ and $\beta = 1$)

various values of q' are provided. Fig. 6.4 also displays the graphical analysis for various values of q' . As can be observed in Fig. 6.4, the fractional RLC circuit's graphical behaviour for $\beta = 1$ is very similar to the classical solution.

Conclusion

In this thesis, we have discussed both analytical and numerical solutions of fractional differential equations by using fractional integral transforms with exponential type kernels and wavelet based numerical schemes. First, with the help of a generalized fractional integral transform with exponential type kernel and Aboodh transform, we obtained analytical solutions of fractional differential equations. We also discussed the properties of these transform techniques and proved the simplicity and the effectiveness of these transform techniques for fractional differential equations. Many researchers are interested in the formation of new integral transforms because of their applications in science and engineering fields.

As certain wavelet-based algorithms appear to be somewhat complex and need a lot of processing time, this encourages us to think of efficient, straightforward, and fast wavelet-based numerical techniques for the fractional differential equations.

The main advantage of wavelet based numerical schemes is its simplicity, small computation costs and less computational errors due to the sparsity of the transform matrices and the small number of significant wavelet coefficients. Additionally, the

inaccuracy could be greatly decreased while the level of resolution might be increased with more collocation points.

Euler wavelet-based numerical scheme is quite simple, effective and expedient for obtaining numerical solutions of fractional differential equations in compared with analytical approaches via Finite Difference Method, Admian Decomposition Method, Finite Differential Transform Method, Variational Iteration Method and numerical approaches via Legendre Wavelet Method, Haar Wavelet Method. Next, we have obtained the numerical solutions of fractional differential equations with variable coefficients by an efficient numerical scheme based on Bernoulli wavelets and proved the fast convergency of this method compared with Adams type Predictor-corrector method and Haar wavelet method. After that, we have attained numerical solutions of multi-order fractional differential equations by Chebyshev wavelet method. Finally, the application of Bernoulli wavelets based numerical scheme in solving fractional electrical circuits was discussed.

As the numerical results have been represented by graphs and tables which depict the efficiency and convergency of numerical solutions, it is evident from our findings that the generalized fractional integral transform with exponential type kernel and wavelet based numerical schemes are simple and efficient for solving fractional differential equations. Many real-world fractional models in the fields of economics, computer science, psychology, medicine, etc. can be investigated with the help of

integral transforms and wavelet based numerical schemes. Moreover, the numerical schemes based on Euler wavelets, Bernoulli wavelets and Chebyshev wavelets could be effectively applied for higher order fractional integro differential equations arising in science and engineering fields.

Bibliography

- [1] W. Abd-Elhameed and Y. Youssri. New spectral solutions of multi-term fractional order initial value problems with error analysis. *Comput. Model. Eng. Sci*, 105(5):375–398, 2015.
- [2] K. S. Aboodh. The new integral transform'aboodh transform. *Global Journal of Pure and Applied Mathematics*, 9(1):35–43, 2013.
- [3] O. P. Agrawal. A general formulation and solution scheme for fractional optimal control problems. *Nonlinear Dynamics*, 38(1):323–337, 2004.
- [4] A. Alsaedi, J. J. Nieto, and V. Venktesh. Fractional electrical circuits. *Advances in Mechanical Engineering*, 7(12):1687814015618127, 2015.
- [5] S. Altaf and S. Y. Khan. Numerical solution of fractional electrical circuits by haar wavelet. *Matematika*, 35, 2019.
- [6] A. Arikoglu and I. Ozkol. Solution of fractional differential equations by using differential transform method. *Chaos, Solitons & Fractals*, 34(5):1473–1481, 2007.
- [7] R. Arora and N. Chauhan. An application of legendre wavelet in fractional

- electrical circuits. *Global Journal of Pure and Applied Mathematics*, 13(2):183–202, 2017.
- [8] A. Atangana and J. J. Nieto. Numerical solution for the model of rlc circuit via the fractional derivative without singular kernel. *Advances in Mechanical Engineering*, 7(10):1687814015613758, 2015.
- [9] A. Bhattacharyya, P. Nandi, S. Hazra, and T. Dutta. Memory of rheological stress in polymers using fractional calculus. *arXiv preprint arXiv:2001.06620*, 2020.
- [10] A. H. Bhrawy, A. Alofi, and S. S. Ezz-Eldien. A quadrature tau method for fractional differential equations with variable coefficients. *Applied Mathematics Letters*, 24(12):2146–2152, 2011.
- [11] İ. CELİK. Generalization of chebyshev wavelet collocation method to the rth-order differential equations. *Communication in Mathematical Modeling and Applications*, 3(2):31–47, 2018.
- [12] P. Chang and A. Isah. Legendre wavelet operational matrix of fractional derivative through wavelet-polynomial transformation and its applications in solving fractional order brusselator system. In *Journal of Physics: Conference Series*, volume 693, page 012001. IOP Publishing, 2016.
- [13] M. K. U. Dattu. New integral transform: fundamental properties, investigations and applications. *IAETSD Journal for Advanced Research in Applied Sciences*, 5(4):534–539, 2018.
- [14] I. Daubechies. *Ten lectures on wavelets*. SIAM, 1992.

- [15] L. Debnath and D. Bhatta. *Integral transforms and their applications*. Chapman and Hall/CRC, 2016.
- [16] A. Demir, M. A. Bayrak, and E. Ozbilge. A new approach for the approximate analytical solution of space-time fractional differential equations by the homotopy analysis method. *Advances in Mathematical Physics*, 2019, 2019.
- [17] K. Diethelm, N. J. Ford, and A. D. Freed. A predictor-corrector approach for the numerical solution of fractional differential equations. *Nonlinear Dynamics*, 29(1):3–22, 2002.
- [18] E. Doha, W. Abd-Elhameed, and Y. Youssri. New ultraspherical wavelets collocation method for solving 2nth-order initial and boundary value problems. *Journal of the Egyptian Mathematical Society*, 24(2):319–327, 2016.
- [19] M. Duarte Ortigueira and J. Tenreiro Machado. Fractional signal processing and applications. *Signal processing*, 83(11), 2003.
- [20] A. El-Sayed, A. El-Mesiry, and H. El-Saka. Numerical solution for multi-term fractional (arbitrary) orders differential equations. *Computational & Applied Mathematics*, 23:33–54, 2004.
- [21] T. M. Elzaki. The new integral transform elzaki transform. *Global Journal of pure and applied mathematics*, 7(1):57–64, 2011.
- [22] T. M. Elzaki and S. M. Elzaki. On the relationship between laplace transform and new integral transform tarig transform'. *Applied Mathematics, Elixir Appl. Math*, 36:3230–3233, 2011.

- [23] U. Farooq, H. Khan, D. Baleanu, and M. Arif. Numerical solutions of fractional delay differential equations using chebyshev wavelet method. *Computational and Applied Mathematics*, 38(4):1–13, 2019.
- [24] V. Gafiychuk, B. Datsko, and V. Meleshko. Mathematical modeling of time fractional reaction–diffusion systems. *Journal of Computational and Applied Mathematics*, 220(1-2):215–225, 2008.
- [25] R. Garra. Analytic solution of a class of fractional differential equations with variable coefficients by operatorial methods. *Communications in Nonlinear Science and Numerical Simulation*, 17(4):1549–1554, 2012.
- [26] J. Gómez, C. Astorga, R. Escobar, M. Medina, R. Guzmán, A. González, and D. Baleanu. Overview of simulation of fractional differential equation using numerical laplace transform. *Cent. Eur. J. Phys.(CEJP)*, pages 1–14, 2012.
- [27] W. Han, Y.-M. Chen, D.-Y. Liu, X.-L. Li, and D. Boutat. Numerical solution for a class of multi-order fractional differential equations with error correction and convergence analysis. *Advances in Difference Equations*, 2018(1):1–22, 2018.
- [28] M. R. Islam. Wavelets, its application and technique in signal and image processing. *Global Journal of Computer Science and Technology*, 2011.
- [29] R. B. D. Ismirate. *Data Compression with Wavelets*. PhD thesis, An-Najah National University, 2009.
- [30] A. K. Jabber and L. N. M. Tawfiq. New transform fundamental properties and its applications. *Ibn Alhaitham Journal for Pure and Applied Science*, 31(1):151–163, 2018.

- [31] S. Javeed, D. Baleanu, A. Waheed, M. Shaukat Khan, and H. Affan. Analysis of homotopy perturbation method for solving fractional order differential equations. *Mathematics*, 7(1):40, 2019.
- [32] G. Jumarie. Laplace's transform of fractional order via the mittag-leffler function and modified riemann-liouville derivative. *Applied Mathematics Letters*, 22(11):1659–1664, 2009.
- [33] A. Kashuri and A. Fundo. A new integral transform. *Advances in Theoretical and Applied Mathematics*, 8(1):27–43, 2013.
- [34] E. Keshavarz, Y. Ordokhani, and M. Razzaghi. The bernoulli wavelets operational matrix of integration and its applications for the solution of linear and nonlinear problems in calculus of variations. *Applied Mathematics and Computation*, 351:83–98, 2019.
- [35] M. Khader. Introducing an efficient modification of the homotopy perturbation method by using chebyshev polynomials. *Arab Journal of Mathematical Sciences*, 18(1):61–71, 2012.
- [36] Z. H. Khan and W. A. Khan. N-transform properties and applications. *NUST journal of engineering sciences*, 1(1):127–133, 2008.
- [37] A. Kilicman and Z. A. A. Al Zhour. Kronecker operational matrices for fractional calculus and some applications. *Applied mathematics and computation*, 187(1):250–265, 2007.
- [38] A. Kilicman and O. Altun. Some remarks on the fractional sumudu transform and applications. *Applied Mathematics & Information Sciences*, 8(6):2881, 2014.

- [39] S. Kiwne and S. M. Sonawane. Mahgoub transform fundamental properties and applications. *International Journal of Computer and Mathematical Sciences*, 7(2):500–511, 2018.
- [40] V. V. Kulish and J. L. Lage. Application of fractional calculus to fluid mechanics. *J. Fluids Eng.*, 124(3):803–806, 2002.
- [41] M. Kumar and S. Pandit. Wavelet transform and wavelet based numerical methods: an introduction. *International Journal of Nonlinear Science*, 13(3):325–345, 2012.
- [42] P. Kumar and O. P. Agrawal. An approximate method for numerical solution of fractional differential equations. *Signal processing*, 86(10):2602–2610, 2006.
- [43] S. Kundu. Analytical solutions of one-dimensional space-fractional advection–diffusion equation for sediment suspension using homotopy analysis method. *Journal of Engineering Mechanics*, 145(7):04019048, 2019.
- [44] W. Li and Y. Pang. Application of adomian decomposition method to nonlinear systems. *Advances in Difference Equations*, 2020(1):1–17, 2020.
- [45] Y. Li and W. Zhao. Haar wavelet operational matrix of fractional order integration and its applications in solving the fractional order differential equations. *Applied mathematics and computation*, 216(8):2276–2285, 2010.
- [46] A. Loverro et al. Fractional calculus: history, definitions and applications for the engineer. *Rapport technique, Univeristy of Notre Dame: Department of Aerospace and Mechanical Engineering*, pages 1–28, 2004.

- [47] J. T. Machado, V. Kiryakova, and F. Mainardi. Recent history of fractional calculus. *Communications in nonlinear science and numerical simulation*, 16(3):1140–1153, 2011.
- [48] M. M. A. Mahgob and A. A. Alshikh. On the relationship between abodh transform and new integral transform zz transform. *Mathematical Theory and Modeling*, 6(9):71–26, 2016.
- [49] S. G. Mallat. Multifrequency channel decompositions of images and wavelet models. *IEEE Transactions on Acoustics, Speech, and Signal Processing*, 37(12):2091–2110, 1989.
- [50] Y. Meyer. basis of $l_2(0, 2\pi)$. *Analysis at Urbana: Volume 1, Analysis in Function Spaces*, 1:256, 1989.
- [51] S. Momani and Z. Odibat. Numerical comparison of methods for solving linear differential equations of fractional order. *Chaos, Solitons & Fractals*, 31(5):1248–1255, 2007.
- [52] M. Omran and A. Kiliçman. Natural transform of fractional order and some properties. *Cogent Mathematics*, 3(1):1251874, 2016.
- [53] Ö. Oruç, A. Esen, and F. Bulut. A haar wavelet approximation for two-dimensional time fractional reaction–subdiffusion equation. *Engineering with Computers*, 35(1):75–86, 2019.
- [54] P. Rahimkhani, Y. Ordokhani, and E. Babolian. Numerical solution of fractional pantograph differential equations by using generalized fractional-order bernoulli wavelet. *Journal of Computational and Applied Mathematics*, 309:493–510, 2017.

- [55] M. Razzaghi and S. Yousefi. Legendre wavelets method for the solution of nonlinear problems in the calculus of variations. *Mathematical and Computer Modelling*, 34(1-2):45–54, 2001.
- [56] B. Ross. A brief history and exposition of the fundamental theory of fractional calculus. *Fractional calculus and its applications*, pages 1–36, 1975.
- [57] P. Sahu and S. Saha Ray. A new bernoulli wavelet method for numerical solutions of nonlinear weakly singular volterra integro-differential equations. *International Journal of Computational Methods*, 14(03):1750022, 2017.
- [58] E. Schmidt. Zur theorie der linearen und nichtlinearen integralgleichungen. In *Integralgleichungen und Gleichungen mit unendlich vielen Unbekannten*, pages 190–233. Springer, 1989.
- [59] P. Shah, A. Patel, I. Salehbhai, and A. Shukla. Analytic solution for the electric circuit model in fractional order. In *Abstract and applied analysis*, volume 2014. Hindawi, 2014.
- [60] S. L. Shaikh. Introducing a new integral transform: Sadik transform. *American International Journal of Research in Science, Technology, Engineering & Mathematics*, 22(1):100–102, 2018.
- [61] M. Sifuzzaman, M. R. Islam, and M. Ali. Application of wavelet transform and its advantages compared to fourier transform. 2009.
- [62] A. Turan Dincel. Solution to fractional-order riccati differential equations using euler wavelet method. *Scientia Iranica*, 26(3):1608–1616, 2019.

- [63] M. ur Rehman and R. A. Khan. The legendre wavelet method for solving fractional differential equations. *Communications in Nonlinear Science and Numerical Simulation*, 16(11):4163–4173, 2011.
- [64] D. Verotta. Fractional dynamics pharmacokinetics–pharmacodynamic models. *Journal of pharmacokinetics and pharmacodynamics*, 37(3):257–276, 2010.
- [65] J. Wang, T.-Z. Xu, Y.-Q. Wei, and J.-Q. Xie. Numerical solutions for systems of fractional order differential equations with bernoulli wavelets. *International Journal of Computer Mathematics*, 96(2):317–336, 2019.
- [66] Y. Wang and Q. Fan. The second kind chebyshev wavelet method for solving fractional differential equations. *Applied Mathematics and Computation*, 218(17):8592–8601, 2012.
- [67] Y. Wang, T. Yin, and L. Zhu. Sine-cosine wavelet operational matrix of fractional order integration and its applications in solving the fractional order riccati differential equations. *Advances in Difference Equations*, 2017(1):1–16, 2017.
- [68] Y. Wang and L. Zhu. Solving nonlinear volterra integro-differential equations of fractional order by using euler wavelet method. *Advances in difference equations*, 2017(1):1–16, 2017.
- [69] Y. Wang, L. Zhu, and Z. Wang. Solving the nonlinear variable order fractional differential equations by using euler wavelets. *Computer Modeling in Engineering & Sciences*, 118(2):339–350, 2019.
- [70] S. Westerlund. Dead matter has memory! *Physica scripta*, 43(2):174, 1991.

- [71] J. Xie, T. Wang, Z. Ren, J. Zhang, and L. Quan. Haar wavelet method for approximating the solution of a coupled system of fractional-order integral-differential equations. *Mathematics and Computers in Simulation*, 163:80–89, 2019.
- [72] F. Zhou and X. Xu. The third kind chebyshev wavelets collocation method for solving the time-fractional convection diffusion equations with variable coefficients. *Applied Mathematics and Computation*, 280:11–29, 2016.
- [73] D. Ziane and M. H. Cherif. Variational iteration transform method for fractional differential equations. *Journal of Interdisciplinary Mathematics*, 21(1):185–199, 2018.



An expeditious wavelet-based numerical scheme for solving fractional differential equations

R. Aruldoss¹ · R. Anusuya Devi¹ · P. Murali Krishna²

Received: 19 July 2020 / Revised: 5 November 2020 / Accepted: 24 November 2020
© SBMAC - Sociedade Brasileira de Matemática Aplicada e Computacional 2021

Abstract

In this article, a numerical scheme based on Euler wavelets for solving fractional differential equations is proposed. An Euler wavelet operational matrix of fractional integration is derived and employed to reduce fractional differential equations into simultaneous algebraic equations. Some examples are given to illustrate the applicability and the high accuracy of the proposed numerical scheme.

Keywords Fractional Calculus · Euler wavelet · Fractional differential equations · Operational matrix · Fractional electrical circuit

Mathematics Subject Classification 26A33 · 34A08

1 Introduction

The fractional calculus is an ancient mathematical tool that is 300 years old and it has been developed progressively up to now. Fractional calculus is the generalization of ordinary calculus to an arbitrary order. In the past few decades, many fractional models have attracted great attention in variety of disciplines, such as chaotic systems (Ma and Li 2020; Hajipour et al. 2018), bioengineering (Magin 2012), dynamics of interfaces between nano-particles and substrates (Chow 2015), optimal control problems (Jajarmi et al. 2018), and non-linear dynamical systems (Baleanu et al. 2018).

Communicated by José Tenreiro Machado.

✉ R. Anusuya Devi
anushya3sai@gmail.com

R. Aruldoss
krvarul@gmail.com

P. Murali Krishna
mkpanthangi@gmail.com

¹ Department of Mathematics, Government Arts College(Autonomous), Kumbakonam (Affiliated to Bharathidasan University), Tiruchirapalli, Tamil Nadu, India

² Department of Mathematics, Amrita Vishwa Vidhyapeetham, Coimbatore, India

However, most of the fractional differential equations do not have analytical solutions. Owing to the wide range of applications of fractional differential equations, remarkable interest has been initiated for developing numerical techniques to find solutions of fractional differential equations. These numerical techniques include Separation of variables (Shen et al. 2019), Variational iteration method (Ziane and Cherif 2018), Adomian decomposition method (Li and Pang 2020), Finite difference method (Karamali et al. 2019), Homotopy analysis method (Demir et al. 2019; Kundu 2019), Homotopy perturbation method (Javeed et al. 2019; Khader 2012), etc.

Besides these numerical techniques, many researchers have applied comparatively a new numerical technique based on wavelets for analyzing problems of high computational complexity and have proved that wavelets are powerful tools to explore new directions in solving fractional differential equations.

In recent years, wavelets have been widely used for data segmentation, data compression, and time–frequency analysis. Wavelets permit the accurate representation of a variety of functions and establish a connection with fast numerical algorithms (Beylkin et al. 1991).

Recently, the operational matrices of fractional-order integrations for Haar wavelets (Xie et al. 2019; Oruc et al. 2019), Chebyshev wavelets (Farooq et al. 2019; Celik 2018), Second kind Chebyshev wavelets (Wang and Fan 2012), Legendre wavelets (ur Rehman and Khan 2011; Chang and Isah 2016), Bernoulli wavelets (Keshavarz et al. 2019; Rahimkhani et al. 2017), Ultra spherical wavelets (Abd-Elhameed and Youssri 2015; Doha et al. 2016), Third kind Chebyshev wavelets (Zhou and Xiaoyong 2016), CAS wavelets (Wang and Yin 2017), and Euler wavelets (Wang and Zhu 2017; Dincel 2019; Wang et al. 2019) have been proposed to solve fractional differential equations.

The main characteristic of wavelet-based techniques is that after the discretization process, the co-efficient matrix of the algebraic equations is obtained which is a sparse matrix. The resulting matrix decreases the computational load and expedites the simulation.

The proposed numerical technique is based on Euler wavelet approximations. We first construct the Euler wavelets, and then, by expanding these wavelets into block pulse functions, we find the operational matrix of fractional-order integration of Euler wavelets. The resulting matrix is used to reduce the solution of the fractional differential equations to the solution of algebraic equations.

We organize the rest of the paper as follows. In Sect. 2, we introduce some basic definitions and discuss some properties of fractional calculus. Section 3 is devoted to the basic formulation of Euler wavelets and operational matrix of the fractional-order integration for Euler wavelets. In Sect. 4, we report our numerical findings and demonstrate the accuracy of the proposed numerical scheme by considering some numerical examples. The conclusion is given in Sect. 5.

2 Preliminary concepts

In this section, we present some basic definitions and mathematical preliminary facts of fractional calculus.

Definition 2.1 The Riemann–Liouville fractional integral of order $\gamma \geq 0$ of $f(x) \in L^2(\mathbb{R})$ is defined as:

$$(I^\gamma f)(x) = \begin{cases} \frac{1}{\Gamma(\gamma)} \int_0^x \frac{f(\zeta)}{(x-\zeta)^{(1-\gamma)}} d\zeta, & \gamma > 0 \\ f(x), & \gamma = 0. \end{cases}$$

If $f(x), g(x) \in L^2(\mathbb{R})$ and $\gamma \geq 0, \lambda, \mu \in (\mathbb{R})$, then we have the following properties:

$$(i) I^\gamma (\lambda f(x) + \mu g(x)) = \lambda I^\gamma f(x) + \mu I^\gamma g(x)$$

$$(ii) I^\gamma x^u = \frac{\Gamma(u + 1)}{\Gamma(u + 1 + \gamma)} x^{u+\gamma}, u > -1$$

The Riemann–Liouville fractional derivative of order $\gamma \geq 0$ of $f(x) \in L^2(\mathbb{R})$ is normally defined as:

$$(D^\gamma f)(x) = \left(\frac{d}{dx}\right)^m (I^{m-\gamma} f)(x), \quad m - 1 < \gamma \leq m,$$

where m is a positive integer and $x > 0$.

Definition 2.2 The Caputo fractional derivative of order $\gamma \geq 0$ of $f(x) \in L^2(\mathbb{R})$ is defined as:

$$(D^\gamma f)(x) = \frac{1}{\Gamma(m - \gamma)} \int_0^x (x - \zeta)^{m-\gamma-1} f^{(m)}(\zeta) d\zeta, \quad m - 1 < \gamma \leq m,$$

where m is a positive integer and $x > 0$.

If $f(x) \in L^2(\mathbb{R})$ and $\gamma \geq 0$, then it has the following two basic properties:

$$(i) (D^\gamma I^\gamma f)(x) = f(x)$$

$$(ii) (I^\gamma D^\gamma f)(x) = f(x) - \sum_{j=0}^{m-1} f^{(j)}(0^+) \frac{x^j}{j!}, \quad m - 1 < \gamma \leq m,$$

where m is a positive integer, $x > 0$ and $f^{(j)}(0^+) := \lim_{x \rightarrow 0^+} D^j f(x), j = 0, 1, \dots, m - 1$.

3 Euler wavelets

In this section, we discuss Euler polynomials and some of their properties to construct Euler wavelets.

3.1 Wavelets and Euler wavelets

Wavelets consist of a family of functions generated from dilations and translations of a single function $\psi(x)$, called the mother wavelet. If the dilation parameter c and the translation parameter d change continuously, we attain the following family of continuous wavelets:

$$\psi_{cd}(x) = |c|^{-\frac{1}{2}} \psi\left(\frac{x - d}{c}\right), c, d \in (\mathbb{R}), c \neq 0.$$

If the translation and dilation parameters are chosen to have discrete values, that is, $c = c_0^{-p}, d = qd_0c_0^{-p}, c_0 > 1, d_0 > 0$ and $p, q \in \mathbb{Z}^+$, then we have the following family of discrete wavelets:

$$\psi_{pq}(x) = |c_0|^{\frac{p}{2}} \psi(c_0^p x - qd_0),$$

where the functions ψ_{pq} form a wavelet basis for $L^2(\mathbb{R})$. In particular, if $c_0 = 2$ and $d_0 = 1$, we can attain an orthonormal basis from $\psi_{pq}(x)$ for $L^2(\mathbb{R})$.

The Euler wavelets are defined on the interval [0,1) as:

$$\psi_{mn}(x) = \begin{cases} 2^{\frac{j-1}{2}} \widetilde{E}_n(2^{j-1}x - m + 1), & \frac{m-1}{2^{j-1}} \leq x < \frac{m}{2^{j-1}} \\ 0, & \text{otherwise} \end{cases}$$

for $m = 1, 2, \dots, 2^{j-1}, n = 0, 1, \dots, M - 1$, and $j, M \in \mathbb{N}$:

$$\text{where } \widetilde{E}_n(x) = \begin{cases} 1, & n = 0 \\ \frac{1}{\sqrt{\binom{2(-1)^{n-1}(n!)^2}{(2n)!}}} E_n(x), & n > 0, \end{cases}$$

the co-efficient

$$\frac{1}{\sqrt{\binom{2(-1)^{n-1}(n!)^2}{(2n)!}}} E_{2n+1}(0)$$

is for normality, the dilation parameter is $2^{-(j-1)}$ and the translation parameter is $(m - 1)2^{-(j-1)}$. Here, $E_n(x)$ denote Euler polynomials of degree n which can be defined by the generating functions:

$$\frac{2e^{xs}}{e^s + 1} = \sum_{n=0}^{\infty} E_n(x) \frac{s^n}{n!}, \quad |s| < \pi.$$

We can also define the first kind Euler polynomials by the relation:

$$\sum_{j=0}^n \binom{n}{j} E_j(x) + E_n(x) = 2x^n,$$

where $\binom{n}{j}$ is a binomial co-efficient.

The first few Euler polynomials are:

$$E_0(x) = 1, E_1(x) = x - \frac{1}{2}, E_2(x) = x^2 - x, E_3(x) = x^3 - \frac{2}{3}x^2 + \frac{1}{4}, \dots$$

These polynomials satisfy the following formula:

$$\int_0^1 E_n(x) E_m(x) dx = (-1)^{m-1} \frac{n!(m+1)!}{(n+m+1)!} E_{n+m+1}(0), \quad n, m \geq 1,$$

and the Euler polynomials form a complete basis for $L^2(\mathbb{R})$.

3.2 Function approximation

A function $f(x) \in L^2[0, 1)$ can be expressed in terms of the Euler wavelets as:

$$f(x) = \sum_{m=0}^{\infty} \sum_{n \in \mathbb{Z}} C_{mn} \psi_{mn}(x), \tag{1}$$

where the co-efficients C_{mn} are given by:

$$C_{mn} = \langle f(x), \psi_{mn} \rangle = \int_0^1 f(x) \psi_{mn}(x) dx.$$

By truncating the infinite series in (1), $f(x)$ is approximated as:

$$\widetilde{f}(x) \approx \sum_{m=1}^{2^{j-1}} \sum_{n=0}^{M-1} C_{mn} \psi_{mn}(x) = C^T \psi(x),$$

where the co-efficient vector C and the Euler function vector $\psi(x)$ are $2^{j-1}M \times 1$ matrices, given by:

$$C = [C_{10}, C_{11}, \dots, C_{1(M-1)}, C_{20}, \dots, C_{2(M-1)}, \dots, C_{2^{j-1}0}, \dots, C_{2^{j-1}(M-1)}]^T$$

and

$$\psi(x) = [\psi_{10}, \psi_{11}, \dots, \psi_{1(M-1)}, \psi_{20}, \dots, \psi_{2(M-1)}, \dots, \psi_{2^{j-1}0}, \dots, \psi_{2^{j-1}(M-1)}]^T. \tag{2}$$

We define the Euler wavelet co-efficient matrix $\phi_{k \times k}$, $k = 2^{j-1}M$ at the collocation points $x_i = \frac{2i-1}{2k}$, $i = 1, 2 \dots k$ as:

$$\phi_{k \times k} = \left[\psi\left(\frac{1}{2k}\right), \psi\left(\frac{3}{2k}\right), \dots, \psi\left(\frac{2k-1}{2k}\right) \right].$$

Specifically, the Euler wavelet co-efficient matrix for $j = 2$ and $M = 3$ becomes:

$$\phi_{6 \times 6} = \begin{pmatrix} 1.4142 & 1.4142 & 1.4142 & 0 & 0 & 0 \\ -0.9428 & 0 & 0.9428 & 0 & 0 & 0 \\ -0.4811 & -0.8660 & -0.4811 & 0 & 0 & 0 \\ 0 & 0 & 0 & 1.4142 & 1.4142 & 1.4142 \\ 0 & 0 & 0 & -0.9428 & 0 & 0.9428 \\ 0 & 0 & 0 & -0.4811 & -0.8660 & -0.4811 \end{pmatrix}.$$

Correspondingly, we have:

$$\widetilde{f}_k = [\widetilde{f}(x_1), \widetilde{f}(x_2) \dots \widetilde{f}(x_k)] = C^T \phi_{k \times k}.$$

Since the Euler wavelet co-efficient matrix $\phi_{k \times k}$ is invertible, the Euler wavelet co-efficient vector C^T can be attained by:

$$C^T = \widetilde{f}_k \phi_{k \times k}^{-1}.$$

3.3 Error Analysis

Theorem 3.1 *If the function $f : [0, 1) \rightarrow \mathbb{R}$ is $n + 1$ times continuously differentiable, that is, and $f \in C^{n+1}[0, 1)$, then $\widetilde{f}(x) = C^T \psi(x)$ approximates $f(x)$ with mean error bounded:*

$$\|f(x) - \widetilde{f}(x)\|_2 \leq \frac{\sqrt{2\widetilde{M}}}{2^{(j-1)(n+1)}(n+1)!\sqrt{(2n+3)}}, \text{ where } \widetilde{M} = \max_{x \in [0,1)} |f^{(n+1)}(x)|.$$

Proof We first divide the interval $[0,1)$ into subintervals $I_{j,m} = [\frac{m-1}{2^{j-1}}, \frac{m}{2^{j-1}})$, $m = 1, 2, \dots, 2^{j-1}$, $j \in \mathbb{N}$ with the restriction that $\widetilde{f}(x)$ is a polynomial of degree less than $n + 1$ that approximates f with minimum mean error. Using Lemma 3 (Wang and Zhu 2017), we

attain:

$$\begin{aligned} \|f(x) - \tilde{f}(x)\|_2^2 &= \int_0^1 [f(x) - \tilde{f}(x)]^2 dx \\ &= \sum_m \int_{I_{j,m}} [f(x) - \tilde{f}(x)]^2 dx \\ &\leq \sum_m \left[\frac{\sqrt{(2)\tilde{M}_m \left(\frac{1}{2^{j-1}}\right)^{\frac{2n+3}{2}}}}{(n+1)! \sqrt{(2n+3)}} \right]^2 \\ &\leq \frac{2\tilde{M}^2}{2^{(j-1)(2n+2)} [(n+1)!]^2 (2n+3)} \\ &\quad \text{where } \tilde{M}_m = \max_{x \in I_{j,m}} |f^{(n+1)}(x)|. \end{aligned}$$

By taking the square roots, we arrive at the upper bound. The error of the approximation $\tilde{f}(x)$ of $f(x)$, therefore, decays like $2^{-(n+1)(j-1)}$. Meanwhile, we notice that the number of wavelets is $k = 2^{j-1}M$, where M is the degree of the Euler polynomials and usually takes small values in computation. When M is fixed, with the values of j increasing, the numerical results become more accurate and we infer that the approximate solutions converge to the exact solution. \square

3.4 Operational matrix of the fractional integration

We now explore the basic idea of finding the fractional integration operational matrix of the Euler wavelets.

A k -set of block pulse functions (BPFs) over the interval $[0, 1)$ is defined as:

$$b_i(x) = \begin{cases} 1, & (i-1)/k \leq x < i/k \\ 0, & \text{otherwise,} \end{cases}$$

where $i=1,2,3\dots k, k \in \mathbb{N}$, For $x \in [0, 1)$:

$$b_i(x)b_j(x) = \begin{cases} 0, & i \neq j \\ b_i(x), & i = j \end{cases}$$

and

$$\int_0^1 b_i(x)b_j(x) = \begin{cases} 0, & i \neq j \\ \frac{1}{k}, & i = j. \end{cases}$$

It is known that any square integrable function $f(x)$ defined over $[0,1)$ can be expanded in terms of BPFs as:

$$f(x) \simeq \sum_{i=1}^k f_i b_i(x) = f^T B_k(x)$$

where $f = [f_1, f_2, \dots, f_k]^T, f_i = \frac{1}{k} \int_{(i-1)/k}^{i/k} f(x)b_i(x)dx$ and $B_k(x) = [b_1(x), b_2(x), \dots, b_k(x)]^T$.

There is a relation between the block pulse functions and Euler wavelets:

$$\psi(x) = \phi_{k \times k} B_k(x). \tag{3}$$

The block pulse operational matrix of the fractional integration $F^\alpha, \alpha \geq 0$ is defined as in (Kilicman 2007), that is:

$$(I^\alpha B_k)(x) \approx F^\alpha B_k(x), \tag{4}$$

where

$$F^\alpha = \frac{1}{k^\alpha} \frac{1}{\Gamma(\alpha + 2)} \begin{pmatrix} 1 & \xi_1 & \xi_2 & \xi_3 & \dots & \xi_{k-1} \\ 0 & 1 & \xi_1 & \xi_2 & \dots & \xi_{k-2} \\ 0 & 0 & 1 & \xi_1 & \dots & \xi_{k-3} \\ \vdots & \vdots & \ddots & \ddots & \ddots & \vdots \\ 0 & 0 & \dots & 0 & 1 & \xi_1 \\ 0 & 0 & \dots & 0 & 0 & 1 \end{pmatrix}$$

with $\xi_s = (s + 1)^{\alpha+1} - 2s^{\alpha+1} + (s - 1)^{\alpha+1}$.

The fractional integration of order $\alpha \geq 0$ of the vector $\psi(x)$ defined in (2) can be approximated as:

$$(I^\alpha \psi)(x) \approx P_{k \times k}^\alpha \psi(x), \tag{5}$$

where $P_{k \times k}^\alpha$ is called Euler wavelet operational matrix of order $\alpha \geq 0$. Using (3) and (4), we attain:

$$(I^\alpha \psi)(x) \approx (I^\alpha \phi_{k \times k} B_k)(x) = \phi_{k \times k} (I^\alpha B_k)(x) \approx \phi_{k \times k} F^\alpha B_k(x). \tag{6}$$

Thus, combining (5) and (6), we attain:

$$P_{k \times k}^\alpha \psi(x) \approx (I^\alpha \psi)(x) \approx \phi_{k \times k} F^\alpha B_k(x) = \phi_{k \times k} F^\alpha \phi_{k \times k}^{-1} \psi(x) \text{ and so}$$

$$P_{k \times k}^\alpha \approx \phi_{k \times k} F^\alpha \phi_{k \times k}^{-1}.$$

For example, the Euler wavelet operational matrix of the fractional integration for $j = 2, M = 3$ and $\alpha = 0.5$ yields:

$$P_{6 \times 6}^{0.5} = \begin{pmatrix} 0.4616 & 0.3150 & -0.1631 & 0.5012 & -0.1509 & 0.1404 \\ 0.0878 & 0.2243 & 0.4203 & 0.0717 & -0.0449 & 0.0626 \\ -0.1305 & -0.1591 & 0.2354 & -0.2110 & 0.0615 & -0.0545 \\ 0 & 0 & 0 & 0.4616 & 0.3150 & -0.1631 \\ 0 & 0 & 0 & 0.0878 & 0.2243 & 0.4203 \\ 0 & 0 & 0 & -0.1305 & -0.1591 & 0.2354 \end{pmatrix}.$$

Since the operational matrix $P_{6 \times 6}^{0.5}$ contains many zeros, the calculations are fast using this phenomena.

4 Numerical examples

To demonstrate the efficiency of the proposed numerical scheme based on Euler wavelets, we discuss some numerical examples.

Example 4.1 Consider:

$$AD^\alpha y(x) + BD^\beta y(x) + Cy(x) = g(x), \text{ with}$$

$$y(0) = y_0, y'(0) = y_1, 0 < \beta < \alpha \leq 2, 0 \leq x < 1, \tag{7}$$

Table 1 Comparisons between numerical solutions attained by proposed numerical scheme (EWM) for $M = 3$ and various numerical methods

x	y_{exact}	y_{EWM} ($j = 9$)	y_{FDM} (Arikoglu and Ozkal 2007)	y_{ADM} (Momani and Odibat 2007)	y_{FDTM} (Arikoglu and Ozkal 2007)	y_{VIM} (Momani and Odibat 2007)	y_{LWM} ($j = 10$) (ur Rehman and Khan 2011)
0.0	0.000000	0.000000	0.000000	0.000000	0.000000	0.000000	0.000000
0.1	0.039750	0.039750	0.039473	0.039874	0.039750	0.039874	0.039750
0.2	0.157036	0.157036	0.157703	0.158512	0.157036	0.158512	0.157035
0.3	0.347370	0.347370	0.352402	0.353625	0.347370	0.353625	0.347370
0.4	0.604695	0.604695	0.620435	0.622083	0.604695	0.622083	0.604695
0.5	0.921768	0.921768	0.957963	0.960047	0.921768	0.960047	0.921767
0.6	1.290457	1.290456	1.360551	1.363093	1.290457	1.363093	1.290456
0.7	1.702008	1.702008	1.823267	1.826257	1.702008	1.826257	1.702007
0.8	2.147287	2.147286	2.340749	2.344224	2.147287	2.344224	2.147286
0.9	2.617001	2.617000	2.907324	2.911278	2.617001	2.911278	2.617000

where $A \neq 0, B, C \in \mathbb{R}, g(x) \in L^2[0, 1]$, and $y(x)$ is the solution to be determined(ur Rehman and Khan 2011).

For $\alpha = 2, \beta = \frac{3}{2}$, Eq. (7) reduces to the Bagley–Torvik equation which arises in modelling the motion of a rigid plate immersed in a Newtonian fluid.

$$\text{Suppose } D^\alpha y(x) \simeq C^T \psi(x) \text{ and } g(x) \simeq F^T \psi(x), \text{ where } F^T = [g_1, g_2, \dots, g_k] \quad (8)$$

$$\text{Then } D^\beta y(x) = I^{\alpha-\beta} (D^\alpha y)(x) = C^T P_{k \times k}^{\alpha-\beta} \psi(x) \quad (9)$$

and

$$y(x) = C^T P_{k \times k}^\alpha \psi(x) + y_0 + y_1 x. \quad (10)$$

Using (8), (9), and (10) in (7), we have the following system of algebraic equations:

$$AC^T \psi(x) + BC^T P_{k \times k}^{\alpha-\beta} \psi(x) + C[C^T P_{k \times k}^\alpha \psi(x) + y_0 + y_1(x)] = F^T \psi(x).$$

If $\alpha = 2, \beta = \frac{1}{2}, A = B = C = 1, g(x) = 8$ and $y_0, y_1 = 0$, the numerical solutions of (7) obtained by the proposed numerical scheme based on Euler wavelets (EWM) are compared with the numerical solutions obtained by finite difference method (FDM), adomian decomposition method (ADM), finite difference transform method (FDTM), variational iteration method (VIM), and Legendre Wavelet Method (LWM) in Table 1. Clearly, comparisons of numerical solutions in Table 1 show that the numerical scheme based on Euler wavelets is superior to those mentioned above numerical schemes.

Example 4.2 In Example 4.1, suppose $A = B = C = 1$:

$$\alpha = 2, 0 \leq \beta \leq 1, y_0 = 0, y_1 = 0 \text{ and } g(x) = 6x^3 \left(\frac{x^{-\alpha}}{\Gamma(4-\alpha)} - \frac{x^{-\beta}}{\Gamma(4-\beta)} \right).$$

The exact solution is given as $y(x) = x^3$. Table 2 shows the absolute errors attained by the proposed numerical scheme (EWM), Legendre wavelet method (LWM), and Haar wavelet method (HWM). From Table 2, we find that the absolute errors become smaller and smaller

Table 2 Comparisons of maximum absolute errors for different values of k and β

EWM β	LWM $k = 24$			HWM $k = 32$		
	$k = 32$	$k = 128$	$k = 96$	$k = 32$	$k = 96$	$k = 128$
0.25	1.4205×10^{-5}	5.1634×10^{-6}	8.546×10^{-4}	4.807×10^{-4}	5.343×10^{-5}	3.005×10^{-5}
0.50	1.0680×10^{-4}	5.3760×10^{-7}	7.963×10^{-4}	4.479×10^{-4}	4.978×10^{-5}	2.800×10^{-5}
0.75	1.0605×10^{-4}	1.1484×10^{-5}	7.405×10^{-4}	4.166×10^{-4}	4.631×10^{-5}	2.605×10^{-5}
1.00	6.8563×10^{-5}	4.1935×10^{-5}	6.946×10^{-4}	3.907×10^{-4}	4.341×10^{-5}	2.442×10^{-5}

Table 3 Comparisons between numerical solutions attained by proposed numerical scheme and Legendre wavelet method

x	$\beta = 0.50$		$\beta = 0.75$		$\beta = 0.999$		Exact($\beta = 1$)
	EWM	LWM	EWM	LWM	EWM	LWM	
0.1	19.3564	19.3481	19.6378	19.6340	19.8017	19.8012	19.8010
0.2	19.0219	19.0500	19.3599	19.3717	19.6042	19.6039	19.6040
0.3	18.8214	18.8163	19.1422	19.1413	19.4091	19.4086	19.4089
0.4	18.6545	18.6471	18.9462	19.9428	19.2165	19.2154	19.2158
0.5	18.4927	18.4976	18.7530	18.7573	19.0238	19.0242	19.0246
0.6	18.3680	18.3669	18.5861	18.5854	18.8359	18.8349	18.8353
0.7	18.2432	18.2450	18.4193	18.4207	18.6480	18.6475	18.6479
0.8	18.1312	18.1319	18.2623	18.2630	18.4625	18.4620	18.4623
0.9	18.0285	18.0275	18.1131	18.1124	18.2793	18.2784	18.2786

with k increasing. Also, Table 2 shows that the proposed numerical scheme can reach a higher degree of accuracy than Legendre and Haar wavelets. This confirms that numerical results attained by the proposed numerical scheme are in good agreement with the exact solution compared to the results obtained by the Legendre and Haar wavelet methods.

Example 4.3 Consider the fractional differential equation (11) given below of an Electrical Circuit with charged capacitor having capacitance C farads and resistor having resistance R ohms (Arora and Chauhan 2017; Altaf and Khan 2019):

$$D^\beta Q(x) + \kappa Q(x) = 0, \quad \beta \in (0, 1], x \in [0, 1) \tag{11}$$

with initial state $Q(0) = Q_0$, where $\kappa = \frac{1}{RC}$:

The exact solution of (11) for $\beta = 1$ is $Q(x) = Q_0 e^{-\kappa x}$.

$$\text{Suppose } D^\beta Q(x) \simeq C^T \psi(x) \tag{12}$$

$$\text{Then } Q(x) = C^T P^\beta \psi(x) + Q_0 \tag{13}$$

Thus, using (12) and (13) in (11), we attain:

$$C^T \psi(x) + \kappa [C^T P^\beta \psi(x) + Q_0] = 0. \tag{14}$$

By solving the matrix equation (14), we can obtain the co-efficients vector C . In Table 3, we show the numerical solutions of (11) attained by the proposed numerical scheme (EWM) and Legendre wavelet method (LWM) for $R = 10, C = 1, Q_0 = 20$ and for some different values of β . Clearly, Table 3 shows the proposed numerical scheme based on Euler wavelets is superior to Legendre wavelet method.

Example 4.4 Consider the multi-term fractional differential equation (Diethelm et al. 2002; Kumar and Agarwal 2006):

$$D^2 y(x) + 3Dy(x) + 2D^{q_2} y(x) + D^{q_1} y(x) + 5y(x) = f(x), \tag{15}$$

where $0 < q_1 < q_2 < 1, 0 \leq x < 1$ and:

$$f(x) = 1 + 3x + \frac{2}{\Gamma(3 - q_2)} x^{2-q_2} + \frac{1}{\Gamma(3 - q_1)} x^{2-q_1} + 5(1 + 0.5x^2)$$

Table 4 Absolute errors for $M = 3$ and different values of j

x	$j = 3$	$j = 5$	$j = 7$	$j = 9$	$j = 11$
0.1	2.7746e-04	1.7346e-05	1.0839e-06	6.7737e-08	4.2335e-09
0.2	2.4925e-04	1.5530e-05	9.7013e-07	6.0625e-08	3.7889e-09
0.3	2.1031e-04	1.3092e-05	8.1761e-07	5.1091e-08	3.1930e-09
0.4	1.6732e-04	1.0390e-05	6.4872e-07	4.0535e-08	2.5332e-09
0.5	1.2436e-04	7.6988e-06	4.8055e-07	3.0024e-08	1.8763e-09
0.6	8.4086e-05	5.2128e-06	3.2527e-07	2.0321e-08	1.2699e-09
0.7	4.9432e-05	3.0575e-06	1.9067e-07	1.1909e-08	7.4420e-10
0.8	2.1033e-05	1.2979e-06	8.0809e-08	5.0447e-09	3.1518e-10
0.9	7.3449e-07	4.8261e-08	3.2143e-09	2.0522e-10	1.2910e-11

with the initial states $y(0) = 1$ and $y'(0) = 0$.

If $q_1 = 0.0159$ and $q_2 = 0.1379$, then the exact solution of (15) is given by $y(x) = 1 + 0.5x^2$.

$$\text{Suppose } D^2 y(x) \simeq C^T \psi(x) \text{ and } f(x) \simeq F^T \psi(x) \tag{16}$$

$$\text{Then } Dy(x) = C^T P_{k \times k} \psi(x) \tag{17}$$

$$D^{q_2} y(x) = C^T P_{k \times k}^{2-q_2} \psi(x) \tag{18}$$

$$D^{q_1} y(x) = C^T P_{k \times k}^{2-q_1} \psi(x) \tag{19}$$

and

$$y(x) = C^T P_{k \times k}^2 \psi(x) + 1. \tag{20}$$

Using (16)-(20) in (15), we arrive:

$$C^T \psi(x) + 3C^T P_{k \times k} \psi(x) + 2C^T P_{k \times k}^{2-q_2} \psi(x) + C^T P_{k \times k}^{2-q_1} \psi(x) + 5[C^T P_{k \times k}^2 \psi(x) + [1, 1, \dots, 1] \phi_{k \times k}^{-1} \psi(x)] = F^T \psi(x). \tag{21}$$

Solving the system of algebraic equations (21), we can attain the co-efficient vector C^T , and so, we can get the approximate output response $y(x)$. Table 4 shows that the absolute errors attained by the proposed numerical scheme with $M = 3$ and the values of j increasing become smaller and smaller. From Table 4, we also infer that the approximate solutions converge to the exact solution. Table 5 shows that the proposed numerical scheme(EWM) can reach a higher degree of accuracy than Adams-type predictor–corrector method.

Example 4.5 Consider the linear fractional differential equation (El-Sayed et al. 2004; Keshavarz et al. 2014):

$$D^\alpha y(x) + y(x) = 0 \text{ with } 0 < \alpha \leq 2, 0 \leq x < 1, \tag{22}$$

and

$$y(0) = 1, y'(0) = 0.$$

Table 5 Comparison of maximum absolute errors for proposed numerical scheme with $j = 3, M = 3$ and Adams-type predictor–corrector method

Step size	Maximum absolute errors	
	EWM	Adams-type predictor–corrector method
0.1	7.3449e−07	0.051115750000
0.01	7.3449e−07	0.004546523000
0.001	1.1577e−08	0.000409626200

Table 6 Absolute errors for different values of k and for $\alpha = 1.5$

x	$k = 12$	$k = 24$	$k = 48$	$k = 96$	$k = 192$	$k = 384$
0.1	6.8808e−04	6.9051e−05	2.2513e−05	7.0231e−06	1.7455e−06	4.156e−07
0.2	7.9552e−05	3.5316e−05	1.3415e−05	3.3178e−06	7.608e−07	1.911e−07
0.3	9.4834e−05	2.2910e−05	2.9444e−06	7.7780e−07	2.384e−07	5.91e−08
0.4	1.0088e−04	8.0418e−06	2.1604e−06	8.1000e−07	1.974e−07	4.58e−08
0.5	3.6805e−04	6.4931e−05	1.2401e−05	2.5924e−06	5.859e−07	1.4209e−07
0.6	1.6556e−04	5.2566e−05	1.3004e−05	3.0970e−06	7.968e−07	2.225e−07
0.7	2.7243e−04	6.6998e−05	1.5649e−05	4.0075e−06	1.1023e−06	3.5728e−07
0.8	2.8032e−04	7.0973e−05	1.9028e−05	5.0157e−06	1.5096e−06	6.49e−07
0.9	3.4727e−04	8.0723e−05	2.1038e−05	6.1479e−06	2.316e−06	1.3906e−06

Table 7 Comparison of maximum absolute errors for $\alpha = 1.5, M = 3$, and different values of j

	$j = 4$	$j = 5$	$j = 8$
EWM	8.042e−06	2.160e−06	4.58e−08
LWM	1.178e−05	2.948e−06	4.605e−08

The second initial condition is only for $1 < \alpha \leq 2$. The exact solution of (22) is:

$$y(x) = E_\alpha(-x^\alpha), \text{ where } E_\alpha(z) = \sum_0^\infty \frac{z^k}{\Gamma(\alpha k + 1)}$$

is the Mittag–Leffler function of order α

$$\text{Suppose } D^\alpha y(x) \simeq C^T \psi(x); \tag{23}$$

$$\text{Then } y(x) = C^T P_{k \times k}^\alpha \psi(x) + 1. \tag{24}$$

Using (23) and (24) in (22), we arrive:

$$C^T \psi(x) + C^T P_{k \times k}^\alpha \psi(x) + 1 = 0. \tag{25}$$

Solving the system (25) at the collocation points, we can obtain the Euler co-efficient vector C^T . For $\alpha = 1$, the exact solution of (22) is $y(x) = e^{-x}$, and for $\alpha = 2$, the exact solution of (22) is $y = \cos x$. Table 6 shows that the absolute errors attained by the proposed numerical scheme with the values of k increasing become smaller and smaller. From Table 6, we also infer that the approximate solutions converge to the exact solution. In Table 7, we show the maximum absolute errors attained by the proposed numerical scheme (EWM) and Legendre wavelet method (LWM) for $\alpha = 1.5, M = 3$, and different values of j . Clearly

from Table 7, we infer that the numerical scheme based on Euler wavelets is superior to Legendre wavelets method.

5 Conclusion

In this article, an expeditious Euler wavelet operational matrix was derived to attain numerical solutions of fractional differential equations. Numerical examples elucidated the solution process and the efficiency of the proposed numerical scheme. Also, numerical results attained by the proposed numerical scheme were in a better agreement with the exact solutions, and so, the proposed numerical scheme based on Euler wavelet is superior to many other numerical schemes.

Acknowledgements The authors are grateful to the anonymous reviewers for several comments and suggestions which contributed to the improvement of this paper.

References

- Abd-Elhameed WM, Youssri YH (2015) New spectral solutions of multi-term fractional order initial value problems with error analysis. *Comput Model Eng Sci* 105:375–398
- Altaf S, Khan SY (2019) Numerical Solution of Fractional Electrical Circuits by Haar wavelet. *MATHEMATIKA:MIAM* 35(3):331–343
- Arikoglu A, Ozkal I (2007) Solution of fractional differential transform method. *Chaos Solitons Fractal* 34:1473–81
- Arora R, Chauhan NS (2017) An application of Legendre wavelet in fractional electrical circuits. *Glob J Pure Appl Math* 13(2):183–202
- Baleanu D, Jajarmi A, Hajjipour M (2018) On the nonlinear dynamical systems within the generalized fractional derivatives with Mittag-Leffler kernel. *Nonlinear Dyn* 94:397–414. <https://doi.org/10.1007/s11071-018-4367-y>
- Beylkin G, Coifman R, Rokhlin V (1991) Fast wavelet transforms and numerical algorithms, I. *Commun Pure Appl Math* 44:141–183
- Celik I (2018) Generalization of Chebyshev wavelet collocation method to the rth-order differential equations. *CMMA* 3(2):31–47
- Chang P, Isah A (2016) Legendre wavelet operational matrix of fractional derivative through wavelet-polynomial transformation and its applications in solving Fractional order Brusselator system. *J Phys Conf Ser* 693:012001
- Chow TS (2015) Fractional dynamics of interfaces between soft-nanoparticles and rough substrates. *Phys Lett A* 342:148–155
- Demir A, Bayrak MA, Ozbilge E (2019) A new approach for the approximate analytic solution of space-time fractional differential equations by the homotopy analysis method. *Adv Math Phys* (2019) (Article ID 5602565). <https://doi.org/10.1155/2019/5602565>
- Diethelm K, Ford NJ, Freed AD (2002) A predictor corrector approach for the numerical solution of fractional differential equation. *Nonlinear Dyn* 29:3–22
- Dincel AT (2019) Solution to fractional-order Riccati differential equations using Euler wavelet method. *Scientia Iranica D* 26(3):1608–1616
- Doha EH, Abd-Elhameed WM, Youssri YH (2016) New ultraspherical wavelets collocation method for solving 2nth-order initial and boundary value problems. *J Egypt Math Soc* 24(2):319–327
- El-Sayed AMA, El-Mesiry AEM, El-Saka HAA (2004) Numerical solution for multi-term fractional (arbitrary) orders differential equations. *Comput Appl Math* 23:33–54
- Farooq U, Khan H, Baleanu D, Arif M (2019) Numerical solutions of fractional delay differential equations using Chebyshev wavelet method. *Comput Appl Math* 38:195
- Hajjipour M, Jajarmi A, Baleanu D (2018) An efficient nonstandard finite difference scheme for a class of fractional chaotic systems. *J Comput Nonlinear Dyn* 13(2):021013
- Jajarmi A, Hajjipour M, Mohammadzadeh E, Baleanu D (2018) A new approach for the nonlinear fractional optimal control problems with external persistent disturbances. *J Frankl Inst* 355(9):3938–3967

- Javeed S, Baleanu D, Waheed A, Shaukat Khan M, Affan H (2019) Analysis of homotopy perturbation method for solving fractional order differential equations. *Mathematics* 7(1):40
- Karamali G, Dehghan M, Abbaszadeh M (2019) Numerical solution of a time-fractional PDE in the electro-analytical chemistry by a local meshless method. *Eng Comput* 35(1):87–100
- Keshavarz E, Ordokhani Y, Razzaghi M (2014) Bernoulli wavelet operational matrix of fractional order integration and its applications in solving the fractional order differential equations. *Appl Math Model* 38:6038–6051
- Keshavarz E, Ordokhani Y, Razzaghi M (2019) The Bernoulli wavelets operational matrix of integration and its applications for the solution of linear and nonlinear problems in Calculus of variations. *Appl Math Comput* 351:83–98
- Khader MM (2012) Introducing an efficient modification of the homotopy perturbation method by using Chebyshev polynomials. *Arab J Math Sci* 18:61–71
- Kilicman A (2007) Kronecker operational matrices for fractional calculus and some applications. *Appl Math Comput* 187:250–265
- Kumar P, Agarwal OP (2006) An approximate method for numerical solution of fractional differential equations. *Signal Process* 86:2602–10
- Kundu S (2019) Analytical solutions of one-dimensional space-fractional advection–diffusion equation for sediment suspection using homotopy analysis method. *J Eng Mech* 145(2):04019048
- Li W, Pang Y (2020) Application of Adomian decomposition method to nonlinear systems. *Adv Differ Equ* 2020:67
- Ma Y, Li W (2020) Application and research of fractional differential equations of dynamic analysis of supply chain financial chaotic system. *Chaos. Solitons Fractals* 130:109417
- Magin RL (2012) Fractional calculus in bioengineering: A tool to model complex dynamics. In: Proceedings of the 13th International Carpathian Control Conference (ICCC), High Tatras, 2012, pp. 464–469. <https://doi.org/10.1109/CarpathianCC.2012.6228688>
- Momani S, Odibat Z (2007) Numerical comparison of methods for solving linear differential equations of fractional order. *Chaos Solitons Fract* 31:1248–55
- Oruc O, Esen A, Bulut F (2019) A Haar wavelet approximation for two-dimensional time fractional reaction-subdiffusion equation. *Eng Comput* 35(1):75–86
- Rahimkhani P, Ordokhani Y, Babolian E (2017) Numerical solution of fractional pantograph differential equations by using generalized fractional-order Bernoulli wavelet. *J Comput Appl Math* 309:493–510
- Shen S, Liu F, Anh VV (2019) The analytical solution and numerical solutions for a two-dimensional multi-term time fractional diffusion and diffusion-wave equation. *J Comput Appl Math* 345:515–534
- ur Rehman M, Khan RA (2011) The Legendre wavelet method for solving fractional differential equations. *Commun Nonlinear Sci Numer Simul* 16:4163–4173
- Wang Y, Fan Q (2012) The Second kind Chebyshev wavelet method for solving fractional differential equations. *Appl Math Comput* 218:8592–8601
- Wang Y, Yin T (2017) Sine-Cosine wavelet operational matrix of fractional order integration and its applications in solving the fractional order Riccati differential equations. *Adv Differ Equ* 2017:222
- Wang Y, Zhu L (2017) Solving nonlinear Volterra integro-differential equations of fractional order by using Euler wavelet method. *Adv Differ Equ* 2017:27
- Wang Y, Zhu L, Wang Z (2019) Solving the nonlinear variable order fractional differential equations by using Euler wavelets. *CMES* 118(2):339–350
- Xie J, Wang T, Ren Z, Zhang J, Quan L (2019) Haar wavelet method for approximating the solution of a coupled system of fractional-order integral-differential equations. *Math Comput Simul* 163:80–89
- Zhou F, Xiaoyong X (2016) The third kind Chebyshev wavelets collocation method for solving the time-fractional convection diffusion equations with variable coefficients. *Appl Math Comput* 280:11–29
- Ziane D, Cherif MH (2018) Variational iteration transform method for fractional differential equations. *J Interdiscip Math* 21(1):185–199

Publisher's Note Springer Nature remains neutral with regard to jurisdictional claims in published maps and institutional affiliations.



A NOVEL NUMERICAL SCHEME BASED ON BERNOULLI WAVELETS FOR FRACTIONAL DIFFERENTIAL EQUATIONS WITH VARIABLE COEFFICIENTS

R. ARULDOSS and R. ANUSUYA DEVI

Department of Mathematics
Government Arts College (Autonomous)
Kumbakonam (Affiliated to Bharathidasan University)
Tiruchirapalli, Tamil Nadu, India
E-mail: krvarul@gmail.com
anushya3sai@gmail.com

Abstract

This article presents a novel numerical scheme based on the operational matrix of Bernoulli wavelets to transform fractional differential equations with variable coefficients into simultaneous algebraic equations. The uniform convergence analysis for Bernoulli wavelets expansion is investigated. The computational algorithm of the proposed method is also presented for the numerical solutions of fractional differential equations with variable coefficients. Applicability and efficiency of the proposed numerical scheme are illustrated by some numerical examples.

1. Introduction

Fractional Calculus is a valuable tool and an old mathematical topic from 17th century. For many researchers in various fields of science and technology, fractional differential equations have been the focus of interest in recent years. As a result, finding solutions to fractional differential equations is an essential part of scientific research.

Furthermore, analytic solutions to the majority of fractional differential equations are not available. Due to this fact, many numerical schemes have

2020 Mathematics Subject Classification: 26A33, 65T60, 34A08.

Keywords: Riemann-Liouville fractional integral, Caputo fractional derivative, Bernoulli wavelets, Block pulse functions, Fractional integration operational matrix.

Received May 25, 2021; Accepted July 31, 2021

been suggested to find approximate solutions of fractional differential equations, namely, Variational Iteration Method, Finite volume method, Finite element method, Adomian Decomposition Method, and Wavelet methods [1, 4, 8-12].

There have been several methods for solving fractional differential equations with variable coefficients. These types of problems have been studied by many authors using different methods [2, 5, 7].

In this work, we present a numerical method based on Bernoulli wavelets for solving fractional differential equations with variable coefficients. Our aim is to derive Bernoulli wavelets' operational matrices to convert the fractional differential equations with variable coefficients into a system of algebraic equations. It not only simplifies the problem, but also speeds up the computation. Numerical solutions of the proposed method are compared with the solutions of some existing numerical techniques and analytical solutions to manifest the applicability, the computational efficiency and the high precision of the proposed method.

The article is summarized as follows. In Section 2, some basic definitions and mathematical preliminaries of fractional calculus are given. Section 3 is devoted to the basic formulation of Bernoulli wavelets, function approximation, and the operational matrix of fractional order integration for Bernoulli wavelets. Computational algorithm of the scheme is given in Section 4. In Section 5, some numerical examples and absolute errors are presented. Finally, we conclude our work in Section 6.

2. Preliminaries

In this section, we briefly recall some essential definitions and preliminary mathematical facts of fractional calculus which are used further in this paper.

Definition 2.1. Fractional integral of order $\gamma \geq 0$ of $h(x) \in L^1(\mathbb{R}^+)$ in terms of Riemann-Liouville, is defined by

$$(I^\gamma h)(x) = \begin{cases} \frac{1}{\Gamma(\gamma)} \int_0^x \frac{h(\zeta)}{(x-\zeta)^{(1-\gamma)}} d\zeta, & \gamma > 0, \\ h(x), & \gamma = 0. \end{cases} \quad (1)$$

Fractional derivative of order $\gamma > 0$ of $h(x) \in L^1(\mathbb{R}^+)$ in terms of Riemann-Liouville, is normally defined by

$$(I^{-\gamma}h)(x) = \left(\frac{d}{dx}\right)^s (I^{s-\gamma}h)(x), \quad s - 1 < \gamma \leq s, \tag{2}$$

where s is a positive integer and $x > 0$.

Definition 2.2. The Caputo fractional derivative of order $\gamma \geq 0$ of $h(x) \in L^1(\mathbb{R}^+)$ is given by

$$(D^\gamma h)(x) = \frac{1}{\Gamma(s-\gamma)} \int_0^x (x-\zeta)^{s-\gamma-1} h^{(s)}(\zeta) d\zeta, \quad s - 1 < \gamma \leq s, \tag{3}$$

where s is a positive integer and $x > 0$.

If $h(x) \in L^1(\mathbb{R}^+)$ and $\gamma \geq 0$ then it has the following two basic properties.

$$(D^\gamma I^\gamma h)(x) = h(x), \tag{4}$$

and

$$(I^\gamma D^\gamma h)(x) = h(x) - \sum_{l=0}^{s-1} h^{(l)}(0^+) \frac{x^l}{l!}, \quad s - 1 < \gamma \leq s, \tag{5}$$

where s is a positive integer, $x > 0$ and $h^{(l)}(0^+) := \lim_{x \rightarrow 0^+} D^l h(x)$, $l = 0, 1, 2, \dots, s - 1$.

3. Bernoulli Wavelets

We here discuss Bernoulli polynomials and some of their properties in order to construct Bernoulli wavelets.

3.1. Properties of Bernoulli polynomials and Bernoulli wavelets

Wavelets represent a family of functions constructed from dilations and translations of a single function $\Psi(x)$ called the mother wavelet. When the dilation parameter c and the translation parameter d change continuously, the following family of continuous wavelets is obtained.

$$\psi_{cd}(x) = |c|^{-\frac{1}{2}} \psi\left(\frac{x-d}{c}\right), \quad c, d \in \mathbb{R}, c \neq 0. \quad (6)$$

If the discrete values are selected for the translation and dilation parameters, that is, $c = c_0^{-p}$, $d = qd_0c_0^{-p}$, $c_0 > 1$, $d_0 > 0$, $p, q \in \mathbb{Z}^+$, then we have the following family of discrete wavelets,

$$\psi_{pq}(x) = |c_0|^{\frac{p}{2}} \psi(c_0^p x - qd_0), \quad (7)$$

where the functions ψ_{pq} form a wavelet basis for $L^2(\mathbb{R})$. Specifically, when $c_0 = 2$ and $d_0 = 1$, the functions $\psi_{pq}(x)$ form an orthonormal basis for $L^2(\mathbb{R})$.

The Bernoulli wavelets are defined on $[0, 1)$ as

$$\psi_{pq}(x) = \begin{cases} 2^{\frac{j-1}{2}} \tilde{E}_n(2^{j-1}x - m + 1), & \frac{m-1}{2^{j-1}} \leq x < \frac{m}{2^{j-1}}, \\ 0, & \text{otherwise,} \end{cases} \quad (8)$$

for $m = 1, 2, \dots, 2^{j-1}$, $n = 0, 1, \dots, N-1$ and $j, N \in \mathbb{N}$, where

$$\tilde{E}_n(x) = \begin{cases} 1, & n = 0, \\ \frac{1}{\sqrt{\left(\frac{(-1)^{n-1}(n!)^2}{(2n)!}\right) \beta_{2n}}} E_n(x), & n > 0, \end{cases}$$

the coefficient $\frac{1}{\sqrt{\left(\frac{(-1)^{n-1}(n!)^2}{(2n)!}\right) \beta_{2n}}}$ is used for normality, the dilation

parameter is $2^{-(j-1)}$ and the translation parameter is $(m-1)2^{-(j-1)}$. Here $E_n(x)$, $n = 0, 1, \dots, N-1$, denote Bernoulli polynomials of order n which can be defined by the relation

$$E_n(x) = \sum_{r=0}^n \binom{n}{r} \beta_r x^{n-r}, \quad (9)$$

where β_r , ($r = 0, 1, 2, \dots, n$) are Bernoulli numbers. Bernoulli numbers can

be defined by the following generating function

$$\frac{x}{e^x - 1} = \sum_{r=0}^{\infty} \beta_r \frac{x^r}{r!}. \tag{10}$$

The first few Bernoulli numbers are

$$\beta_0 = 1, \beta_1 = -\frac{1}{2}, \beta_2 = \frac{1}{6}, \beta_4 = -\frac{1}{30}, \dots, \tag{11}$$

with $\beta_{2r+1} = 0, r = 1, 2, 3, \dots$

The first few Bernoulli polynomials are

$$E_0(x) = 1, E_1(x) = x - \frac{1}{2}, E_2(x) = x^2 - x + \frac{1}{6}, E_3(x) = x^3 - \frac{3}{2}x^2 + \frac{1}{2}x, \dots \tag{12}$$

The properties of Bernoulli polynomials and Bernoulli wavelets have been discussed by Sahu and Saha Ray [10] and Jiao et al. [13].

Moreover,

$$\int_0^1 E_m(x)E_n(x)dx = (-1)^{m-1} \frac{n!m!}{(n+m)!} \beta_{m+n}, \quad n, \quad m \geq 1, \tag{13}$$

and

$$\int_0^1 |E_n(x)|dx \leq 16 \frac{n!}{(2\pi)^{n+1}}, \quad n \geq 0. \tag{14}$$

Let $\psi(x) = [\psi_1(x), \psi_2(x), \dots, \psi_k(x)]^T$, where $\psi_i(x) = \psi_{mn}(x), i = N(m-1) + n + 1, k = 2^{j-1}N, m = 1, 2, \dots, 2^{j-1}, n = 0, 1, \dots, N-1$ and $j, N \in \mathbb{N}$. Then Bernoulli wavelets have the following orthonormality properties.

$$\langle \psi_r(x), \psi_s(x) \rangle = \int_0^1 \psi_r(x)\psi_s(x)dx = \{1, r = s, 0, r \neq s, \tag{15}$$

and

$$\int_0^1 \Psi(x)\Psi^T(x)dx = E, \tag{16}$$

where $\langle \dots \rangle$ denotes the inner product and E indicates identity matrix.

3.2. Function approximation

A function $h(x) \in L^2[0, 1)$ can be expressed in terms of Bernoulli wavelets as

$$h(x) = \sum_{m=0}^{\infty} \sum_{n \in Z} a_{mn} \psi_{mn}(x), \quad (17)$$

where the coefficients a_{mn} are given by

$$a_{mn} = \langle h(x), \psi_{mn}(x) \rangle = \int_0^1 h(x) \psi_{mn}(x) dx.$$

By truncating the infinite series in Equation (17), $h(x)$ is approximated as

$$\widetilde{h(x)} \approx \sum_{m=1}^{2^{j-1}} \sum_{n=0}^{N-1} a_{mn} \psi_{mn}(x). \quad (18)$$

For simplicity, Equation (18) is written as

$$\widetilde{h(x)} = \sum_{i=1}^k a_i \psi_i(x) = A^T \Psi(x), \quad (19)$$

where $a_i = a_{mn}$, $\psi_i = \psi_{mn}$, $k = 2^{j-1}N$, $A = [a_1, a_2, \dots, a_k]^T$, (20)

and

$$\Psi(x) = [\psi_1(x), \psi_2(x), \dots, \psi_k(x)]^T. \quad (21)$$

The index i is determined by the relation $i = N(m-1) + n + 1$.

We define the Bernoulli wavelet coefficient matrix $\phi_{k \times k}$, $k = 2^{j-1}N$, at the collocation points $x_r = \frac{2r-1}{2k}$, $r = 1, 2, \dots, k$ as

$$\phi_{k \times k} = \left[\Psi\left(\frac{1}{2k}\right), \Psi\left(\frac{3}{2k}\right), \dots, \Psi\left(\frac{2k-1}{2k}\right) \right]. \quad (22)$$

Specifically, the Bernoulli wavelet coefficient matrix for $j = 2$ and $N = 3$ becomes

$$\phi_{6 \times 6} = \begin{pmatrix} 1.4142 & 1.4142 & 1.4142 & 0 & 0 & 0 \\ -1.6330 & 0 & 1.6330 & 0 & 0 & 0 \\ 0.5270 & -1.5811 & 0.5270 & 0 & 0 & 0 \\ 0 & 0 & 0 & 1.4142 & 1.4142 & 1.4142 \\ 0 & 0 & 0 & -1.6330 & 0 & 1.6330 \\ 0 & 0 & 0 & 0.5270 & -1.5811 & 0.5270 \end{pmatrix}. \tag{23}$$

Here, we have

$$\tilde{h}_k = [\tilde{h}(x_1), \tilde{h}(x_2), \dots, \tilde{h}(x_k)] = A^T \phi_{k \times k}.$$

Since the Bernoulli wavelet coefficient matrix $\phi_{k \times k}$ is invertible, it is possible to obtain the Bernoulli wavelet coefficient vector A^T by $\tilde{h}_k \phi_{k \times k}^{-1}$.

3.3. Operational matrix of fractional order integration

In this section, we explore the basic idea of finding the operational matrix of fractional order integration for the Bernoulli wavelets.

A k -set of Block pulse functions (BPFs) over the interval $[0, 1)$ is defined as

$$b_r(x) = \begin{cases} 1, & (r - 1) / k \leq x < r / k, \\ 0, & \text{otherwise,} \end{cases} \tag{24}$$

where $r = 1, 2, 3, \dots, k$.

It is known that any square integrable function $h(x)$ defined on the interval $[0, 1)$ can be extended in terms of BPFs, and by using orthogonality of BPFs as

$$h(x) = \sum_{r=1}^k h_r b_r(x) = h^T B_k(x), \tag{25}$$

where $h = [h_1, h_2, \dots, h_k]^T$, h_r for $r = 1, 2, \dots, k$ are given by

$$h_r = \frac{1}{k} \int_{(r-1)/k}^{r/k} h(x) b_r(x) dx, \text{ and } B_k(x) = [b_1(x), b_2(x), \dots, b_k(x)]^T.$$

There is a connection between the block pulse functions and Bernoulli

wavelets, which is,

$$\Psi(x) = \phi_{k \times k} B_k(x). \quad (26)$$

The block pulse operational matrix H^β , $\beta \geq 0$ of fractional integration of order $\beta \geq 0$ is defined by Kilicman [6] as,

$$(I^\beta B_k)(x) \approx H^\beta B_k(x), \quad (27)$$

where

$$H^\beta = \frac{1}{k^\beta} \frac{1}{\Gamma(\beta + 2)} \begin{pmatrix} 1 & \zeta_1 & \zeta_2 & \zeta_3 & \dots & \zeta_{k-1} \\ 0 & 1 & \zeta_1 & \zeta_2 & \dots & \zeta_{k-2} \\ 0 & 0 & 1 & \zeta_1 & \dots & \zeta_{k-3} \\ \vdots & \vdots & \ddots & \ddots & \vdots & \vdots \\ 0 & 0 & \dots & 0 & 1 & \zeta_1 \\ 0 & 0 & \dots & 0 & 0 & 1 \end{pmatrix},$$

with $\zeta_j = (j+1)^{\beta+1} - 2j^{\beta+1} + (j-1)^{\beta+1}$.

The fractional integration of order $\beta \geq 0$ of the vector $\Psi(x)$ defined in Equation (21) can be approximated as

$$(I^\beta \Psi)(x) \approx P_{k \times k}^\beta \Psi(x), \quad (28)$$

where $P_{k \times k}^\beta$ is called Bernoulli wavelet operational matrix of order $\beta \geq 0$.

Using Equations (26) and (27), we attain

$$(I^\beta \Psi)(x) \approx (I^\beta \phi_{k \times k} B_k)(x) = \phi_{k \times k} (I^\beta B_k)(x) \approx \phi_{k \times k} H^\beta B_k(x). \quad (29)$$

Thus combining Equations (28) and (29), we attain

$$P_{k \times k}^\beta \Psi(x) \approx (I^\beta \Psi)(x) \approx \phi_{k \times k} H^\beta B_k(x) = \phi_{k \times k} H^\beta \phi_{k \times k}^{-1} \Psi(x), \text{ and so} \quad (30)$$

$$P_{k \times k}^\beta \approx \phi_{k \times k} H^\beta \phi_{k \times k}^{-1}. \quad (31)$$

For example, the Bernoulli wavelet operational matrix of the fractional order integration for $j = 2$, $N = 3$ and $\beta = 0.5$ yields

$$P_{6 \times 6}^{0.5} = \begin{pmatrix} 0.5282 & 0.1819 & -0.0298 & 0.4438 & -0.0871 & 0.0256 \\ -0.1452 & 0.2243 & 0.1329 & 0.0799 & -0.0449 & 0.0198 \\ -0.0598 & -0.0964 & 0.1688 & -0.0417 & -1.8589e - 04 & 0.0029 \\ 0 & 0 & 0 & 0.5282 & 0.1819 & -0.0298 \\ 0 & 0 & 0 & -0.1452 & 0.2243 & 0.1329 \\ 0 & 0 & 0 & -0.0598 & -0.0964 & 0.1688 \end{pmatrix}. \tag{32}$$

Since the operational matrix $P_{6 \times 6}^{0.5}$ contains several zeros, the proposed technique reduces the computation greatly.

3.4. Convergence analysis

In the following theorem, we establish the convergence of the Bernoulli wavelets expansion [10].

Theorem 3.1. *If $h(x) \in L^2[0, 1)$ is a continuous function and $|h(x)| \leq \eta$, $\eta \in \mathbb{R}$, then the Bernoulli wavelets expansion of $h(x)$ defined in Equation (17) converges uniformly and also*

$$|a_{mn}| < \eta \frac{F}{2^{\frac{j-1}{2}}} \frac{16n!}{(2\pi)^{n+1}}, \tag{33}$$

where

$$F = \frac{1}{\sqrt{\left(\frac{(-1)^{n-1}(n!)^2}{(2n)!}\right)\beta_{2n}}}.$$

Proof. Any function $h(x) \in L^2[0, 1)$ can be approximated in terms of Bernoulli wavelets as

$$h(x) \approx \sum_{m=1}^{2^{j-1}} \sum_{n=0}^{N-1} a_{mn} \psi_{mn}(x), \tag{34}$$

Here

$$a_{mn} = \int_0^1 h(x) \psi_{mn}(x) dx$$

$$= \sum_m \int_{I_{j,m}} h(x) \psi_{mn}(x) dx, \text{ where } I_{j,m} = \left[\frac{m-1}{2^{j-1}}, \frac{m}{2^{j-1}} \right), m = 1, 2, \dots, 2^{j-1}, \quad (35)$$

$$= 2^{\frac{j-1}{2}} F \sum_m \int_{I_{j,m}} h(x) E_n(2^{j-1}x - m + 1) dx, \text{ where } F = \frac{1}{\sqrt{\left(\frac{(-1)^{n-1} (n!)^2}{(2n)!} \right) \beta_{2n}}}. \quad (36)$$

Using $2^{j-1}x - m + 1 = t$, we have

$$a_{mn} = \frac{F}{2^{j-1}} \sum_m \int_{I_{j,m}} h\left(\frac{t+m-1}{2^{j-1}}\right) E_n(x) dt, \quad (37)$$

and so

$$\begin{aligned} |a_{mn}| &= \left| \frac{F}{2^{\frac{j-1}{2}}} \sum_m \int_{I_{j,m}} h\left(\frac{t+m-1}{2^{j-1}}\right) E_n(t) dt \right| \leq \frac{F\eta}{2^{\frac{j-1}{2}}} \int_0^1 E_n(t) |dt| \\ &< \frac{F\eta}{2^{\frac{j-1}{2}}} 16 \frac{n!}{(2\pi)^{n+1}}. \end{aligned} \quad (38)$$

Thus the series $\sum_{m=1}^{2^{j-1}} \sum_{n=0}^{N-1} a_{mn}$ is absolutely convergent, and so the series $\sum_{m=1}^{2^{j-1}} \sum_{n=0}^{N-1} a_{mn} \psi_{mn}(x)$ is uniformly convergent. \square

4. Algorithm for the Proposed Numerical Scheme

Step 1. Assign the values for j and N for step size $k = 2^{j-1}N$ in Equation (20).

Step 2. Compute Bernoulli wavelet coefficient matrix $\phi_{k \times k}$ at the collocation points $x_r = \frac{2r-1}{2k}$, $r = 1, 2, \dots, k$ from Equation (22).

Step 3. Compute the block pulse operational matrix H^β from Equation (27).

Step 4. Construct Bernoulli wavelet operational matrix $P_{k \times k}^\beta$ of order $\beta \geq 0$ using Equation (31).

Step 5. Dispersing the coefficients of the given fractional differential equations at the collocation points, construct diagonal matrices.

Step 6. Express all Caputo fractional derivatives in the given fractional differential equations in terms of Bernoulli wavelets.

Step 7. Solve the system of algebraic equations using MATLAB2015a to compute the unknown vector.

Step 8. Compute the solution using the unknown vector and the Bernoulli wavelet operational matrix.

5. Numerical Experiments

To show the applicability and the effectiveness of the proposed numerical scheme, we consider here some fractional differential equations with variable coefficients.

Example 5.1. Consider the following fractional order linear differential equation with variable coefficients

$$r[D^2h(x)] + s(x)[D^{\gamma_2}h(x)] + t(x)[Dh(x)] + u(x)[D^{\gamma_1}h(x)] + v(x)h(x) = w(x), \tag{39}$$

with $0 \leq x < 1$, $0 < \gamma_1 \leq 1$, $1 < \gamma_2 \leq 2$, $h(0) = 2$ and $h'(0) = 0$,

where $r \in \mathbb{R}$, $s(x)$, $t(x)$, $u(x)$, $v(x)$, $h(x)$, $w(x) \in L^2[0, 1]$,

$$w(x) = -r - \frac{s(x)}{\Gamma(3 - \gamma_2)} x^{2-\gamma_2} - t(x)x - \frac{u(x)}{\Gamma(3 - \gamma_2)} x^{2-\gamma_2} + u(x)(2 - \frac{1}{2} x^2).$$

Suppose

$$D^2h(x) \approx A^T \Psi(x) \text{ where } A = [a_1, a_2, \dots, a_k]^T, \text{ and}$$

$$w(x) \approx W^T \Psi(x) \text{ where } w = [w_1, w_2, \dots, w_k]. \tag{40}$$

$$\text{Then } D^{\gamma_2}h(x) = A^T P_{k \times k}^{2-\gamma_2} \Psi(x), \tag{41}$$

$$D^{\gamma_1}h(x) = A^T P_{k \times k}^{2-\gamma_1} \Psi(x), \tag{42}$$

$$Dh(x) = A^T P_{k \times k} \Psi(x), \tag{43}$$

$$\text{and } h(x) = A^T P_{k \times k}^2 \Psi(x) + 2. \tag{44}$$

Using Equations (40)-(44) in (39), we attain

$$[rA^T] \Psi(x) + [A^T P_{k \times k}^{2-\gamma_2}] \Psi(x) s(x) + [A^T P_{k \times k}] \Psi(x) t(x) + [A^T P_{k \times k}^{2-\gamma_1}] \Psi(x) u(x) + [A^T P_{k \times k}^2] \Psi(x) v(x) + 2v(x) = W^T \Psi(x). \tag{45}$$

Dispersing the coefficients $s(x), t(x), u(x), v(x)$ at the collocation points, construct the following matrices.

$$S = \begin{pmatrix} s(x_1) & 0 & \dots & 0 \\ 0 & s(x_1) & \dots & 0 \\ \vdots & \ddots & \ddots & \vdots \\ 0 & \dots & 0 & s(x_k) \end{pmatrix}, T = \begin{pmatrix} t(x_1) & 0 & \dots & 0 \\ 0 & t(x_2) & \dots & 0 \\ \vdots & \ddots & \ddots & \vdots \\ 0 & \dots & 0 & t(x_k) \end{pmatrix},$$

$$U = \begin{pmatrix} u(x_1) & 0 & \dots & 0 \\ 0 & u(x_1) & \dots & 0 \\ \vdots & \ddots & \ddots & \vdots \\ 0 & \dots & 0 & u(x_k) \end{pmatrix}, V = \begin{pmatrix} v(x_1) & 0 & \dots & 0 \\ 0 & v(x_2) & \dots & 0 \\ \vdots & \ddots & \ddots & \vdots \\ 0 & \dots & 0 & v(x_k) \end{pmatrix}.$$

Table 1. Maximum absolute errors for various choices of j and N .

k	48	96	192	384	768
	$(j = 3, N = 3)$	$(j = 4, N = 3)$	$(j = 5, N = 3)$	$(j = 6, N = 3)$	$(j = 7, N = 3)$
The Proposed method	1.5100e-05	3.8168e-06	9.6282e-07	2.4249e-07	6.0990e-08

Table 2. Adams type Predictor-Corrector method [3].

Step size	Maximum absolute errors
0.1	0,023658990000
0.01	0.000986218500
0.001	0.000043988230

Discretizing Equation (45), we can achieve

$$rA^T\phi_{k \times k} + A^T P^{2-\gamma_2}\phi_{k \times k} \cdot S + A^T P\phi_{k \times k} \cdot T + A^T P^{2-\gamma_1}\phi_{k \times k} \cdot U + [A^T P^2\phi_{k \times k} + Y] \cdot V = W^T\phi_{k \times k}, \tag{46}$$

where $Y = [2, 2, \dots, 2]_{1 \times k}$. At the collocation points $x_i = (2i - 1)/2k, i = 1, 2, \dots, k$, we transform Equation (46) into a system of algebraic equations. Solving this system of algebraic equations using MATLAB2015a, we can easily obtain A^T .

Suppose

$$r = 1, s(x) = x^{1/2}, t(x) = x^{1/3}, u(x) = x^{1/4}, v(x) = x^{1/5}, \gamma_1 = 0.333, \gamma_2 = 1.234.$$

Then the exact solution of Equation (39) for $\gamma_1 = 0.333$ and $\gamma_2 = 1.234$ is $h(x) = 2 - \frac{1}{2}x^2$.

In Tables 1 and 2, the maximum absolute error obtained using Adams type Predictor-Corrector method is 4.40e-05 in 1000th step, while the maximum absolute error using the proposed method is 1.51e-05 in 48th step. We also see clearly from Table 1 that the numerical solutions are in perfect agreement with the exact solutions for larger values of k . Numerical results of this problem demonstrate that the proposed method converges rapidly and is more efficient than the Adams type predictor-corrector method [3]. Also from Figure 1, we see clearly that the numerical solutions are in perfect agreement with the exact solutions.

Example 5.2. Consider the following fractional differential equation

$$D^{1/3}h(x) + x^{1/3}h(x) = w(x), x \in [0, 4), \tag{47}$$

with the initial state $h(0) = 0$ and $w(x) = \frac{3}{2\Gamma(2/3)}x^{(2/3)} + x^{(4/3)}$. The exact solution of Equation (47) is $h(x) = x$.

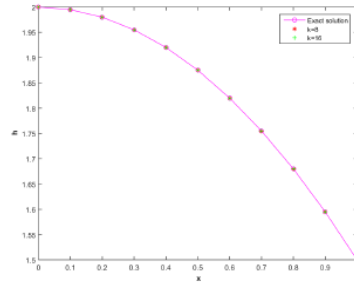


Figure 1. Comparison of Numerical solutions of Example 5.1 for $k = 8 (j = 3, N = 2)$ and $k = 16 (j = 4, N = 2)$ with the exact solutions.

Let $t = x/4$. Then $x = 4t$, $t \in [0, 1)$. Thus

$$D^{1/3}h(4t) + (4t)^{1/3}h(4t) = v(t), \quad (48)$$

where

$$v(t) = w(4t) = \frac{3 \cdot 2^{1/3}}{\Gamma(2/3)} t^{2/3} + (4t)^{4/3}, \quad t \in [0, 1).$$

Approximating

$$D^{1/3}h(4t) \text{ as } A^T \Psi(t) \text{ where } A = [a_1, a_2, \dots, a_k]^T, \quad (49)$$

we have

$$h(4t) = A^T P^{1/3} \Psi(t). \quad (50)$$

Similarly, $v(t)$ can be approximated by the Bernoulli wavelet functions as

$$v(t) = V^T \Psi(t), \text{ where } V = [v_1, v_2, \dots, v_k]^T. \quad (51)$$

Using Equations (49), (50) and (51) in Equation (48), we have

$$A^T \Psi(t) + (4t)^{1/3} A^T P^{1/3} \Psi(t) = V^T \Psi(t). \quad (52)$$

Table 3. Absolute errors for various choices of j and for $N = 2$.

x	$k = 8$		$k = 16$		$k = 32$	
	$(j = 3, N = 2)$		$(j = 4, N = 2)$		$(j = 5, N = 2)$	
	The proposed method	HWM	The proposed method	HWM	The proposed method	HWM
0.25	3.4042e-02	4.6972e-02	1.0979e-02	2.5554e-02	1.6860e-03	6.3723e-03
0.75	5.2261e-03	1.8818e-02	1.7086e-03	7.7490e-03	4.8561e-04	2.6655e-03
1.25	2.9291e-03	1.2333e-02	9.1120e-04	4.9465e-03	2.7618e-04	1.7841e-03
1.75	1.8933e-03	9.2464e-03	5.9425e-04	3.6780e-03	1.8461e-04	1.3549e-03
2.25	1.3507e-03	7.4107e-03	4.2765e-04	3.2651e-03	1.3471e-04	1.3549e-03
2.75	1.0238e-03	6.1850e-03	3.2668e-04	2.6691e-03	1.0387e-04	1.0953e-03
3.25	8.0889e-04	5.3060e-03	2.5985e-04	2.0961e-03	8.3183e-05	9.1997e-04
3.75	6.5879e-04	4.6437e-03	2.1286e-04	1.8332e-03	6.8503e-05	6.9676e-04

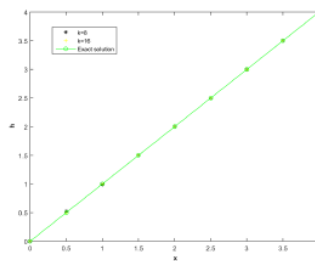


Figure 2. Comparison of Numerical solutions of Example 5.2 for $k = 8 (j = 3, N = 2)$ and $k = 16 (j = 4, N = 2)$ with the exact solutions.

Dispersing the coefficient $(4t)^{1/3}$ of Equation (52) at the collocation points, construct the following matrix.

$$R = \begin{pmatrix} (4t_1)^{(1/3)} & 0 & \dots & 0 \\ 0 & (4t_2)^{(1/3)} & \dots & 0 \\ \vdots & \ddots & \ddots & \vdots \\ 0 & \dots & 0 & (4t_k)^{(1/3)} \end{pmatrix}.$$

Discretizing Equation (52), we get

$$A^T \phi_{k \times k} + A^T P^{1/3} \phi_{k \times k} \cdot R = V^T \phi_{k \times k}. \quad (53)$$

At the collocation points $t_i = \frac{2i-1}{2^j N}$, $i = 1, 2, \dots, 2^{j-1} N$, we transform Equation (53) into a system of algebraic equations. Solving this system of algebraic equations using MATLAB2015a, we can easily obtain the coefficients vector A^T . Then we get the numerical solutions $h(4t)$ of Equation (48). The numerical solutions $h(x)$ of Equation (47) are obtained by $h(x) = A^T P^{1/3} \psi(x/4)$.

The numerical results for $k = 8$ ($j = 3$, $N = 2$) and $k = 16$ ($j = 4$, $N = 2$) are shown in Figure 2. From Figure 2, we find easily that the numerical solutions are in good agreement with the exact solutions. The absolute errors for different values of k are shown in Table 3. We also see from Table 3 that as k increases, the errors become smaller and the proposed method is more accurate compared with the Haar wavelets method.

6. Conclusion

In this paper, an efficient numerical scheme based on Bernoulli wavelets for solving a class of fractional differential equations with variable coefficients was proposed. By the advantages of sparse and orthogonal nature, the proposed technique reduces the computation greatly to give numerical solutions with good coincidence. Tables 2 and 3 depict the advantages of the proposed method over other methods, namely Adams type Predictor-Corrector method and Haar wavelet method, in terms of less computational effort and time, accuracy and simplicity. Absolute errors and graphical representations in the two numerical examples demonstrate the high degree accuracy of the proposed numerical scheme.

References

- [1] Ahmed Kareem Mohsin Al-Mosawi, Variational iteration method for solving delay integro-differential equation of fractional order, *Al-Mustansiriyah Journal of Science* 26(2) (2015), 62-68.
- [2] A. H. Bhrawy, A. S. Alofi and S. S. Ezz-Eldien, A quadrature tau method for fractional differential equations with variable coefficients, *Appl. Math. Lett.* 24 (2011), 2146-2152.

- [3] A. M. A. El-Sayed, A. E. M. El-Mesiry and H. A. A. El-Saka, Numerical solution for multi-term fractional (arbitrary) orders differential equations, *Comput. Appl. Math.* 23 (2004), 33-54.
- [4] Li Fangli, Fu Hongfei and Jun Liu, An efficient quadratic finite volume method for variable coefficient Riesz space-fractional diffusion equations, *Math. Meth. Appl. Sci.* (2020), 1-18, <https://doi.org/10.1002/mma.6306>.
- [5] R. Garra, Analytic solution of a class of fractional differential equations with variable coefficients by operatorial methods, *Commun. Nonlinear Sci. Numer. Simul.* 17(4) (2012), 1549-1554.
- [6] A. Kilicman, Kronecker operational matrices for fractional calculus and some applications, *Appl. Math. Comput.* 187 (2007), 250-265.
- [7] Mingxu Li and Jun Huang, Wavelet operational matrix method for solving fractional differential equations with variable coefficients, *Appl. Math. Comput.* 230 (2014), 383-394.
- [8] O. Oruc, A. Esen and F. Bulut, A Haar wavelet approximation for two-dimensional time fractional reaction-sub diffusion equation, *Engineering with Computers* 35(1) (2019), 75-86.
- [9] Peng Guo, The adomian decomposition method for a type of fractional differential equations, *Journal of Applied Mathematics and Physics* Article ID: 95943, 7(10) (2019), 8.
- [10] P. K. Sahu and S. Saha Ray, A new Bernoulli wavelet method for numerical solutions of nonlinear weakly singular Volterra integro-differential equations, *International Journal of Computational Methods* 14(1) (2017), 175-0022.
- [11] Yanxin Wang and Li Zhu, Solving nonlinear Volterra integro-differential equations of fractional order by using Euler wavelet method, *Advances in Difference Equations* 27 (2017).
- [12] Zhaopeng Hao, Moongyu Park, Guang Lin and Zhiqiang Cai, Finite element method for two-sided fractional differential equations with variable coefficients: Galerkin approach, *Journal of Scientific Computing* 79 (2019), 700-717, <https://doi.org/10.1007/s10915-018-0869-5>.
- [13] Jiao Wang, Tian-Zhou Xu, Yan-Qiao Wei and Jia-Quan Xie, Numerical solutions for systems of fractional order differential equations with Bernoulli wavelets, *International Journal of Computer Mathematics* 96(2) (2019), 317-336.